

DEPARTMENT OF THE INTERIOR

U.S. GEOLOGICAL SURVEY

**The Rapids and Waves of the Colorado River,  
Grand Canyon, Arizona**

by

**Susan Werner Kieffer**

**Flagstaff, Arizona 86001**

**Open-File Report 87-096**

**Prepared in cooperation with the Bureau of Reclamation  
and National Park Service**

**This report is preliminary and has not been reviewed for conformity with U.S.  
Geological Survey editorial standards.**

**1987**

THE RAPIDS AND WAVES OF THE COLORADO RIVER,

GRAND CANYON, ARIZONA

Sediment and/or Hydrology

of the

Glen Canyon Environmental Studies

by

Susan Werner Kieffer

U.S. Geological Survey

Flagstaff, AZ 86001

GCES Report No. D-5

(U.S. Geological Survey Open-File Report 87-096)

Approved for publication by the Director of the U.S. Geological Survey,  
February 6, 1987

## ABSTRACT

The rapids of the Colorado River in the Grand Canyon occur where debris fans constrict the width of the river and elevate the bed, causing supercritical flow and standing waves. The geometry of the channel and the nature of the bed material in it at the rapids have not been documented, and the hydraulic structures in the rapids have never been described. The objective of this project was to obtain data on the channel, and to provide hydraulic descriptions and interpretation of the rapids.

Channel configuration and river hydraulics were studied at twelve of the largest rapids: House Rock, 24.5-Mile, Hance, Cremation, Bright Angel, Horn Creek, Granite, Hermit, Crystal, Deubendorff, Lava Falls, and 209-Mile Rapids. The products of this research consist of this report and analysis; a video cassette showing the major hydraulic features at ten of these rapids (U. S. Geological Survey Open-File Report 86-503); and ten hydraulic maps of the rapids (U.S. Geological Survey I-Map 1897 A-J). The hydraulic maps show the standing wave structures in the rapids on detailed topographic bases of the river channel for discharges of 5,000 cubic feet per second (cfs) and 30,000 cfs and, where data were available, for 92,000 cfs. At each rapid, floats were launched. From their trajectories, streamlines have been plotted on the hydraulic maps and float velocities in different parts of the rapid have been determined. Accelerations of water from the backwaters (where velocities are typically 0.5 m/s) to velocities,  $u$ , as high as 7.5 m/s in the constrictions, and decelerations back to about 4-5 m/s into the jet that emerges into the channel below the rapid have been measured. Typical depths,  $D$ , in these same reaches at 5,000 cfs discharge are: 10 m in the backwater; 5 m in the convergent reach; 1 m in the constriction; and 5-10 m in the divergent reach. The velocities and depths indicate Froude numbers  $[Fr=u/(gD)]^{1/2}$ , where  $g$  is the acceleration of gravity of less than than 0.1 in the backwaters; a Froude number of about unity in the converging flow; of nearly 2 in the constriction; and of order unity in the jet emerging into the diverging section. The flow is therefore supercritical in the constrictions. The standing waves in the rapids are stable features in supercritical flow. Their strength changes with discharge, although their position is typically stable because of the presence of large rocks that are associated with the waves.

Large debris flows from tributaries change the position and strength of the waves because such flows change the constriction of the channel (both laterally and vertically) and, therefore, change the nature of the supercritical flow. Debris flows from the tributary canyons are episodically narrowing the river channel at the rapids; and the Colorado River clears the channel depending on the competence of the flow at different discharges. A study of the boulder size distributions in the channel suggests that boulders of 1-2 m diameter can be moved in the main channel by discharges typical of the power plant discharges at Glen Canyon Dam (a few thousand to 30,000 cfs). However, the pre-dam geometry of the river channel in the vicinity of the rapids was carved by large floods, comparable to or larger than natural mean annual floods that occurred in the Canyon prior to closure of Glen Canyon Dam (order

of magnitude 100,000 to 400,000 cfs). The rapids should be considered in operating criteria for Glen Canyon dam for the following factors: navigability (large rafts cannot navigate some rapids at the extremely low discharges proposed in some scenarios); safety (affected by both discharge and, possibly, by rate of change of discharge); and geologic impact (high discharges can substantially erode the channel of the Colorado River where it has been altered by tributary debris flows since the construction of the dam or since the last high discharges).

#### ACKNOWLEDGMENTS

Margie Dennis aided in field organization and laboratory analysis of data. Owen Baynham and Jim Tichenor, river guides, provided field and river assistance. Jennifer Whipple provided photographic support for both field trips, and numerous others helped with field work on each trip. Nancy Brian, National Park Service, provided the air photographs of the rapids at 30,000 cfs.

The hydraulic maps (U.S. Geological Survey Miscellaneous Investigations Maps I-1897, A-J) were prepared in collaboration with Ray Batson and Sherman Wu of the U.S. geological Survey in Flagstaff, Arizona. Bonnie Redding prepared the contour base maps. Patti Hagarty Gray prepared the air-brush illustrations.

Numerous formal and informal reviewers provided many constructive and stimulating comments, by which the manuscript was much improved. However, the author bears sole responsibility for the final product.

This work performed under Interagency Acquisition No. 6-AA-40-04190 during FY-86 and its amendment in FY-87, with continual support from the U.S. Geological Survey Branch of Igneous and Geothermal Processes since the inception of the work in 1983. For the work accomplished, we all owe Dave Wegner of the Bureau of Reclamation gratitude for his continual dedication to the Glen Canyon Environmental Studies.

## TABLE OF CONTENTS

Title Page	1
Abstract	ii
Acknowledgments	iv
Table of Contents	v
List of Figures	vi
List of Graphs	viii

I. Introduction: The Rapids and Waves of the Colorado River, Grand Canyon, Arizona	1
II. Objective	4
III. Methods	4
IV. Results and Discussion:	5
1. Common hydraulic and geomorphic features of the rapids	5
2. Location of the rapids	15
3. Channel geometry and hydraulic structures	16
4. Hydraulic parameters in pools and rapids	24
5. A generalized hydraulic model for the rapids	26
6. Pools and backwaters	34
7. The tongue and oblique lateral waves	37
8. The breaking waves below the tongue	40
9. Tailwaves and eddies	42
10. The minor effects: river curvature	47
11. Large rocks in the rapids	50
12. Movement of boulders and contouring of the channel	51
13. Rapids and rock gardens	60
14. Summary: Processes and their relative importance	60
V. Operating Criteria	64
VI. Conclusions	65
Literature Cited	67

Appendices: following text

    Appendix A: The 1983 Hydraulic Jump in Crystal Rapid:  
    Implications for River-Running and Geomorphic Evolution in  
    the Grand Canyon, reproduced from Kieffer, S.W., 1985,  
    Journal of Geology, 93 (4), pp. 385-406. A1

    Appendix B: Summary of Project Objectives and  
    Accomplishments B1

    Appendix C: Control for Topographic Maps of the Rapids C1

    Appendix D: Measurement of Water Surface Velocities  
    with "Yogis" D1

## LIST OF FIGURES

	page number
1. Index map	3
2. Granite Rapids (air photos)	7 and 8
3. Bright Angel Rapids (air photos)	9
4. Hance Rapids (air photo)	10
5. Deubendorff Rapids (air photo)	11
6. Boulder at 24.5-Mile Rapids (photos)	12
7. Wave at Horn Creek Rapids (photo)	13
8. Waves at 209-Mile and Hermit Rapids (photos)	14
9. Preliminary hydraulic map of Crystal Rapids	17
10. Preliminary hydraulic maps of House Rock Rapids	18 and 19
11. Cross sections of the Colorado River channel at House Rock Rapids	20
12. Preliminary hydraulic map of Horn Creek Rapids	21
13. Preliminary hydraulic maps of Lava Falls Rapids	22
14. Fathometer data (graphs)	23
15. Energy relations in open channel flow (schematic)	27
16. Depth-energy relations (schematic)	29
17. Comparison of subcritical and supercritical flow (schematic)	32
18. Types of hydraulic waves (schematic)	33
19. Hermit Rapids (air photos)	36
20. Hydraulic jump shapes at different Froude numbers (schematic)	38
21. Jet in diverging channel (schematic)	43
22. Crystal Rapids (air photo)	44
23. 24.5-Rapids (air photos)	45
24. Jet-eddy relations at a corner (schematic)	46
25. Open channel flow in a curved channel (schematic)	48
26. 209-Mile Rapids (photo and air photo)	49
27. Flow over a rock (schematic)	51
28. Erosion-sedimentation relations (graph)	54
29. Boulder size distributions at rapids (graphs)	54-56
30. Evolution of rapid-debris fan relations (schematic)	61
31. Histogram of constrictions along the river (graph)	63
D1. Floats in Granite Rapids (photographs)	following Appendix D1

LIST OF GRAPHS

(by Figure number)

	page number
14. Fathometer data (depth vs. location in rapids)	23
28. Erosion-sedimentation relations	54
29. Boulder size distributions at rapids (cumulative frequency vs. particle diameter of particles on debris fans)	54-56
31. Histogram of constrictions along river	63

I. INTRODUCTION: THE RAPIDS<sup>1</sup> AND WAVES OF THE COLORADO RIVER,  
GRAND CANYON, ARIZONA

*Look, look, it's waving to us with a wave  
to let us know it hears me.*

...  
*The black stream, catching on a sunken rock,  
Flung backward on itself in one white wave,  
And the white water rode the black forever,  
Not gaining but not losing.*

...  
*That wave's been standing off this jut of shore  
Ever since rivers, I was going to say,  
Were made in heaven.*

...  
*Speaking of contraries, see how the brook  
In that white wave runs counter to itself.*

...  
*It is this backward motion towards the source,  
Against the stream, that most we see ourselves in,  
The tribute of the current to the source.*

*(Robert Frost, "West Running Brook", applied to  
hydraulics by Lighthill, 1978, p. 261)*

Each rapid of the Colorado River is unique, but the major rapids have many hydraulic features in common. In this paper I describe the general features of twelve of the major rapids of the river in the Grand Canyon

---

<sup>1</sup> The use of the words "rapid" and "rapids" to indicate "part(s) of a river where the bed forms a steep descent, causing a swift current" is complex. The Compact Edition of the Oxford English Dictionary (1971) says that the word is usually used in the plural; the U.S. Geological Survey has followed this convention on topographic maps, e.g., Crystal Rapids. However, of the examples cited in the Oxford dictionary (p. 2416), the two in which the plural form (rapids) is used indicate multiple stretches of rough water, e.g., "through all the rapids" and "through twenty seven rapids". The other two examples cited use the singular, e.g., "we descend the rapid", and "in such a shallow rapid". Therefore, for clarity, in this paper, the singular form is used in descriptions of one continuous stretch of rough water, and the plural term is used when generalizations to many such stretches are being presented. However, conformity to U.S. Geological Survey nomenclature requires that the plural form be used for the proper name of a rapid, e.g., Crystal Rapids.

(Figure 1), and address the following hydraulic and geomorphic problems posed by the amazing similarity and, simultaneously, individuality of the rapids:

(1) Features: What are the common geomorphic and hydraulic features of rapids? (Section IV-1)

(2) Location: Most rapids occur where debris from tributary canyons has constricted the course of the Colorado River. Why are the tributaries and debris fans located where they are? (Section IV-2)

(3) Channel geometry and hydraulic structures: The gradient of the water surface through the rapids is much steeper than the average gradient of the water surface on the Colorado River in the Grand Canyon. What is the relation of the water surface profile to the channel profile? What do the flow streamlines look like? What are the water velocities in the rapids? What do the waves look like, and where do they occur? (Section IV-3, and hydraulic maps)

(4) Hydraulic parameters in pools and rapids: What are the characteristic Reynolds and Froude numbers along the river? (Section IV-4)

(5) A generalized hydraulic model for rapids: How does the constriction caused by a debris fan affect the flow of the river? What features are stable? Can features in a rapid be related to features identified and understood in simple laboratory flume flow? (Section IV-5)

(6) Pools and backwaters: What causes the pools above the rapids? (Section IV-6)

(7) The tongue and lateral waves: Water accelerates into the rapids through a chute of smooth water (the "tongue"). This tongue is bounded by oblique waves (the "laterals"). There are often non-breaking waves on the tongue ("rollers"). Why do all rapids have tongues? What are the rollers? What determines the angle of the laterals to the shoreline? How does this angle change with discharge? (Section IV-7)

(8) The breaking waves: A series of breaking waves exists below the tongue ("haystacks", "V-waves"). What causes these waves? (Section IV-8)

(9) Tailwaves and eddies: Large eddies typically exist on one or both sides of the river below a rapid. What is the relation between the main current and the eddies typically found above and below rapids? (Section IV-9)

(10) The minor effects, e.g., curvature of the river: The river often curves into and/or out of a rapid. Why? What is the influence of this curvature on the flow? (Section IV-10)

(11) Large rocks in the rapids: There are typically large boulders in

the main channel, and are often large waves associated with the rocks. How is the flow affected by the rocks, and by their position in the channel? How is it affected by different discharges? (Section IV-11)

(12) **Movement of the boulders and contouring of the channel:** Under what conditions can the boulders in a rapid be moved by the flow? How does the channel of the river change shape in response to changing discharges? (Section IV-12)

(13) **Rapids and rock gardens:** There are often rock gardens or cobble bars below the rapids. How do these form? (Section IV-13)

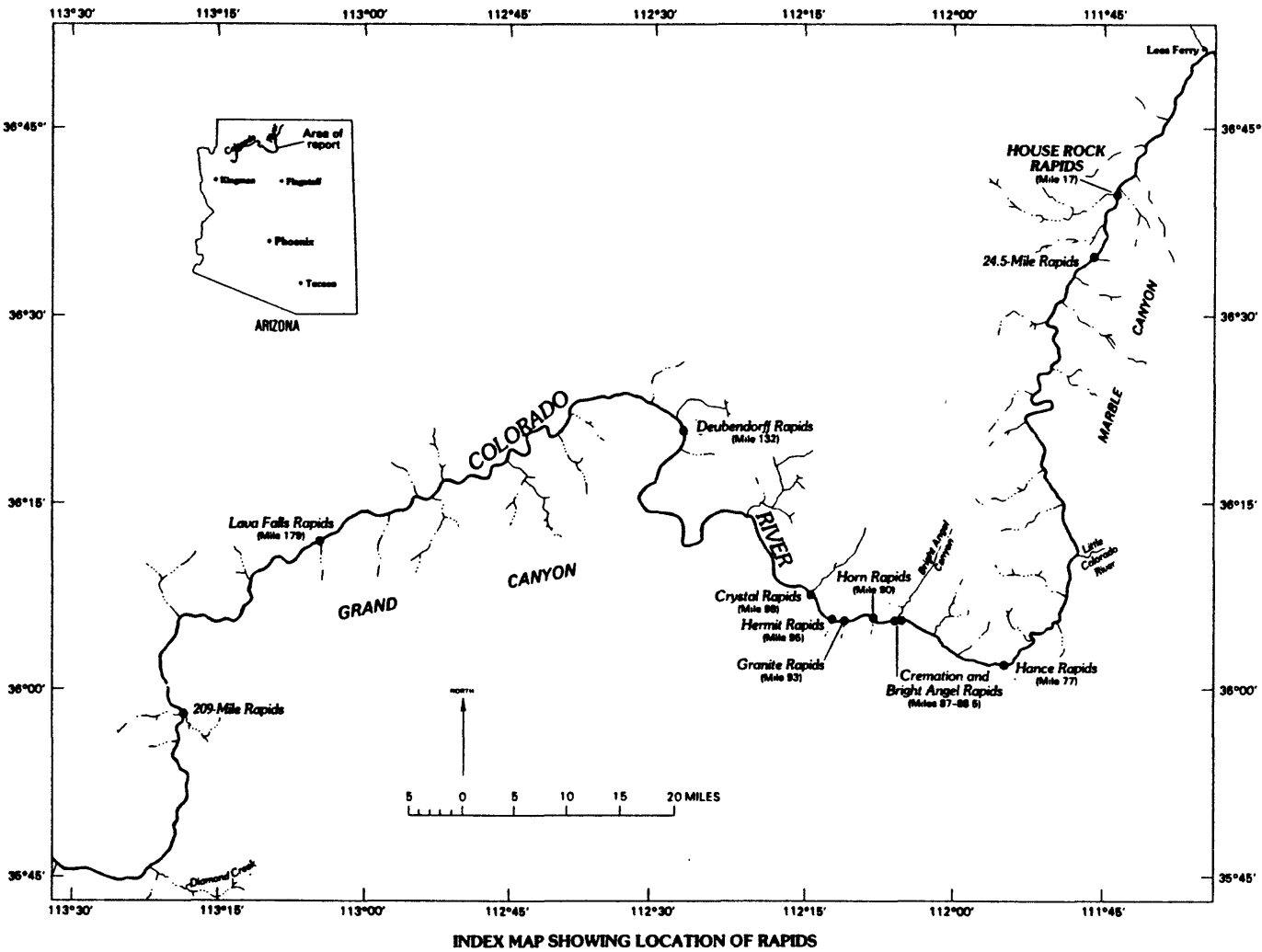


**Figure 1.** Index map showing the location of the major rapids studied. Of the twelve rapids indicated, ten were studied in detail for hydraulic mapping. 209-Mile Rapids was studied only as a topical example of river curvature, and Cremation and Bright Angel Rapids were combined into one map. The hydraulic maps of the rapids indicated by dots will be published as U.S. Geological Survey Miscellaneous Investigations Maps I-1897, A-J (no hydraulic map was made of 209-Mile Rapids).

## II. OBJECTIVE:

Work on the Colorado River by Howard and Dolan (1976), related work by Graf (1980) on similar rivers, and preliminary work done at Crystal Rapids by Kieffer in 1983 (Kieffer 1985, attached as Appendix A) has demonstrated that the rapids have changed since Glen Canyon Dam was closed. Data on the shape of the river channel and the material that lines it have not been available and are needed before response of the rapids to discharges through the dam can be predicted. The objective of this study was to obtain data on the configuration of the channel of the Colorado River in the vicinity of the rapids, on the nature of the material forming the channel bed and walls, and on the hydraulics of the river in the rapids. A brief statement of the more detailed objectives contained in Interagency Agreement No. 6-AA-40-04190 (FY'-86), its amendment in FY'-87, and status report as of the date of submission of this report is given in Appendix B. This work is part of the Glen Canyon Environmental Studies of the Bureau of Reclamation; related reports of these studies are cited herein as GCES (1987).

## III. METHODS

Twelve major rapids were selected for study: House Rock, 24.5-Mile, Hance, Cremation, Bright Angel, Horn Creek, Granite, Hermit, Crystal, Deubendorff, Lava, and 209-Mile Rapids. These rapids are amongst the largest on the river, and are of interest for hydraulic, sediment transport, beach stability, and recreational safety studies.

Two river trips of 16-18 days duration were conducted in October and November, 1985, for the purposes of: (a) filming time-lapse photography of the rapids as discharge varied during fluctuating flow from about 7000 cfs to about 20,000 cfs; (b) surveying in control points to provide data for construction of topographic maps by cartographic methods; (c) recording fathometer data across the channel above the rapids for determination of the specific head of the flow in the rapids; (d) launching and filming the trajectories of floats through the rapids for analysis of streamlines and velocity; and (e) obtaining preliminary data on the size distribution of the large boulders lining the channel of the river. 209-Mile Rapids was not studied in detail, but was selected for topical studies of the single hole formed by a rock fall about a decade ago and of the extreme curvature of the river at the rapid. Cremation Rapids and Bright Angel Rapids<sup>2</sup> are treated as a

---

<sup>2</sup> As of this writing, neither Cremation Rapids nor Bright Angel Rapids are official place names. The name "Bright Angel Rapids" herein means the rapid extending westward from the Kaibab trail bridge that crosses the Colorado River at Bright Angel Creek. The name "Cremation Rapids" herein means the first (small) rapid upstream from this bridge (it is a few hundred meters upstream from the beach popularly known as "Roy's Beach" during the GCES studies, and is formed by the debris fan on the south wall of the Canyon known as "Cremation Camp").

single rapid because of their proximity. Therefore, ten rapids were studied in detail and hydraulic maps were prepared for these ten (U.S. Geological Survey Miscellaneous Investigations Maps I-1897 A-J, hereafter referred to simply as I-1897). Because travel time between the rapids is substantial, even in a motor boat, the average time spent at each of the ten rapids was two days.

In the interest of simplicity, the text of this paper presents hydraulic and geomorphic generalizations, some of which may not be strictly valid at a particular rapid. The purpose is to summarize the data obtained and to present a framework within which detailed studies can be done on a rapid of interest (e.g., a particular rapid might be especially important for hydrologic monitoring as is Bright Angel Rapids; rafting management, as are Crystal and Lava Falls Rapids; or camping beach stability, as are Hance, Hermit, and Granite Rapids).

#### IV. RESULTS AND DISCUSSION:

The questions posed in the Introduction (Section I) are discussed sequentially here.

##### 1. Common Hydraulic and Geomorphic Features of the Rapids

Features found at most rapids are identified on the air photos of Granite Rapids shown in Figures 2a, b, and c, and can be found on the photographs of other rapids referred to throughout the text (particularly Figures 3, 4 and 5). Where possible, the photographs have been printed at the same scale, approximately 1:3000.

Rapids typically form where a debris fan from a tributary canyon constricts the Colorado River. These tributary canyons often have formed along regional faults or joints. In the converging portion of the river channel, standing waves (laterals) bound a tongue of smooth, accelerating water, upon which may stand smooth, undulating, nonbreaking waves (rollers). In the diverging portion of the river channel, criss-crossing, lateral waves typically intersect to give high-amplitude breaking waves (haystacks).

Obstacles in the bed of the channel (rocks, bedrock protrusions) also cause waves (holes, curlers, rooster combs, sculpted waves). Some types of these waves are illustrated in Figures 6, 7, and 8. In this report, the following meanings are attached to these words:

Lateral: A wave standing oblique to the current near the top of a rapid, usually emanating from shore.

Tongue: Smooth water between the first two strong lateral waves (right and left) at the top of a rapid.

Roller: A wave that stands oblique to the current and breaks back onto the current; the term nonbreaking roller is used to indicate the smooth rolling waves often found on the tongue.

Eddy fence: The shear zone between two currents with different velocity magnitudes or directions. An eddy fence usually does not have measurable relief on the water surface, but at high discharges, waves up to 10' high have been observed on eddy fences (e.g., the Slate Creek eddy fence at Crystal Rapids).

Pourover: A zone where water "pours over" an obstacle, obtaining a large downward component of velocity.

Hole: A trough in a standing wave, usually deep.

Runout: A zone of standing, generally nonbreaking (or weakly breaking), waves at the bottom of a rapid.

Haystack: A pyramidal wave (shaped like a haystack) usually breaking on top and sending spray in all directions (e.g., the fourth and fifth waves at Hermit Rapids).

Rooster comb: A haystack elongated in the downstream direction.

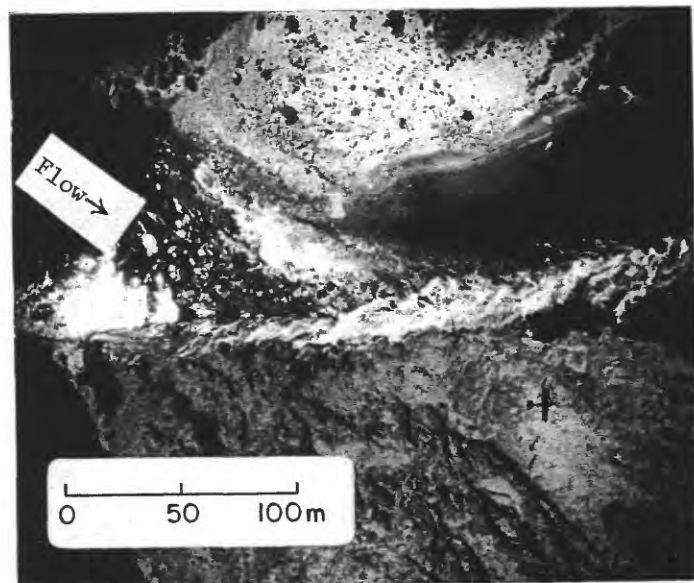
V-wave: The composite wave formed when opposing laterals intersect.

2(a)

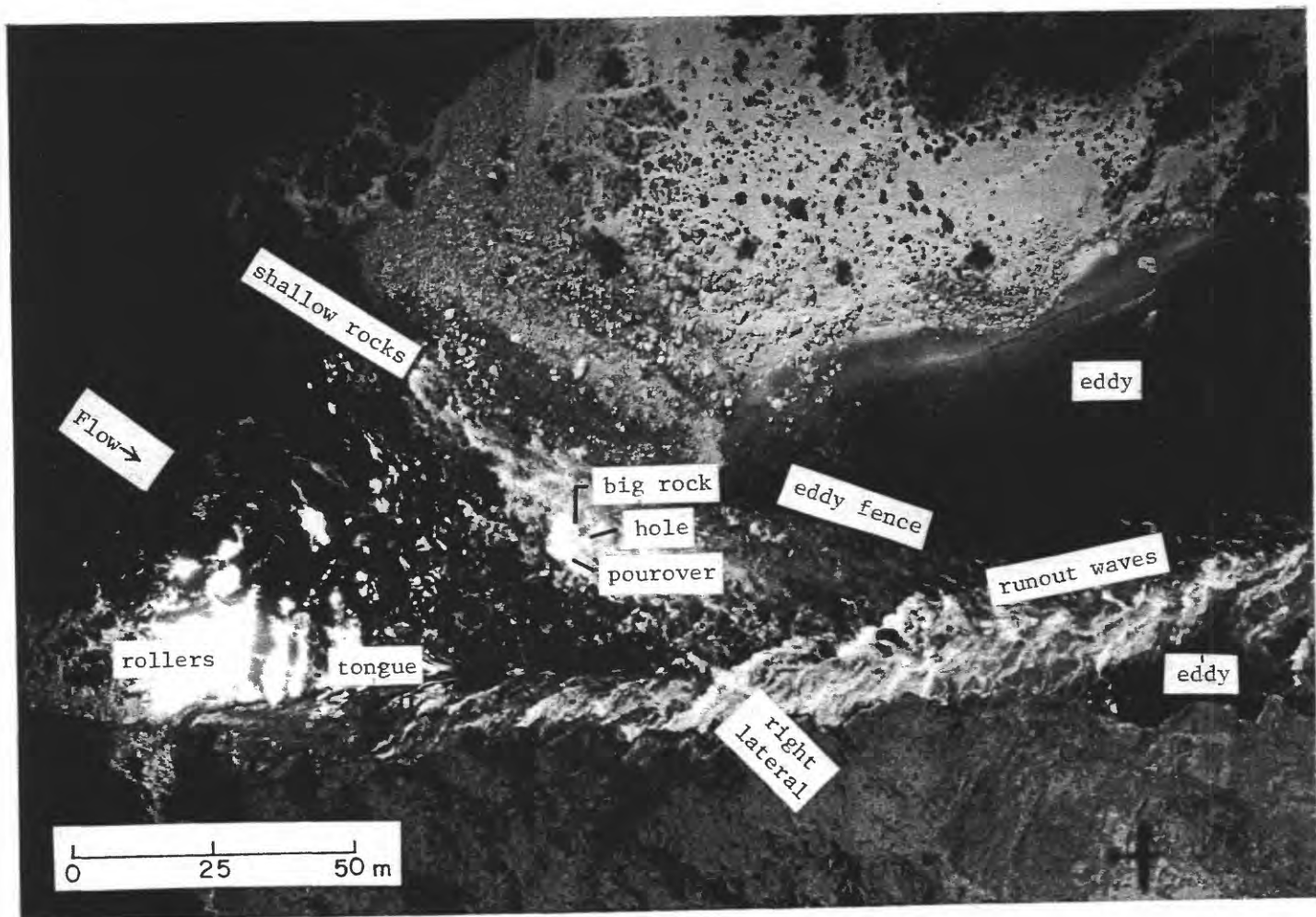


**Figure 2.** (a) Aerial photograph of Granite Rapids at a discharge of 5,000 cfs, showing the geomorphic features common to many rapids. For definitions of the terms, see text. Photograph by U.S. Bureau of Reclamation, 1984. Regional faults from Dolan, Howard and Trimble (1978). (b and c) Aerial photographs of Granite Rapids at 30,000 cfs showing typical wave structures in rapids. Photographs by U.S. National Park Service. (b) is at the same scale as (a); (c) is enlarged so that individual hydraulic features can be identified.

2(b)



2(c)



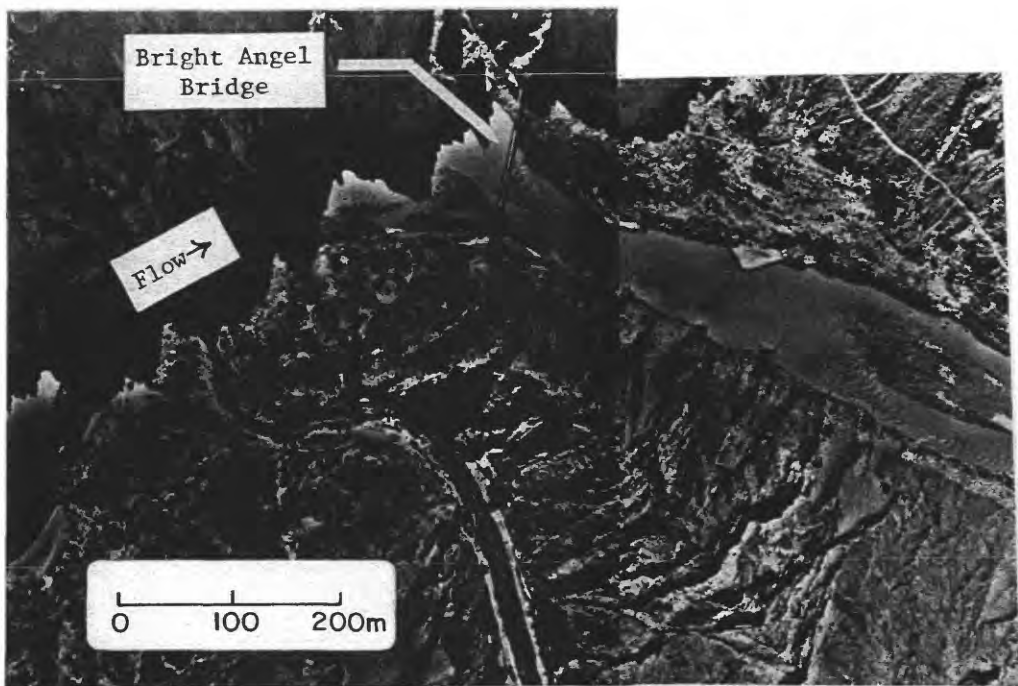


**Figure 3.** Composite aerial photograph of Bright Angel Rapids. Note the long cobble bar downstream of Bright Angel Creek, which enters from the bottom of the photo. Discharge is 5,000 cfs. Photograph by U.S. Bureau of Reclamation, 1984.

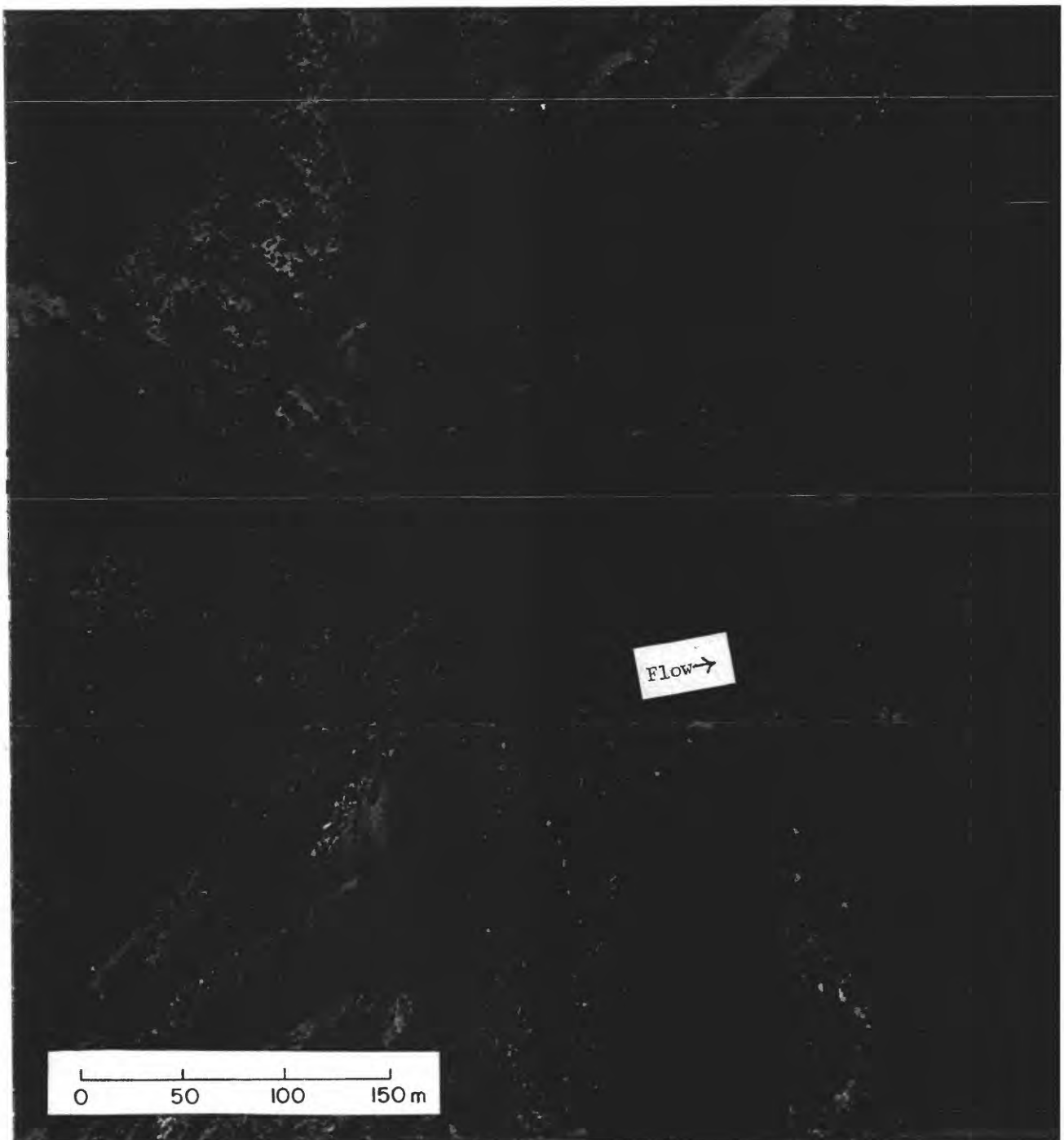


**Figure 4.** The head of Hance Rapids, showing unusual rockiness compared to most rapids. Discharge is 5,000 cfs. Photograph by U.S. Bureau of Reclamation, 1984.

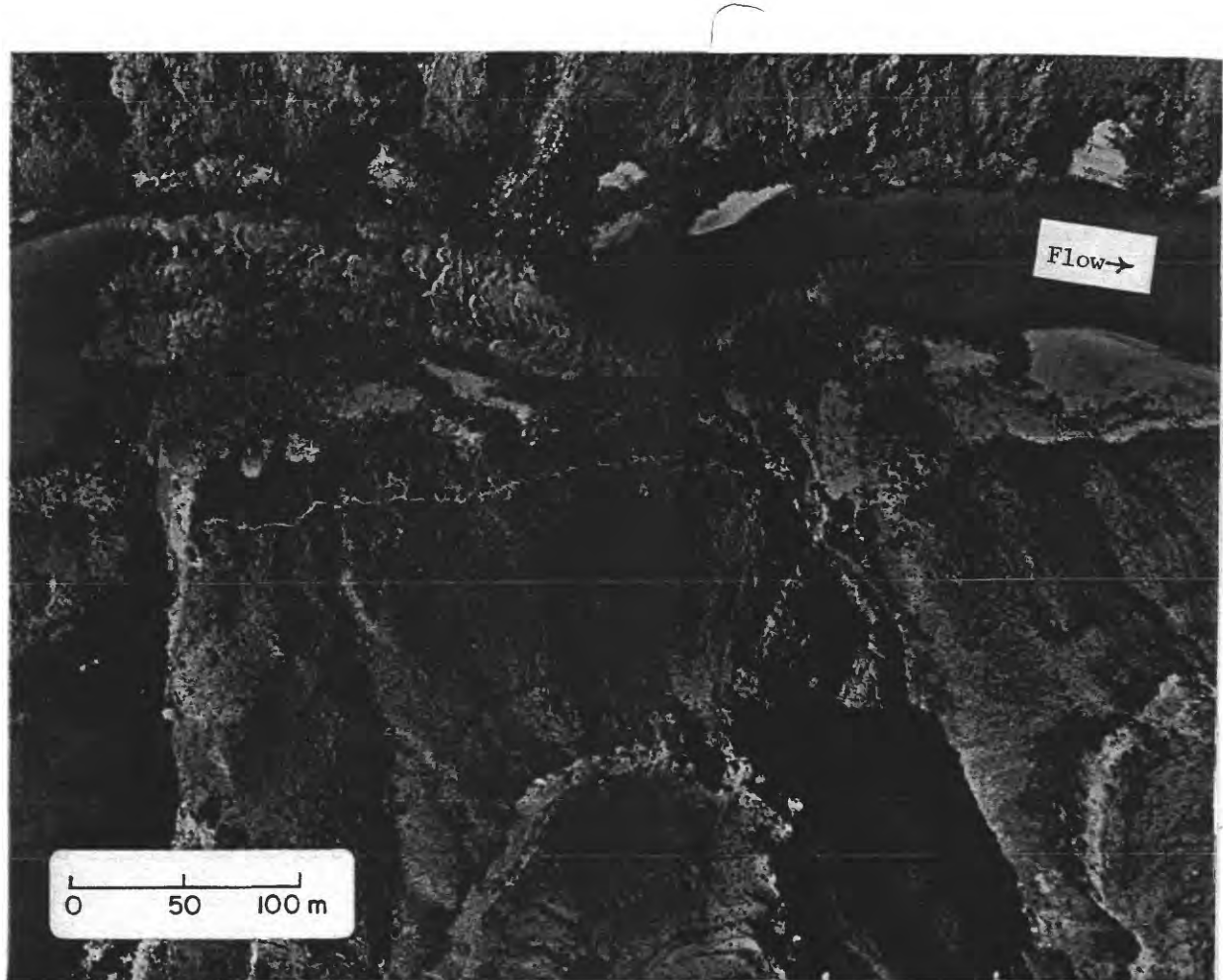


**Figure 5.** Deubendorff Rapids, showing an unusual rocky area at the head of the rapids (similar to Hance Rapids, Figure 4) and different from Granite Rapids, Figure 2a. Note also the unusually close proximity of two tributary canyons entering from the bottom of the photograph - Galloway Canyon at the head of the rapids, and Stone Canyon, with a much smaller debris fan, at the foot of the rapids. The setback of the river channel into the bedrock wall across from Stone Canyon is comparable to the setback across from Galloway Canyon. This observation leads the author to speculate that Stone Canyon has, in the past, produced larger debris fans than the one that exists at present and that these debris fans have diverted the river further to the south (top of photograph). Photograph by U.S. Bureau of Reclamation, 1984.

6(a)



6(b)



**Figure 6.** The unusually large, tabular rock at the head of 24.5-Mile Rapids is exposed at about 7,000 cfs, and (b) nearly submerged at about 15,000 cfs. The wake and eddy that develops in the flow downstream of the rock. This is typical of obstacles embedded in subcritical flow (see section IV, Figure 10).

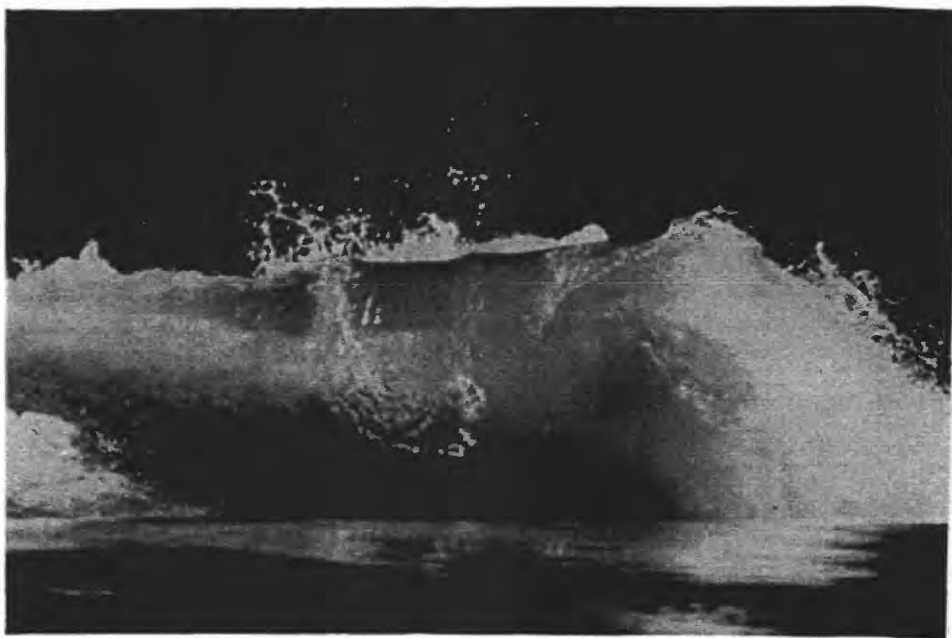


**Figure 7.** A curling wave ("sculptured wave", "rooster tail", "rooster comb") at the head of Horn Creek Rapids at a discharge of about 17,000 cfs. The wave is approximately 1 m in height. Such standing, breaking waves occur around obstacles in the region of supercritical flow in the rapids--in this case, between the two "horns" (rocks) that give Horn Creek Rapids its name. Photograph by Jennifer Whipple.

8(a)



8(b)



**Figure 8.** Two typical waves of Colorado River rapids. (a) The large back-~~—~~  
(or "breaking roller") at 209-Mile Rapids. The wave is about 1-2 m  
approximately 7 m in breadth. The discharge at the time of the ph-~~—~~  
approximately 15,000 cfs. (b) The famous "fifth" wave at Hermit Rapids  
though larger than usual, haystack. The dory is approximately 5 m in  
discharge at the time of the photograph was about 15,000 cfs. ~~—~~  
discussion of breaking waves. Photographs by Jennifer Whipple.

## 2. Location of the Rapids

Description of the Colorado River and its rapids began with exploration of the Grand Canyon by Powell (1875). The survey of the river by the Birdseye (1923) expedition established quantitatively that the descent of the river through the Grand Canyon occurs in a series of steps--the rapids.

In 1965, measurements of depth and velocity were again made along the river (Leopold 1969), and some measurements of velocity were obtained. Although these measurements were made after closure of Glen Canyon Dam in 1963, they were taken prior to closure of the bypass tunnels, and the river was flowing at the moderately high level of 48,500 cfs at the time of the measurements. At this discharge, median values of river width and depth were 220 ft (670 m) and 40 ft (12 m), respectively. Leopold noted that the river flows in alternating sections of long smooth deep pools and short steep shallow rapids. The water-surface gradient in the pools measured at 48,500 cfs was less than 0.002, and typically was of the order of 0.0005. In the rapids the gradient ranged between 0.005 and 0.017. Most (more than 80%) of the 2,200 (67 m) foot drop in elevation that occurs over the 280 miles of the river occurs in the individual rapids, and 50% of the elevation change takes place in only 9% of the distance. A typical velocity "above the rapids" was found to be 7 ft/s (3.3 m/s), and in the rapids, 11 ft/s (2 m/s).<sup>3</sup>

The channel of the river can be divided into stretches with different geomorphic or hydraulic characteristics (Howard and Dolan, 1981), and the severity of the rapids depends, in a general way, on these characteristics:

- (1) a wide valley with a freely meandering channel (e.g., miles 67-70 near Tanner Rapids);
- (2) valleys of intermediate width with tributary fan deposits (in these valleys, the river has usually cut into soft sandstones or limestones, e.g., the few miles just downstream of the Little Colorado River);
- (3) narrow valleys in fractured igneous and metamorphic rocks (e.g., "Granite Narrows" through miles 77-112);
- (4) narrow valleys of roughly uniform width and few constrictions in massive Muav limestone (e.g., miles 140-165);

---

<sup>3</sup> Any description of a rapid should include a specification of the discharge at which the description applies because the stage of the river, the nature of the bed, and the structure of the waves change with discharge. Leopold (1969, p. 142) showed that discharge is accommodated by both increase in stage and by scouring of the river bed (at Lee's Ferry, for example, as the discharge increased from 10,000 cfs to 92,000 cfs in 1948, the water elevation rose 11 ft (3.5 m) and the bed scoured 16 ft (5 m)).

(5) nearly flat stretches where the channel bottom is sandy (e.g., miles 1-10, and parts of Marble Canyon).

In all of these stretches, rapids generally occur where tributary side canyons join the Grand Canyon.<sup>4</sup> The tributary side canyons generally occur along regional faults or joints, and thus the distribution of the rapids is dependent on the regional tectonics (Dolan, Howard and Trimble, 1978, see also Figure 2a of this report). Bright Angel Creek (shown in Figure 3), for example, lies along the major Bright Angel fault. The side canyons are much steeper than the main canyon. This relatively steeper gradient permits delivery to the main channel of boulders that are too large for the main stem to move - even under inferred large natural floods (Graf, 1979). The tributary deposits therefore constrict the river on a large scale, and on a smaller scale, contain individual boulders that can be formidable obstacles in the path of the river. The relation between zones of structural weakness, tributary streams, debris fans, and rapids is well illustrated at Monument Creek where Granite Rapids has been formed (Figure 2). Repeated floods (the most recent in 1984) have poured down Monument Creek, building a debris fan that has pushed the Colorado River against the north wall of its channel. Debris fans form on at least one bank of the Colorado River where tributary streams enter (Howard and Dolan, 1981). Because many tributaries follow zones of structural weakness, it is not uncommon for tributaries to enter the Grand Canyon on both sides of the river at a given location. In such cases, if meteorologic and drainage conditions are conducive, debris fans may be formed by both tributaries. The size of the fans depends on the frequency and magnitude of floods in each drainage, on the drainage gradient (see Webb, GCES, 1987), and on the nature of the material in the contributing drainage. The river then erodes through the weaker debris fan, or even through the bedrock wall if the wall is more erodible than the debris fan. This process can result in the formation of a pronounced meander, and many rapids occur on curves of the river.

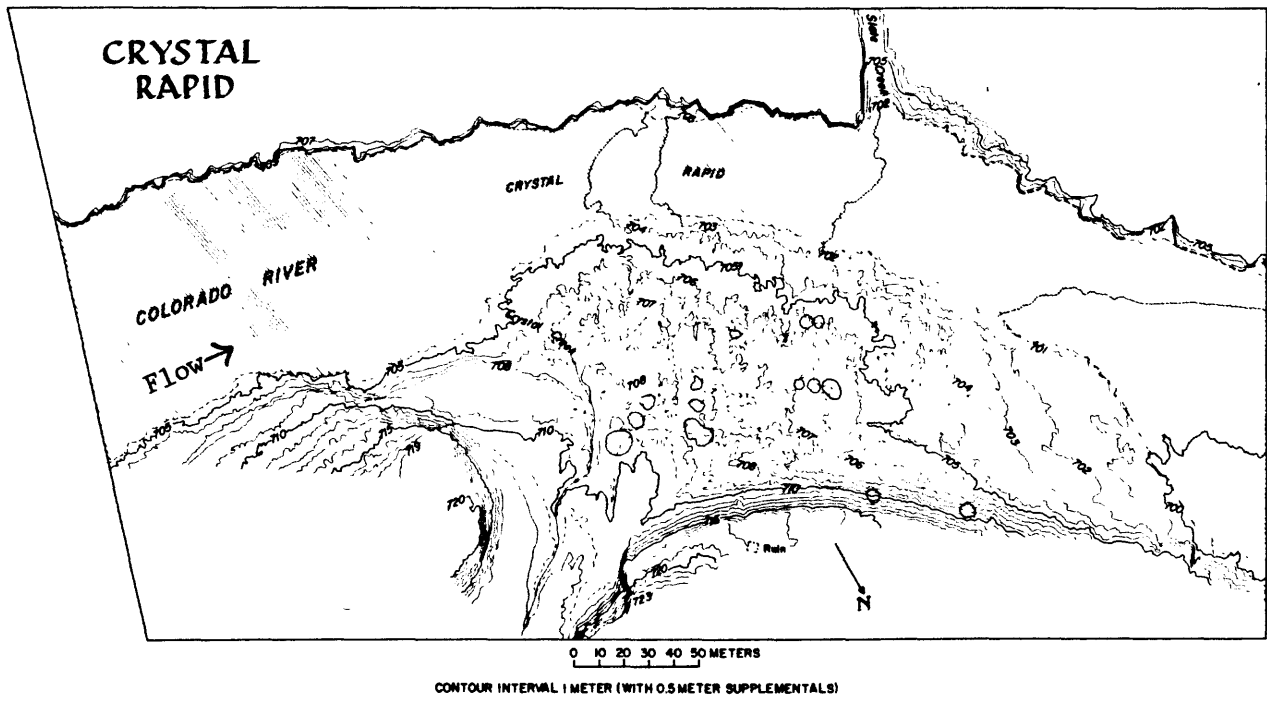
### 3. Channel Geometry and Hydraulic Structures

The topography of the channel in the vicinity of the rapids and the standing wave features of the rapids are portrayed on ten hydraulic maps of the rapids (U.S. Geological Survey Miscellaneous Investigations Maps I-1897, parts A-J). Each map contains: (a) a description of the rapid shown; (b) topographic contours of the channel; (c) hydraulic information at two or more discharges, (d) water surface elevations at different discharges (i.e., rating curves and water surface profiles); (e) velocity and streamline data at one or two discharges; and (f) approximately five channel cross sections. These data for House Rock Rapids, and preliminary maps and velocity and streamline data for Crystal, Horn Creek and Lava Falls Rapids are shown in Figures 9-13.

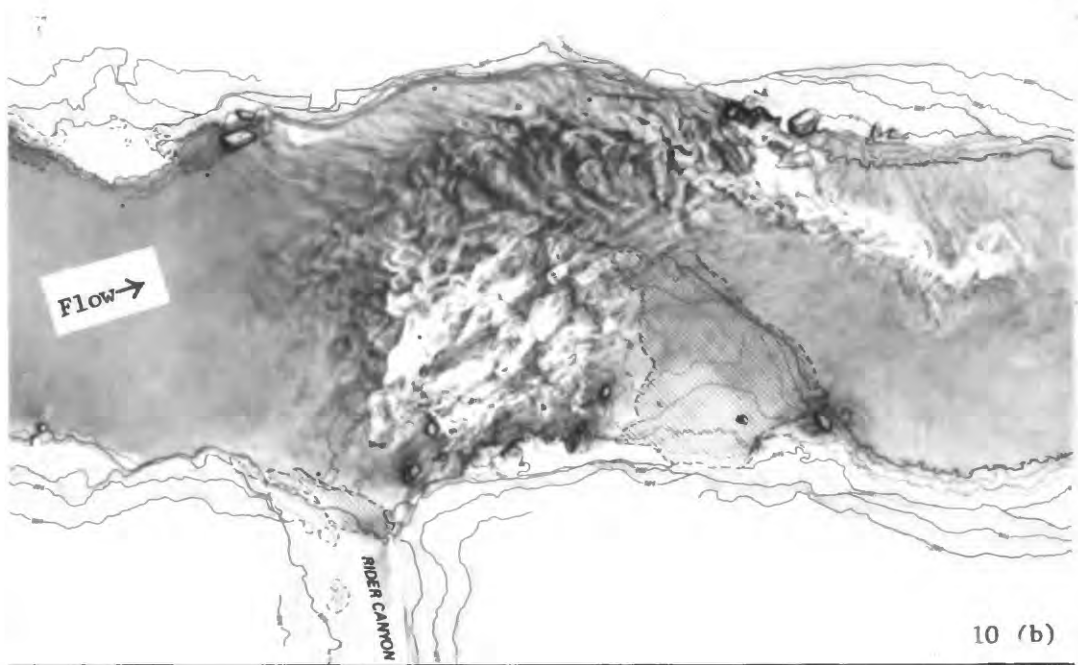
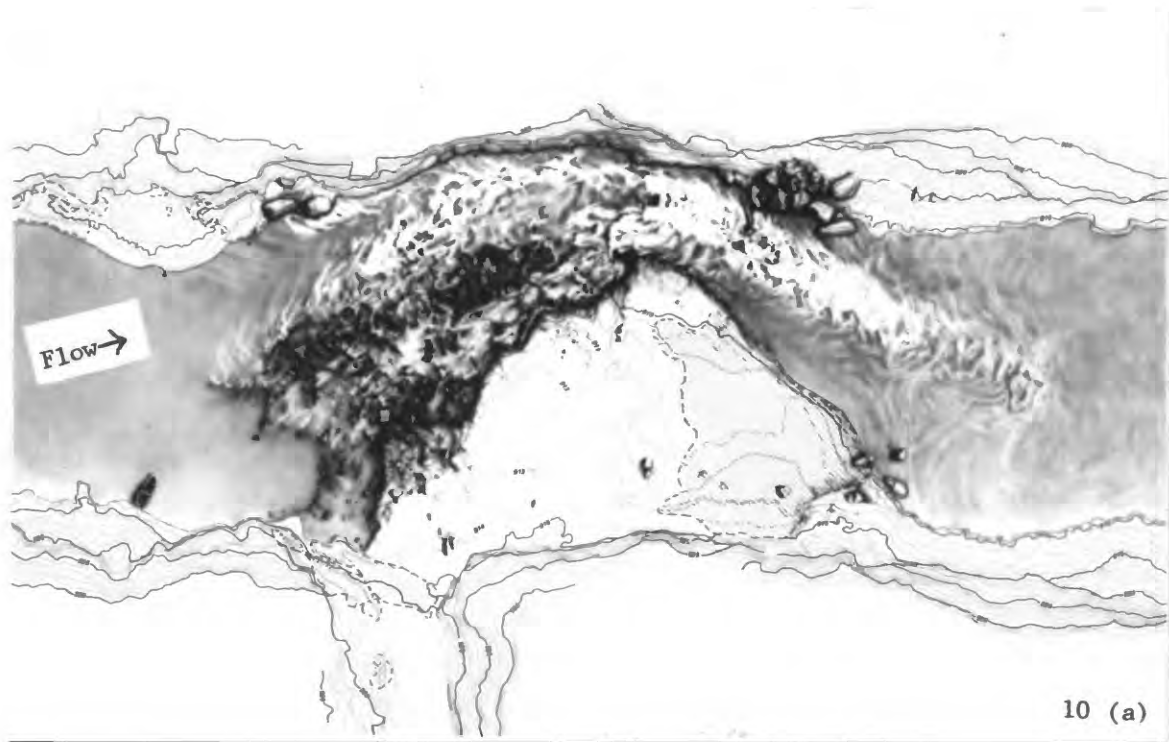
---

<sup>4</sup> Talus deposits and rock falls are a minor cause of rapids and will not be discussed here.

The topographic maps were prepared from 1984 stereo photographs taken by the Bureau of Reclamation when the water discharge was 5,000 cfs (Figures 2a, 3, 5, 19a, and 27a are such photographs). The drop of the water surface through the rapids at this discharge is shown on the maps; an example is shown in Figures 9 and 10c. Description of the techniques used to construct the maps is given in Appendix C. Streamlines and velocities in the rapids were measured by techniques described in Appendix D. Examples of the streamlines and velocity measurements are shown in Figure 10d, and in Figures 12 and 13. The channel configuration under the water could not be measured by analytical mapping techniques. Some fathometer data were obtained to supplement the topographic data shown on the maps (Figure 14). The data were obtained at dramatically different discharges, and, because the rating curves at the individual rapids are not well known, may never be precisely correctable to a fixed discharge, e.g., 5,000 cfs. The fathometer data have been incorporated semiquantitatively into the cross sections, e.g., as shown for House Rock Rapids in Figure 11. In spite of the limitations of the fathometer data, enough data on the channel configuration have been obtained for discussion of the hydraulic parameters in different parts of the rapids.



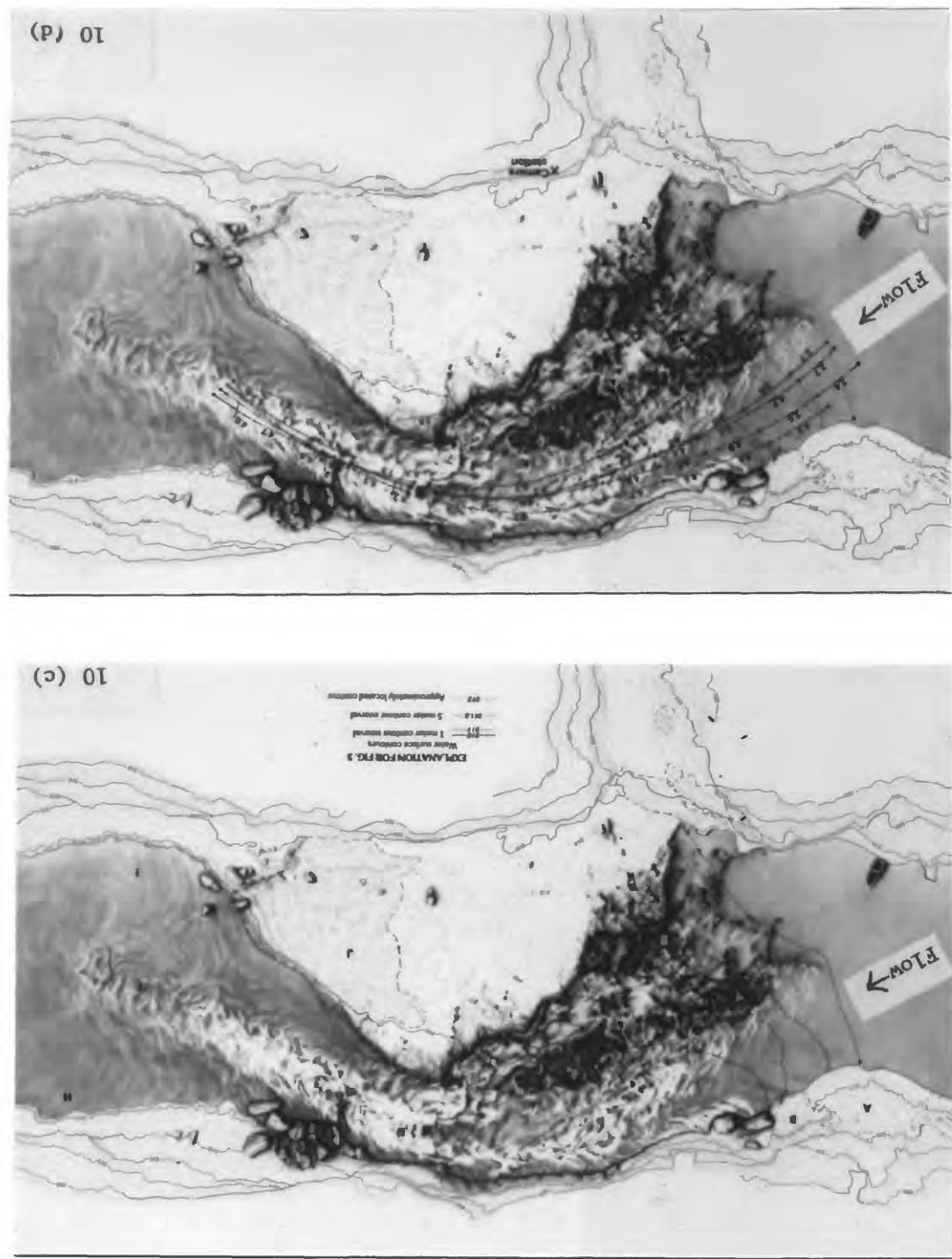
**Figure 9.** Topographic map of Crystal Rapids and its debris fan. This preliminary map has been extended about 50% further downstream; a final version will appear in the 1-1897 maps referenced in the text. Topography in Figures 9-13 prepared from Bureau of Reclamation photographs flown in 1984.

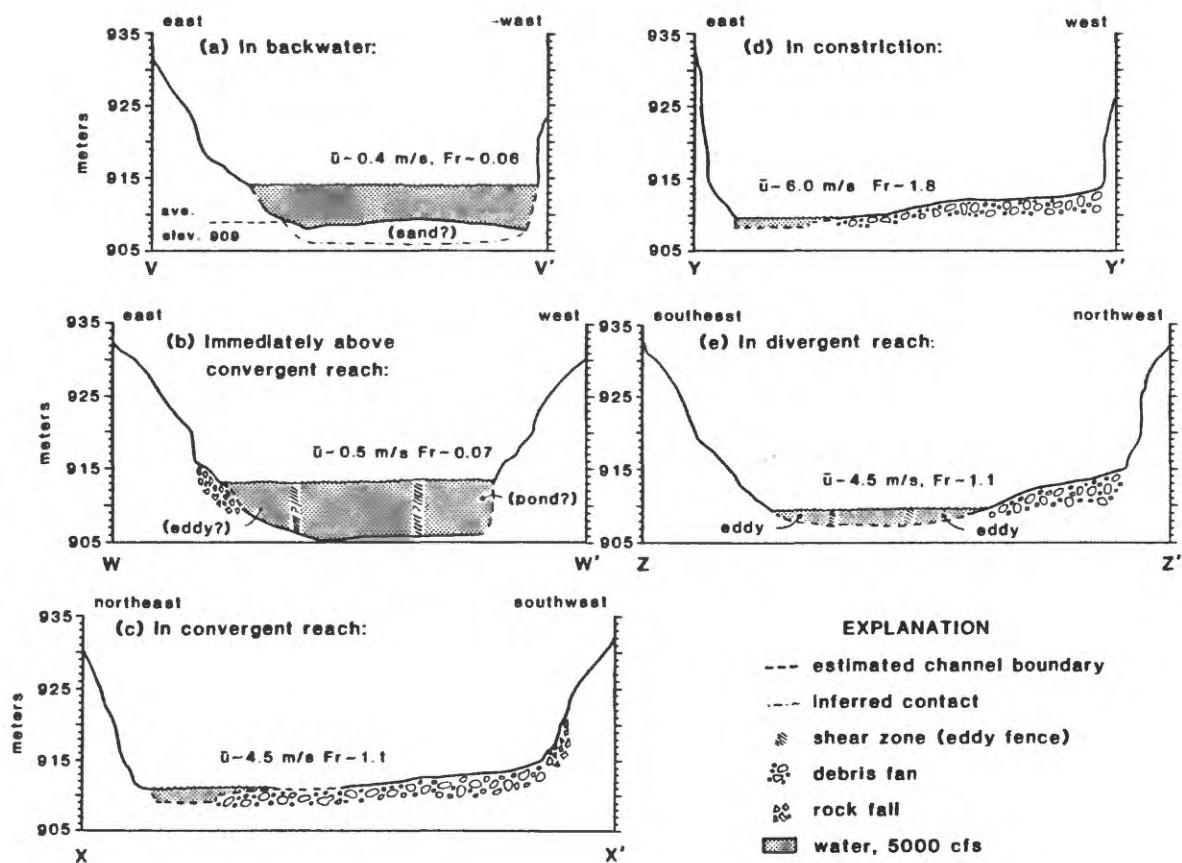


**Figure 10.** Preliminary hydraulic maps for House Rock Rapids showing (a) topographic contours and standing waves at 5,000 cfs; (b) the same at 30,000 cfs; (c) water-surface profile at 5,000 cfs; and (d) velocities and streamlines at 5,000 cfs. Flow direction is from left. Scale is 1:2000. Contour intervals indicated with solid lines are 1 meter (dashed lines = 0.5 m). Diagonal pattern slanting left indicates sand; diagonal pattern slanting right indicates vegetation (continued next page).

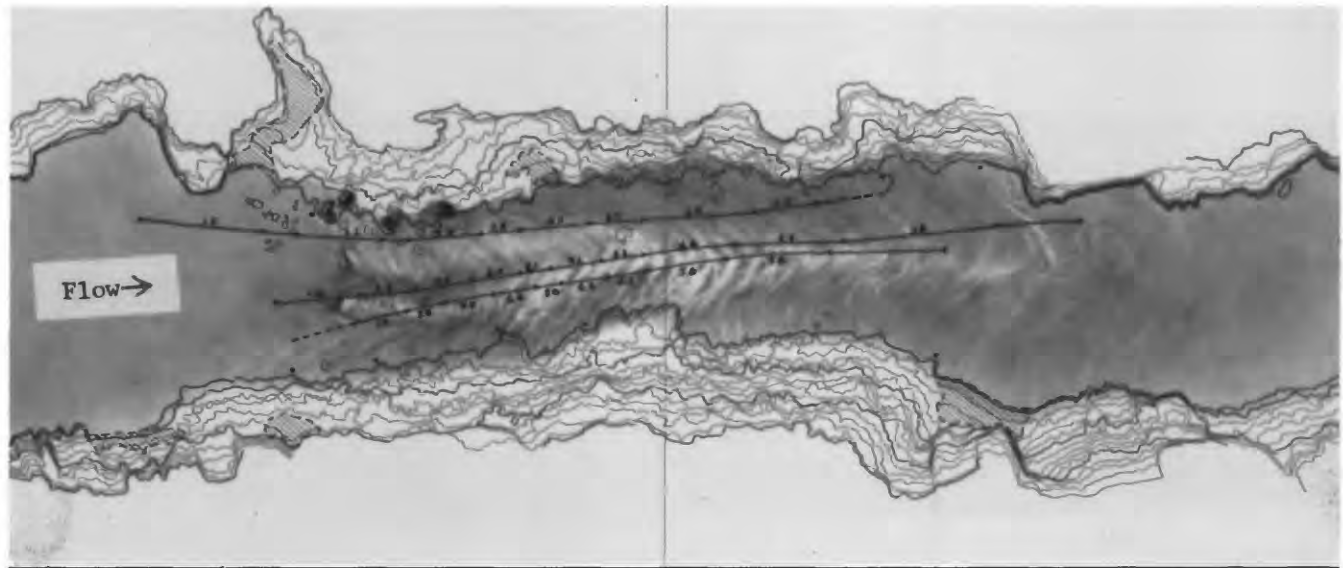
Figure 10 (continued) In (d) the numerals indicate velocitys along the streamlines between the adjacent dots; velocities are in m/s. Trajectories of the floats were determined from movies taken from the camera station indicated. The floats were standard commercial motor raft that is 10 m (33') in length. The boat shown is a standard commercial motor raft that is 10 m (33') in length. The boat is shown only for scale. These maps are for illustration of hydrologic features only and are not for scale.

Figure 10 (continued) In (d) the numerals indicate velocities along the streamlines





**Figure 11.** Five cross sections through different reaches of House Rock Rapids, based on the topographic map shown in Figure 10. Location is approximately described above each cross section.



**Figure 12.** Preliminary hydraulic map of Horn Creek Rapids, including contours, wave patterns, and measurements of streamlines and velocities at about 17,000 cfs discharge. Scale is 1:2000. Contour intervals are 1 m. Diagonal pattern slanting left indicates sand; diagonal pattern slanting right indicates vegetation. Velocities are in meters per second. Each numeral applies to the segment of streamline between the dots. These maps are for illustration of hydraulic features only and are not intended for navigation purposes.

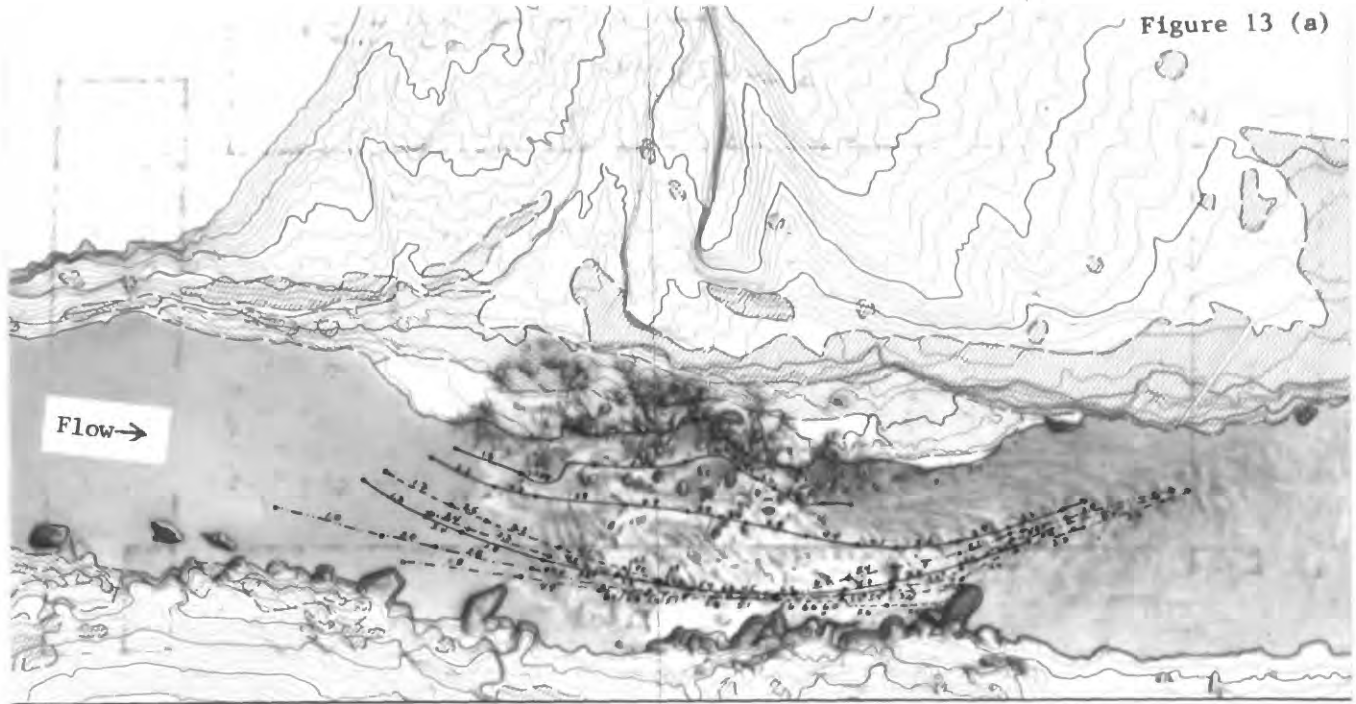


Figure 13 (a)

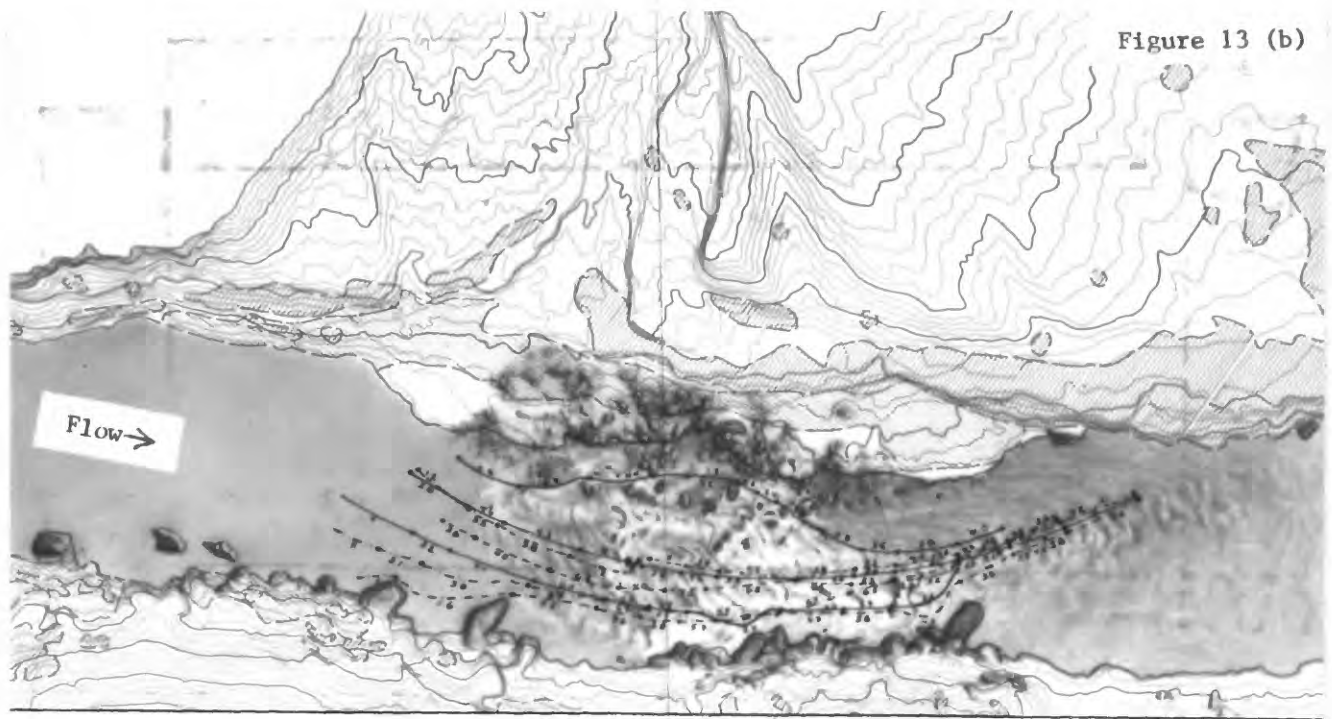


Figure 13 (b)

**Figure 13.** Preliminary hydraulic maps of Lava Falls Rapids, including contours, wave patterns, streamlines and velocities at (a) about 7,000 cfs discharge and (b) at about 10,000 cfs. See Figure 10 for map information, and Appendix D for discussion. The boat shown is a standard paddle or rowed raft, e.g., as used by most private parties, and is approximately 5 m in length (14-16 ft). The boat is shown only for scale. These maps are for illustration of hydraulic features only and are not intended for navigation purposes.

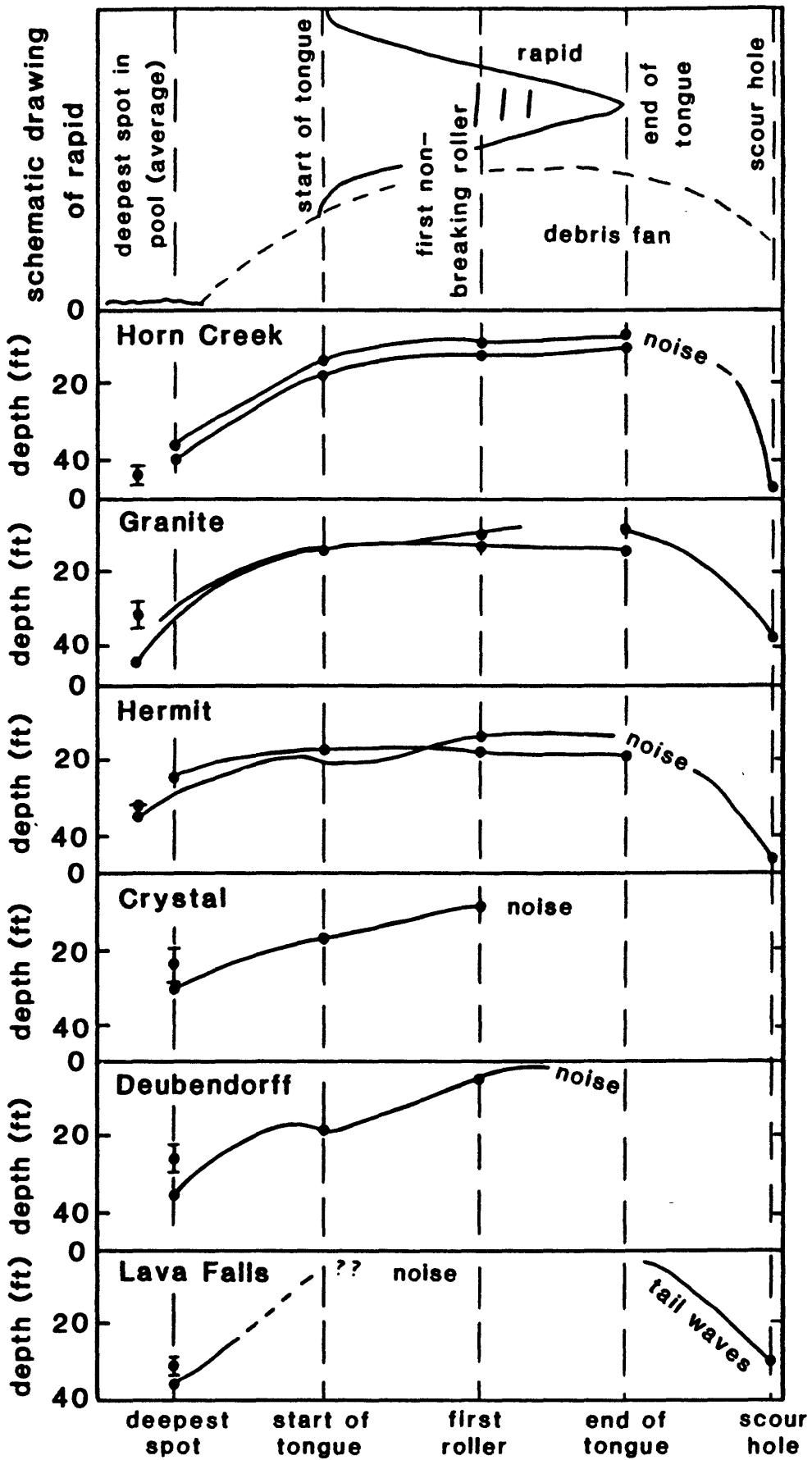


Figure 14. Summary of fathometer tracings obtained by the author and by Julie Graf (U.S. Geological Survey) and Owen Baynham (river guilds). No horizontal dimensions are implied. On each tracing, identifiable hydraulic features are shown, as indicated by the schematic map view of the river at the top of the figure: the top of the tongue, defined as the position at which the lateral waves begin at the shoreline; undulating rollers on the tongue; the end of the tongue; and the bottom of the breaking waves. Where known, discharges are indicated. Similar profiles occur in every rapid for which fathometer data were obtained.

**6. Hydraulic Parameters in Pools and Rapids** In both map view (e.g., as in the air photo in Figure 2) and in cross section (as indicated in Figure 14 by the fathometer tracings, and in more detail in Figure 11 for House Rock Rapids) the channel of the Colorado River is constricted at the rapids. The constrictions are caused by the debris flows from the side canyons. The debris flows narrow the canyon laterally and elevate the bed. The shape and the hydraulic characteristics have given rise to the so-called "pool-rapid" sequence of the Colorado River.

Above a rapid the river is typically wide, relatively deep, and tranquil. I reserve the term "pool" for such sections of the river<sup>5</sup> and will demonstrate below that at most discharges the pool is a hydraulic backwater. Cross section V-V' in Figure 11 shows a typical pool (upstream of House Rock Rapids). The water velocity is slow (about 0.4 m/s) and the water is relatively deep. The channel bottom is, on the average, at 909 m elevation in this particular pool.

At the downstream end of the pool, water accelerates gradually toward the constriction. Cross section W-W' at House Rock (Figure 11b) shows that the water has accelerated slightly to 0.5 m/s. This same cross section is deeper than V-V', with the channel bottom lowered to at least 906 and, in one place, to 905 m. In this region the channel bottom may change from sand (at the higher elevation) to bedrock or very coarse cobbles or boulders. The "rapid" itself is narrow and shallow, and the flow is fast (cross sections X-X' and Y-Y' in Figure 11). Depths of only one or two meters are common (at the discharge of 5,000 cfs shown in the illustrations) and float velocities up to 8 m/s have been measured at this discharge. In the case of House Rock Rapids, the channel bottom appears to have risen from 905 m at the upstream hole at W-W' toward an elevation of 909 m. It is probably not coincidence that this is the same elevation found further upstream at V-V', but the hydraulic explanation for this is not yet clear.

Below the rapid is a deep zone in which the flow is still relatively fast compared to the "pool" upstream of the rapid. For example, the velocity in the jet that emerges from House Rock Rapids is about 4.5 m/s. Gentle waves, known as the "tailwaves" of the rapid, occur within this region. Within the region of tailwaves, the channel bottom drops back toward the depths seen upstream of the rapids. Note, however, that in the region of House Rock Rapids over which we have accurate data (Figure 11), the channel bottom has not yet recovered the lowest base level seen at W-W' upstream of the rapids. The deep region of the channel below a rapid is often referred to as a pool, but this deep zone is more properly called a "scour hole" to emphasize that it is associated with the relatively high-velocity runout from the rapid. It is important to distinguish these higher-velocity stretches of the river immediately below the rapids from the "pools" that are immediately upstream of the rapids.

<sup>5</sup> This use of the word "pool" is consistent with Leopold (1969, p. 133).

Strong vertical motions occur in the water, particularly at the bottom of rapids (Leopold 1969). The water drops in elevation through a rapid, and Leopold (1969) proposed that continued vertical motion at the foot of the rapid causes the deep hole to be scoured. He proposed that water flows along the bed at the base of the rapid and then rises toward the surface in groups of turbulent boils that are characteristic of this region. Some of these boils have as much as 1 ft (0.3 ft/s) of super-elevation, indicating a vertical velocity of at least 8 ft/s (2 m/s).

The data from the hydraulic maps (e.g., figures 10, 12, 13, and unpublished data on the other rapids) allow calculation of two important hydraulic parameters in these the pools, rapids, and scour holes: the Reynolds number, and the Froude number. These two dimensionless numbers indicate the state of the flow: laminar vs. turbulent, and subcritical vs. critical.

The Reynolds number,  $Re=uD/v$  (where  $u$  is a velocity,  $D$  is a characteristic length, and  $v$  is the fluid viscosity) indicates the stability or instability of laminar flow. When this number is large ( $>10^5$ ), flow is turbulent. The viscosity of water is 0.01 poise; a typical minimum dimension of interest is depth, of order 1 m ( $10^2$  cm). Therefore, for all flow velocities above 10 cm/s the flow is fully turbulent. The Reynolds number does not change appreciably from backwater to rapids. Therefore, differences in wave behavior between backwaters and rapids cannot be explained by differences in the Reynolds number; the flow is fully turbulent everywhere.

The Froude number,  $Fr=u/(gD)^{1/2}$ , is a measure of the relative importance of kinetic and potential energies and the stability of standing waves. There are dramatic changes in flow regime as the Froude number changes from less than one to greater than 1. In a typical backwater,  $u \sim 100$  cm/s,  $D \sim 10^3$  cm, so  $Fr \sim 0.1$  (this would be a typical condition at the Bright Angel gage station), and is found, for example, above House Rock Rapids (Figure 11). In a rapid, on the other hand,  $u > 500$  cm/s (as shown by the three figures 10, 12, 13),  $D < 300$  cm (Figure 11 and 14), so  $Fr \sim 1$  or  $Fr > 1$ . In extreme cases,  $u \sim 10^3$  cm/s,  $D \sim 10^2$  cm, so  $Fr \sim 3$ .

Consideration of the Reynolds and Froude numbers then suggests that the dramatic change in flow regime from backwaters to rapids will be caused by differences in the balances of kinetic and potential energy that change the stability of standing waves in the channel. The general principals that apply comprise the classic theory of open channel hydraulics. This subject is briefly reviewed in the next section, (which may be skipped by readers with a background in hydraulics and supercritical flow).

## 5. A Generalized Hydraulic Model for the Rapids

Although complex in detail, the flow of the Colorado River in its channel can be interpreted to first order in terms of open-channel flow principles. The river flows in a channel bounded on its sides and bottom by walls (possibly erodible). The surface of the river is unconfined, subject to atmospheric pressure. This free surface can change shape in time and space. Depth, discharge, bottom slope, and free surface slope are all interdependent--connected by mass, momentum, and energy relations. Although the channel of the Colorado River is not rectangular (except possibly where bounded by bedrock walls), the discussion here is for the simple case of a rectangular channel for simplicity.<sup>6</sup>

A schematic geometry of open-channel flow and of energy relations is shown in Figure 15. The total energy ("head"),  $H$ , of water at any level,  $A$ , in a cross section,  $O$ , relative to an arbitrary level, called the datum, is the sum of its potential energy and its kinetic energy:

$$H = z_A + D_A \cos \theta + u_A^2 / 2g$$

$z_A$  is the elevation of point A above the datum;  $D_A$  is the depth of point A below the water surface;  $\theta$  is the bed slope angle;  $u_A$  is the velocity;  $g$  is the acceleration of gravity.  $u_A^2 / 2g$  is the velocity head. It is common practice to express all energies in terms of an elevation, in dimensions of feet or meters.

The line representing the total head of the flow is the energy line; its slope is the energy gradient,  $S_f$ . The slope of the water surface is  $S_w$ ; the slope of the channel bottom is  $S_0 = \tan \theta$  ( $S_0 \rightarrow \sin \theta$  for small slopes). In uniform flow,  $S_f = S_w = S_0 = \sin \theta$ .

Energy must be conserved between any two cross sections of the flow (Bernoulli's principle):

$$z_1 + D_1 \cos \theta + u_1^2 / 2g = z_2 + D_2 \cos \theta + u_2^2 / 2g + h_f$$

In this equation, the subscripts 1 and 2 represent the two different cross sections in which energy is balanced. The left side of the equation is the total energy at cross section 1; the first three terms of the right side give the total energy at cross section 2, and the last term,  $h_f$ , represents all energy losses (or gains) between the two cross sections.

---

<sup>6</sup> Excellent discussions of the following material can be found in Bakhmeteff (1932), Ippen (1951), or Chow (1959).

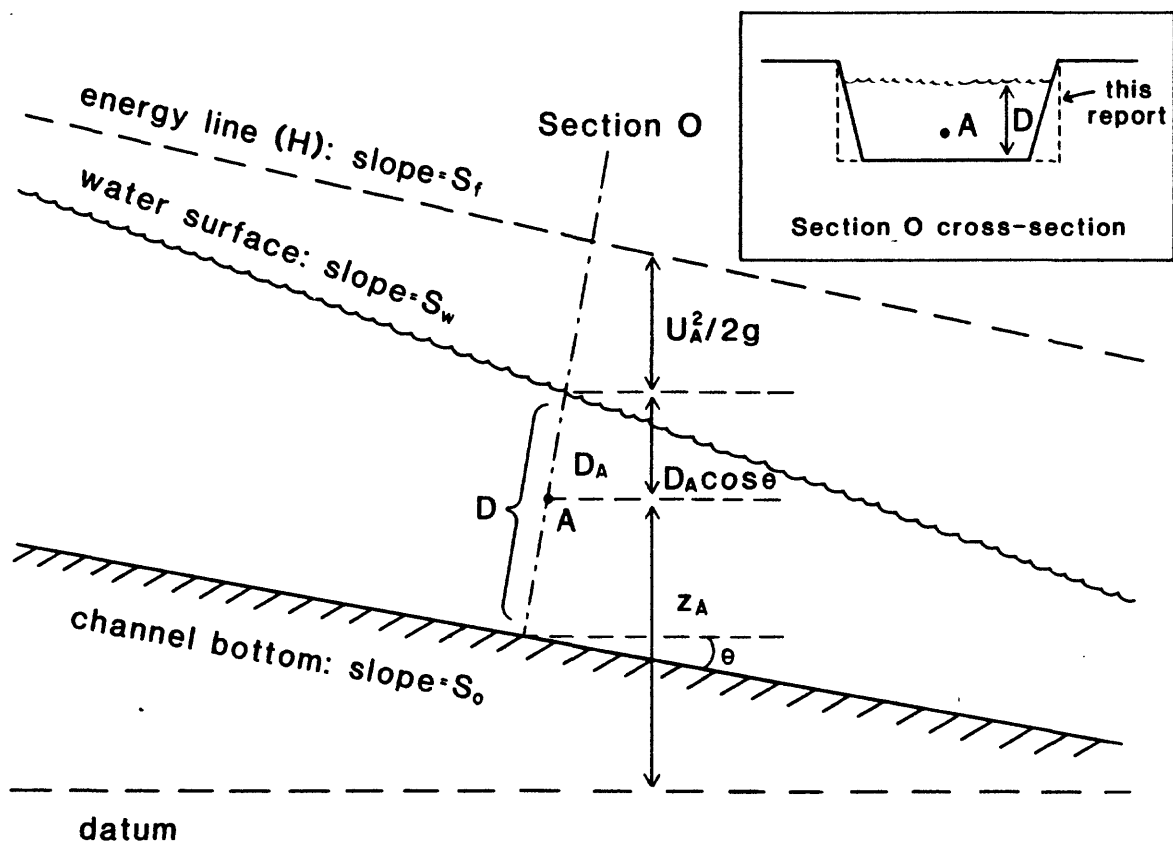


**Figure 15.** Energy relations in open-channel flow (after Chow, 1959, p. 39). See text for discussion of notation. Inset: schematic of open-channel flow in a trapezoidal channel.

If the slope,  $\theta$ , is small,  $\cos \theta \rightarrow 1$ . If energy losses are also small,  $h_f \approx 0$ . The above equation then simplifies to the Bernoulli energy equation:

$$z_1 + D_1 + u_1^2/2g = z_2 + D_2 + u_2^2/2g = \text{constant}$$

or

$$H_1 = H_2.$$

The specific energy of the water is the energy with respect to the channel bottom ( $z_1 = z_2 = 0$ ):

$$E = D \cos \theta + u^2/2g.$$

If the specific energy is the same at two different sections (namely, if  $h_f = z_2 - z_1$ ), then,

$$E_1 = E_2 = D_1 + u_1^2/2g = D_2 + u_2^2/2g$$

This equation demonstrates that changes in depth (D) (i.e., in potential energy) cause changes in velocity (u) (i.e., in kinetic energy). From continuity,

$$u = Q/A$$

where  $Q$  is the discharge, and  $A$  is cross-sectional area.

For a rectangular channel,

$$u = Q/Dw$$

where  $w$  is channel width, and  $D$ ,  $A$ , and  $u$  become mean flow or channel parameters. Then,

$$E = D + \frac{Q^2}{2gD^2w^2}$$

For a given channel section (described by the single parameter  $w$  in a rectangular channel model) and given discharge ( $Q$ ), the specific energy ( $E$ ) is a function only of depth. Therefore, a graph of energy vs. depth (an E-D graph) specifies the flow behavior completely (Figure 16). This energy equation is cubic with two real roots, and therefore the energy-depth (E-D) graph has two real branches. For a given specific energy,  $E$ , there are two possible depths: a low stage,  $D_1$ , and a high stage,  $D_2$ . For a given discharge (i.e., a specific curve in the E-D diagram), there is a minimum specific energy,  $E_c$ , and only one flow depth,  $D_c$ , and one flow velocity,  $u_c$  possible. These are called the critical conditions (critical state, critical depth, and critical velocity). If the depth of flow is greater than the critical depth, the velocity is less than the critical velocity--for these conditions the flow is called subcritical. If the depth of flow is less than the critical depth, the velocity is greater than the critical velocity--the flow is called supercritical.

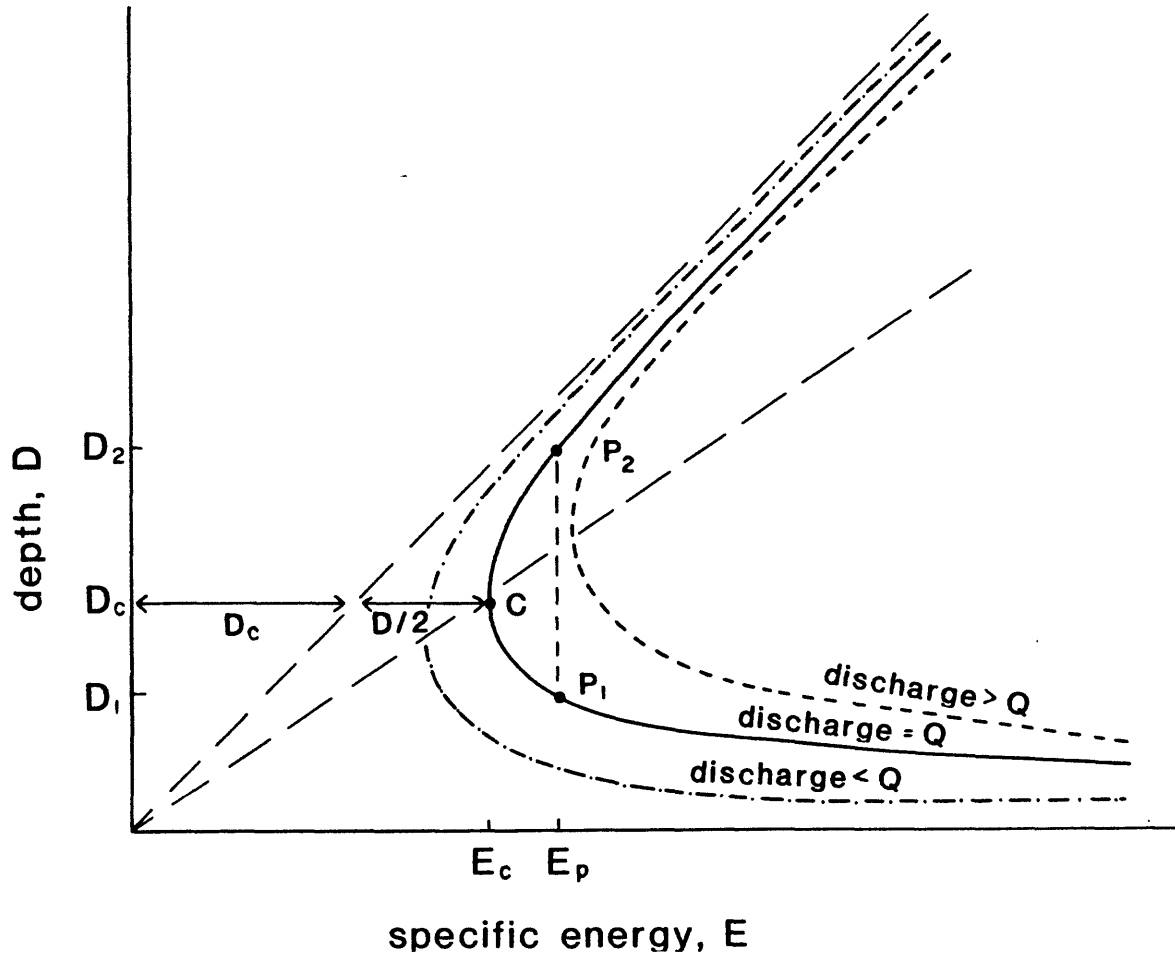


**Figure 16.** Specific-energy - depth relations (after Chow, 1959, p. 42). See text for notation. See Kleffer (1985) [attached as Appendix A] for a specific example of these relations at Crystal Rapids.

If the discharge changes, the specific energy changes, and the E-D relation is therefore a different curve--of similar shape, but offset from the original curve (see Figure 16). It can be shown that at the critical state, the velocity head is equal to half of the depth:

$$u_c^2/2g = D_c/2$$

and

$$D_c = 2H_c/3.$$

The existence or absence of waves in a flow field, and the form of the waves, depends on the state of the flow relative to the critical state, described by the Froude number,  $Fr=u/(gD)^{1/2}$ , discussed in the previous section. The Froude number is the ratio of mean flow velocity to critical velocity which, in turn, depends on water depth. The critical velocity is the velocity at which small disturbances in depth propagate through the fluid by gravity waves.

The Froude number is the ratio of inertial to gravitational forces in the flow. In subcritical flow,  $Fr < 1$ ; in critical flow,  $Fr = 1$ ; and in supercritical flow,  $Fr > 1$ . In subcritical flow the role of gravity forces is more pronounced than the role of inertial forces: the flow velocity is low (the words "tranquil" and "streaming" are used to describe subcritical flow in some hydraulics literature). In supercritical flow, on the other hand, inertial forces are dominant. The flow has high velocity (the words "rapid", "shooting", or "torrential" are used).

In subcritical flow, the velocity head is a small fraction of the specific energy and so the total energy is well-approximated by the potential energy. Changes in channel geometry cause changes in water velocity, and these changes may be large percentages of the velocity head, but they are still small when expressed as depth changes. Therefore, to a first approximation, the pressure is everywhere hydrostatic--even when the channel shape is changing. Large variations in total specific energy are caused by variations of depth.

In supercritical flow, in contrast, the kinetic energy is comparable to, and often exceeds, the potential energy. Large variations in specific head (total energy) are caused by changes in the velocity. Curvature in the boundaries may cause only small dynamic pressures (i.e., changes in velocity head), but large changes in depth or surface elevation.

In critical flow, the velocity and potential heads are similar in magnitude. Slight variations of head cause large variations in both kinetic and potential energy. Curvature in the channel boundaries changes the hydrostatic pressure distribution and, produces slight variations in total energy. In critical flow, the slight variations in total energy can cause large depth and velocity disturbances; these are often manifested by strong undulations in the flow.

The response of a flow field to an obstacle in the channel or to changes in channel alignment depends on whether the flow is subcritical or supercritical. Changes in channel configuration cause subcritical flow to accelerate or decelerate smoothly--there are no standing waves. Flow accelerates through constrictions and decelerates through expansions (Figure 17a).

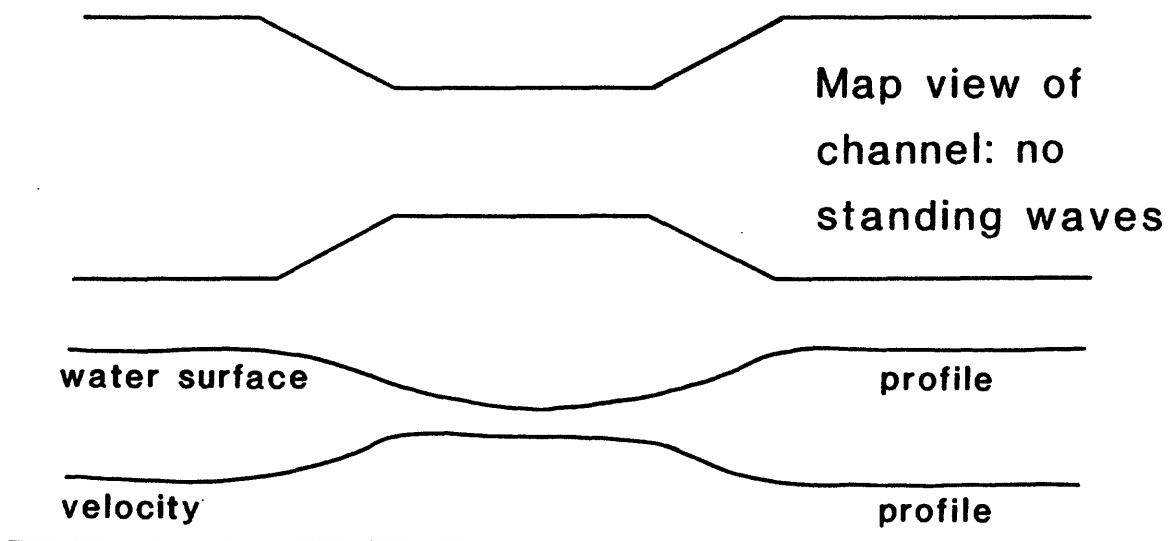
Supercritical flow responds to obstacles and channel alignments in a different way. Disturbances in water depth caused by obstacles in the channel cannot be propagated upstream because the flow velocity,  $u$ , exceeds the critical velocity,  $(gD)^{1/2}$ . Standing wave patterns appear in the flow downstream of the obstacles, and the fluid adjusts to the obstacles only as it passes through these standing waves (Figure 17b).

The terminology used for waves has evolved to depend on the channel geometry being described, and is therefore difficult to invoke for description of waves in rapids where channel geometry is not known. Some useful terms from hydraulics, however, are:

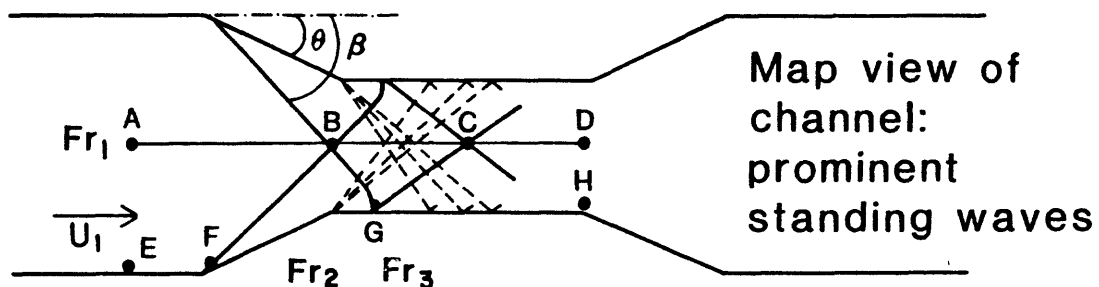
1. **Standing waves**: a general term for waves that maintain a fixed position with respect to the channel.
2. **Traveling waves**: waves that propagate up and down the channel as surges.
3. **Normal waves**: waves that stand perpendicular to the flow.
4. **Oblique waves**: waves that stand at an inclined angle to the flow.
5. **Positive waves**: waves that deflect the flow toward the line of disturbance and cause a rise in water surface elevation (also called compression waves). Such waves are associated with contractions.
6. **Negative waves**: waves that deflect the flow away from the wave front and lower the water surface elevation. Such waves are associated with expansions. Positive and negative waves may cancel when they intersect.
7. **Hydraulic jump**: a wave across which the flow changes from supercritical (fast and shallow) to subcritical (slow and deep).
8. **Hydraulic drop**: a transition region across which the flow changes from subcritical to critical.

Hydraulic drops and jumps can be caused by a variety of geometric changes in the channel. A few such changes are illustrated in the parts of Figure 18. For example, a change in bed slope can cause subcritical flow to become critical (Figure 18a). Obstacles on the bed change subcritical flow upstream of the obstacle to critical or supercritical flow over the obstacle (Figure 18b and c), with the formation of a standing wave ("repelled hydraulic jump") whose position relative to the

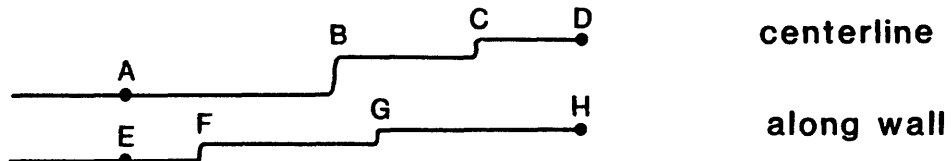
## (a) Subcritical conditions:



## (b) Supercritical conditions:



## (c) Water surface: centerline



## (d) Velocity: centerline

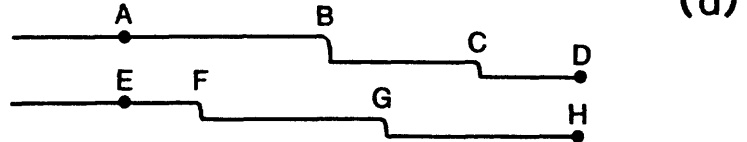


**Figure 17.** Comparison of the flow fields in subcritical and supercritical flow. (a) (top) Schematic map view of subcritical flow through a constriction; (bottom) water surface and velocity profile. (b) Schematic map view of supercritical flow through the same constriction. (c) water surface, and (d) velocity profiles in the channel along the paths A-B-C-D, and E-F-G-H. No energy changes associated with the constriction, expansion, or bed slope are considered. The entrance and exits of constrictions, as well as channel roughness, cause drops in the total energy of the flow; bed slope can, in contrast, increase the total energy. These energy changes affect the flow depth and velocity so that profiles in a real flow are not as simple as shown here.

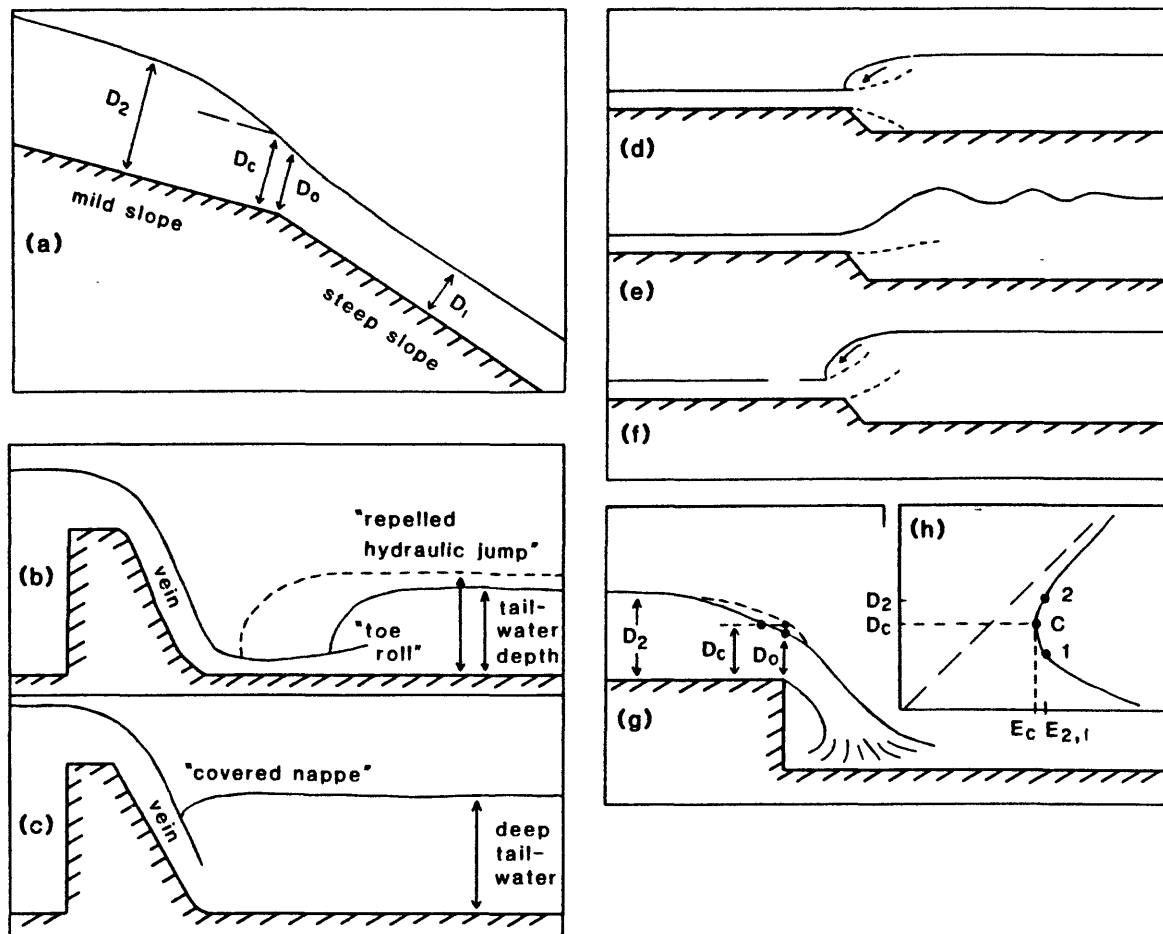


Figure 18. Illustration of some hydraulic features common to flumes and rivers.

(a) A hydraulic drop caused by a steepening of the channel slope (after Bakhmeteff, 1932, p. 8). The flow changes from subcritical conditions with depth  $D_2$ , to supercritical conditions with depth  $D_1$ , and passes through critical conditions,  $D_0$ , at approximately the inflection in slope. For the subtle details of this transition and an explanation of the differences between states c and o, see part (g). (b) A hydraulic jump ("toe roll") below a weir. In this case, the tailwater is not deep. The position of the hydraulic jump depends on the depth of the tailwater, being furthest repelled in shallower tailwater (solid curve) and moving closer to the vein as the tailwater depth increases (dashed line). (c) When the tailwater is deep, as illustrated here, the falling vein is partially covered by the hydraulic jump. (d), (e), and (f) Alternate forms of a hydraulic drop (from Ippen, 1951, p. 360) formed at an abrupt drop. Notice the different forms of the jet in (d) and (f). If the downstream depth is less than that required to produce the standing wave in (e), the pressure on the face of the wave is determined by the upstream depth, and a wave of type (d) is formed. For greater depths, the downstream depth governs the wave type. The conditions for formation of a wave of type (e) must be determined by experiment. (g) A free overfall, a special case of the hydraulic drop (Chow, 1959, p. 44). The solid line shows the theoretical water surface. Water flowing at depth  $D_2$  with energy  $E_2$  decreases in depth as the drop is approached and as energy  $D_E$  is dissipated. Ideally, the critical depth  $D_c$  would be reached at the brink, as shown by the solid curve; the water should not get shallower than this because a further decrease in depth would result in an increase in specific energy, which is impossible unless external energy is supplied. In rivers, however, the assumptions of parallel, gradually varied flow in the simple energy analysis applied here do not hold, and it is found that the calculated depth  $D_c$  occurs upstream from the brink. The depth  $D_0$  at the brink is the true depth of minimum energy, and is typically about  $1/1.4 D_c$ . The dashed line shows the actual water surface under these conditions.

object depends on the downstream hydraulic conditions (the tailwater depth), and whose wave structure also depends on these parameters (Figure 18d,e,f). In many rapids obstacles can be so large that water flowing over them is above the base level of the flow. In this situation air is available as the water descends from the top of the obstacle back into the flow. The air becomes entrained into the flow (Figure 18d) or, in some circumstances, the water cavitates.

Of these geometric possibilities, the three most important for analyses of the rapids are<sup>7</sup>:

1. changing channel gradient (Figure 18a);
2. changing channel cross section (Figure 17b);
3. submerged obstacles (Figure 18 and 21).

The next sections interpret the major features of rapids in terms of the hydraulic concepts presented here.

#### 6. Pools and backwaters

For flow with a constant specific head (a restriction that requires balance of the bed slope by frictional energy dissipation; see Kieffer, 1985, for details), the variation in depth is controlled solely by the specific discharge (discharge per unit area A of the channel):

$$q = Q/w.$$

For a rectangular channel, the area A is equal to the width w times the depth D. The width of the channel upstream of a rapid in the pool will be denoted by  $w_1$ , and the width of the channel at its narrowest point will be denoted by  $w_2$ .

For a given head of the flow, denoted  $H_r$ , where r stands for "reservoir", the equations above show that the specific discharge, q, must be less than a limit,  $q_{\max}$ , given by:

$$[q_{\max}^2/g] = (2/3) H_r = D_c = u_c^2/g$$

If  $Q/w_2$  is greater than  $q_{\max}$ , the ambient river head,  $H_r$ , is not sufficient to allow all of the discharge through the constricted part of the rapid. Then  $H_r$  must be increased by the formation of a backwater to raise the energy to a new head (the backwater head,  $H_b$ ):

---

<sup>7</sup> Leopold (1969) recognized four types of waves in the rapids that roughly correspond to these categories: (a) waves below large rocks and outcrops; (b) deep-water waves caused by convergences; (c) waves and riffles in shallow water (including gravel bars and shallow overbank flow across low-angle debris fans); and, (d) waves in deep, but high-velocity, water.

$$H_b = (3/2)[(Q/w_2)^2/g]^{1/3}$$

The equation above for  $q_{max}$  then describes the flow if  $H_r$  is simply replaced by  $H_b$ .

The only hydraulic analysis done to date for a pool-rapid pair on the Colorado River is that of Kieffer (1985) for Crystal Rapids. The observations made on the 11 other rapids during the course of the field studies reported here suggest that a generalization of the conclusions from Crystal Rapids to other rapids in the Grand Canyon is warranted although a hydraulic model that eliminates some of the simplifying assumptions such as constant specific head and gradually-varied flow is needed. The reader is referred to Kieffer (1985, Appendix A) for details of the calculations.

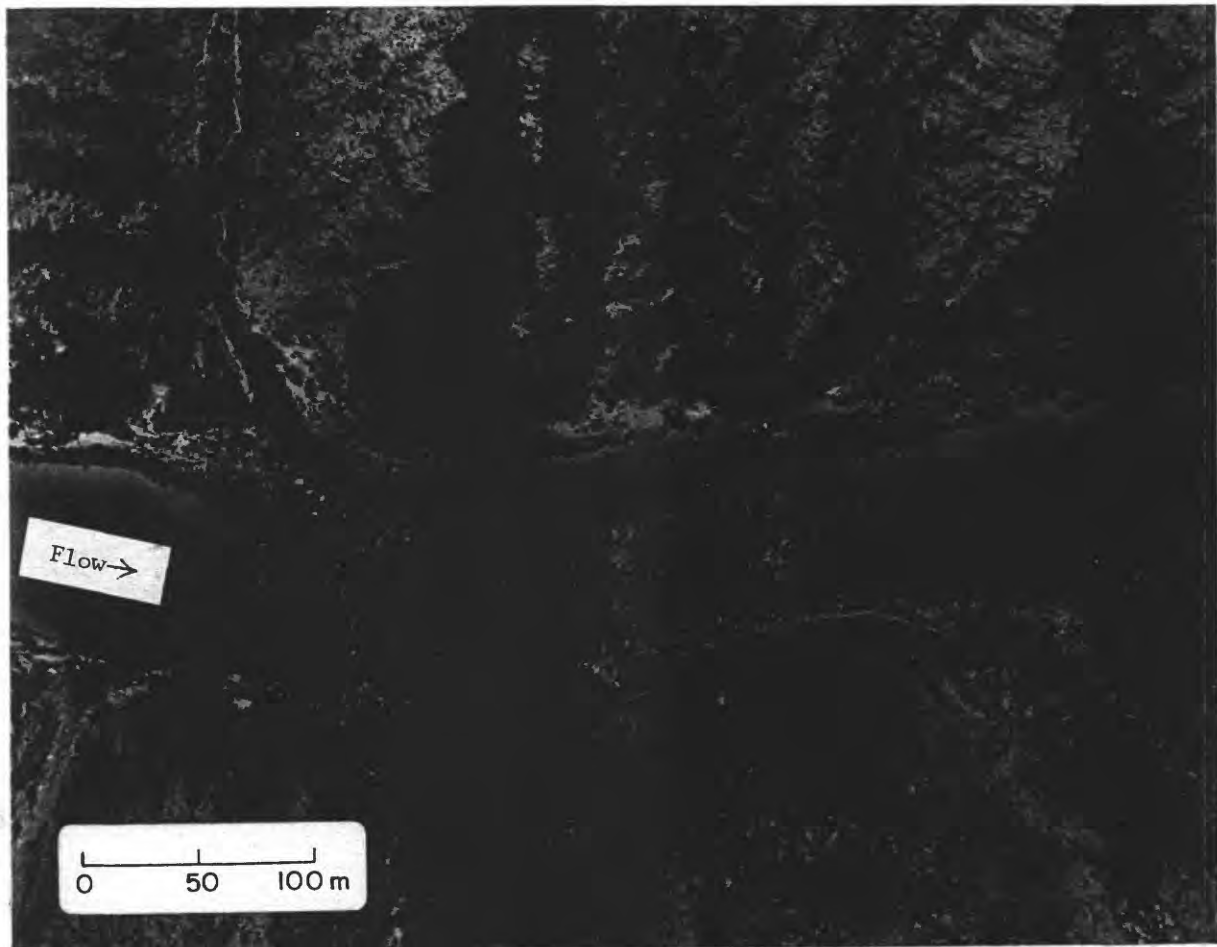
In a channel of the general shape of the Colorado River channel at the constriction at Crystal Rapids, flow may be entirely subcritical, or entirely supercritical, or it may change from one state to the other. The specific discharge,  $q$ , will be the greatest at the constriction. If the specific discharge there is less than  $q_{max}$  for the available specific head, and if the flow is subcritical in the pool above the rapid and in the pool below it, critical conditions will not occur in the constriction. The subcritical flow of the river above the rapid accelerates to higher velocities in the constriction, and then decelerates back to greater depths and slower velocities in the diverging part of the channel (Figure 17a). Under such conditions, the "pool" upstream of the rapid is simply a region of lower channel gradient and slower flow than in the rapid.

On the other hand, if  $Q/w_2$  is greater than  $q_{max}$  allowed by the available head,  $H_r$ , water will pond behind the constriction until a backwater is formed that just allows  $Q/w_2$  to equal  $q_{max}$  for the backwater head,  $H_b$ . The backwater is essentially stagnant; the flow accelerates in the converging part of the channel to critical conditions in the constriction. The relative energies of the main channel flow upstream and downstream of the constriction determine whether the flow will return along a subcritical or supercritical path. In the case where a backwater has formed so that the energy of the river downstream,  $H_r$ , is less than the energy of the backwater,  $H_b$ , the flow will expand supercritically into the divergence. The return to ambient head is accomplished through discontinuous transitions--the hydraulic jumps which occur downstream in the rapid. Under such conditions the pool upstream of the rapid is a hydraulic backwater.

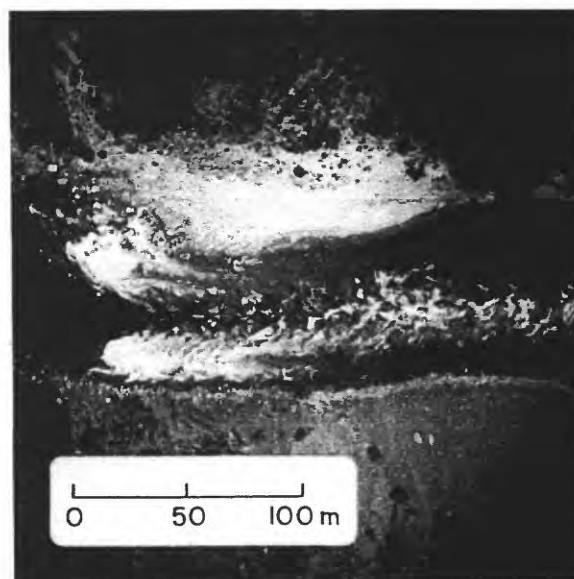
The pools upstream of rapids are therefore interpreted as backwaters caused by the constrictions at the rapids. Only for very low discharges (less than 10,000 cfs), does the normal river energy become adequate to allow subcritical flow through the constrictions. Even at these low discharges where the converging-diverging geometry itself does not force supercritical conditions, the drop in elevation of the channel bottom, and local obstacles in the path of the flow, cause supercritical conditions. Therefore, there are standing waves in the channel at nearly all discharges (e.g., see the air photos, such as in Figures 2a, 4, 5, 19a, and 27a). In these, note that the tongue (an indication of

**Figure 19.** (a) Hermit Rapids, showing the tongue and lateral waves at 5,000 cfs. Photograph by U.S. Bureau of Reclamation, 1984. (b) A view of part of the same rapid at the same scale showing these features at 30,000 cfs. Note differences in tongue lengths, angle of lateral waves to shore, and nonbreaking rollers on the tongue. Photograph (b) by National Park Service, 1986.

19(a)



19(b)



supercritical flow) is very weak, and that the major standing waves are associated with obstacles in the bed.

### 7. The tongue and oblique lateral waves.

Smooth water with nonbreaking waves extends furthest from a pool into a rapid along the "tongue"--the chute of water bounded by oblique lateral waves (Figure 1b). The length of the tongue and the angle of the oblique waves change with increasing discharge, as expected in supercritical flow in which the wave behavior is influenced by depth and flow velocity, which, in turn, depend on discharge. I propose that the flow is supercritical in the region bounded by the top of the tongue and the oblique lateral waves. From the bottom of the tongue to the beginning of the tailwaves the flow appears to be a complex mixture of regions of different Froude number separated by hydraulic jumps--some regions having  $Fr > 1$  and some having  $Fr < 1$ .

The tongue is the region where flow passes from subcritical conditions in the backwater (with Froude numbers less than 0.1 as shown in cross sections V-V' and W-W' of Figure 11) to weakly supercritical conditions. From the tongue, the flow passes into "fully supercritical" conditions in the region of breaking waves in the rapid (with Froude numbers on the order of 2, as shown in cross section Y-Y' of Figure 11). Here I use the term "fully supercritical" to mean  $Fr > 1.7$ , where breaking waves become stable in hydraulic jumps (Figure 20). Changes in wave structure between subcritical flow (with no standing waves) and "fully supercritical flow" with noticeable standing waves occur over a range of Froude numbers often cited as between 1 and 1.7 (Figure 20)<sup>8</sup>. It is important to note here that Froude numbers greater than about 2.0 are required for the formation of strong hydraulic jumps. At Froude numbers between about 2.5 and 4.5 the jump tends to be oscillatory, because the entering supercritical water "flaps" in a vertical plane (Figure 20c). Froude numbers of about 2-3 are calculated

---

<sup>8</sup> There is a well-known analogy between shallow-water flow and flow of a gas through nozzles. In this analogy, sub-critical shallow-water flow is analogous to subsonic flow; supercritical flow is analogous to supersonic flow; and critical conditions are analogous to transonic conditions. The critical velocity of shallow-water flow is analogous to the sound speed of the gas. An important aspect to be noted here is that in supersonic gas flow through a converging-diverging nozzle (the so-called Laval nozzle), flow in the diverging section, and in the gas jet emerging into the atmosphere outside the nozzle, is a complex mixture of subsonic and supersonic flow regions, separated by shock waves which locally decelerate the flow from supersonic to subsonic conditions. Because of the non-linearity of flow fields in which the driving pressure is much higher than the reservoir pressure, there is a complex mixture of subsonic and supersonic flow fields in a zone that is typically many nozzle diameters in extent. Likewise, in shallow-water flow through a constriction, local transitions back and forth between supercritical and subcritical flow across hydraulic jumps cause complex flow fields for many channel widths downstream of a constriction. The excess energy of the backwater is dissipated across the complex system of oblique and normal hydraulic jumps that occur within this region (as well as by boundary layer and internal fluid dissipation).

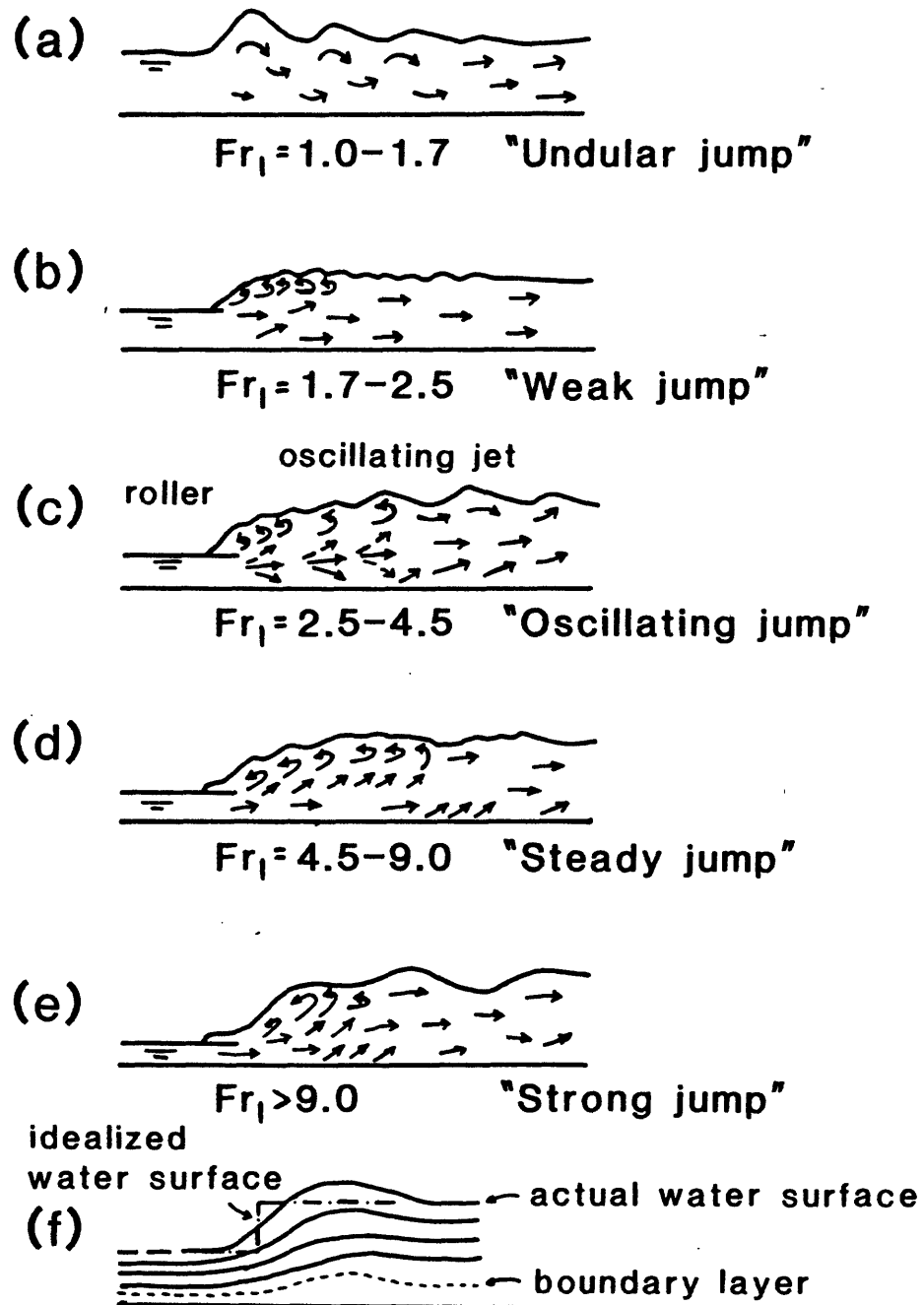


Figure 20. (a) - (e). Idealized cross-sections of hydraulic jumps with the entering flow at different Froude numbers as shown. From Chow, 1959, p. 395. (f) Schematic cross-section of idealized and actual hydraulic jumps, after Ippen (1951) p. 339.

for places in the rapids, and it may be the instability of the jet of water that enters the hydraulic jumps that gives rise to the pulsating phenomena reported by boatmen to be important in determining the success of their navigation through the rapids.

Several pieces of data obtained in this study suggest that this interpretation of the tongue is plausible: (1) the relative depths of the backwaters and tongues; (2) Froude numbers calculated from measured velocities on the tongue; (3) the form of the waves on the tongue; and (4) the angle of the oblique waves from the shore and the change of this angle with changing discharge.

First, recall that the critical depth (where  $Fr=1$ ) is related to the backwater depth by the simple relation

$$D_c = 2/3H$$

The fathometer data show that the channel bottom begins to rise under the water surface upstream of the tongue. As summarized in Figure 14, to first order, the oblique lateral waves that bound the tongue detach from the shore when the water depth is approximately 2/3 of the backwater depth [e.g., under the conditions shown in Figure 14 a typical backwater depth is 30 ft (9 m), and a typical depth at the top of the tongue is 20 ft (6 m)].

On the tongue, the measured Froude numbers are, to within the uncertainty of the field measurements, unity. For example, as shown in cross section X-X' of Figure 11, at House Rock Rapids,  $Fr=1.1$  on the tongue.

The nonbreaking rollers that occur on the tongue are plausibly interpreted as an undular jump, the type of hydraulic jump that forms when the Froude number is just slightly greater than 1 (Figure 20). The oblique waves (laterals) that bound the tongue are interpreted as oblique hydraulic jumps.

The oblique waves bounding the tongue have the following characteristics: (1) They emerge from the shoreline approximately at the beginning of the lateral contraction (Figure 2b, for example), but well downstream of the point where the channel becomes shallower due to the underwater extension of the debris fans in the upstream direction (Figure 14). (2) They emerge from the shore at an angle approaching  $90^\circ$ —that is, nearly perpendicular to the current—and then curve downstream as they project into the flow. Their amplitude increases in the downstream direction.

The angle,  $\beta$ , that waves in supercritical flow make with the downstream flow direction is approximately

$$\beta \sim \sin^{-1} [(gD)^{1/2}/u] \sim \sin^{-1} (1/Fr) \quad (\beta \text{ is defined in Figure 17.})$$

At  $Fr=1$ , the waves (of infinitesimal amplitude) would stand perpendicular to the flow ( $\beta=90^\circ$ ). With increasing Froude number, the waves become stronger and more aligned with the flow direction. For

example, at  $Fr=1.1$ ,  $\beta=65^\circ$ ; at  $Fr=1.5$ ,  $\beta=42^\circ$ ; and at  $Fr=1.7$ ,  $\beta=36^\circ$ . At Crystal Rapids,  $\beta$  changes from approximately  $40^\circ$  at 5,000 cfs (in 1984 with a channel geometry that postdates the 1983 erosional changes discussed below), to  $18^\circ$  at 30,000 cfs (also in 1984), to  $10^\circ$  at 92,000 cfs (at the peak discharges of 1983). The Froude numbers implied by these angles are 1.5 at 5,000 cfs, 3.9 at 30,000 cfs, and 5.8 at 92,000 cfs. These values indicate weakly supercritical flow at 5,000 cfs, and more strongly supercritical flow at the higher discharges, and are consistent with the fact that strong waves are observed in Crystal Rapids at the higher discharges.

At House Rock Rapids, at 5000 cfs (Figure 10), the wave angle becomes about  $35^\circ$ , indicating a Froude number of about 1.7. As shown in Figures 10a and 10b, the wave angle at House Rock decreases as the discharge changes from 5,000 to 30,000 cfs, indicating that the flow is becoming less supercritical with increasing discharge. This is consistent with the fact that at discharges above 30,000 cfs there are almost no waves in House Rock Rapids. The hydraulic geometry of the channel changes with discharge in a way that permits the flow to become subcritical at discharges greater than about 30,000 cfs.

The four types of observations cited here (the relative depths of the backwater and tongue; Froude numbers calculated from measured velocities and discharges; the undular wave forms; and the angles of the oblique waves) suggest that the boundaries of the tongue are oblique hydraulic jumps, and that the nonbreaking rollers on the tongue can be interpreted as an undular jump.

#### 8. The Breaking Waves Below the Tongue

Between the downstream end of the tongue and the beginning of the tailwaves at the end of the rapid, there is typically a region (roughly 100 m in length) of strongly breaking waves. The breaking waves are within the most highly constricted part of the channel (e.g., note their position in Figure 5 of Deubendorff Rapids at 5,000 cfs discharge; in Figure 10a and 10b of House Rock Rapids at 5,000 and 30,000 cfs discharges; and in Figure 12 of Horn Rapids at 17,000 cfs discharge)<sup>9</sup>.

---

<sup>9</sup> Note here the distinction between the breaking waves that occur immediately downstream of the tongue of the rapids, and the "tailwaves" that occur in the diverging part of the channel in the "runout" of the rapid into the tailwater at ambient downstream conditions. The transition between the two types of waves can be gradual--for example, in a weakly supercritical rapid at low discharge--but may sometimes be dramatic if the region of critical and supercritical flow in the top part of the rapid is separated from the region of subcritical flow at the lower end of the rapid by a strong hydraulic jump. The detailed configuration of oblique and normal hydraulic jumps appears to have not been mapped out in detail but, by analogy to gas dynamics flow fields, it seems likely that a strong hydraulic jump will not stand normal to the flow until the Froude number exceeds about 2. At lower Froude numbers, the transition from supercritical flow to subcritical flow will take place through a series of crossing (oblique) hydraulic jumps, of the kind seen in most rapids.

These waves are here interpreted as crossing lateral waves reflected from the sides of the channel (refer to Figure 17b) and hydraulic jumps required to match the supercritical flow to the downstream tailwater conditions. Both positive and negative waves can be generated in a rapid, depending on the details of the convergence, divergence, and river curvature. The waves have their greatest amplitude where positive hydraulic jumps intersect, and "haystacks" mark these points. Boulders commonly, but not always, are found in association with the haystacks.

Breaking waves indicate fairly high Froude numbers (refer to Figure 20). River runners have often noticed surging and pulsing in these waves. Strong surges may indicate the oscillating jet conditions shown in Figure 20c, but no data are directly available to support this speculation.

The Colorado River rarely displays hydraulic jumps of textbook simplicity. A primary reason for the complexity of the wave patterns is the complexity of the channel geometry that disturbs regular wave patterns. Second, where large boulders are associated with the waves they change the local energy of the flow and disturb the hydraulic patterns. Finally, at individual hydraulic jumps two other effects become important: vertical accelerations of the fluid and boundary layer irregularities (Ippen and Dawson, 1949, p. 339).

Basic, two-dimensional theory predicts hydraulic jumps with vertical fronts (i.e., negligible thickness of transition), and constant depths in front of and behind the jumps (as shown in Figure 20f, dashed line). Typically the observed waves have either gently sloping fronts (as in the case of a weak jump, Figure 20a), or fronts that overturn with breaking of the wave crest and formation of surface rollers. The steep fronts cause high vertical accelerations, not accounted for in the theory that assumes hydrostatic pressure distribution in calculation of the height of the wave front. Thus, actual wave fronts tend to be higher than predicted by simple theory, and there is a finite length of transition between sub- and super-critical flow. This length is the distance for the streamlines to become parallel to the channel bottom. The boundary layer of the flow also thickens under the wave front because of the low momentum and adverse pressure gradient there. The thickened boundary layer mimics an obstacle on the channel bottom. The magnitude of this effect is not known. Photographs of a spectacular hydraulic jump of complex geometry in Crystal Rapids in 1983 can be found in Kieffer (1985).

An important aspect of the strongly breaking waves is their foaming and entrainment of air. This plays a significant role in energy dissipation in the wave, e.g., can account for several tens of percent to nearly all of the required energy loss in the jump (Lighthill, 1978).

## 9. Tailwaves and Eddies

The above discussion demonstrates that flow is generally supercritical in the narrowest part of a rapid. The waves (oblique and normal hydraulic jumps) extending from the oblique waves at the top of the rapid through the breaking waves below the tongue dissipate energy from the flow and bring it back toward the subcritical tailwater conditions downstream. Under certain conditions, e.g., as at Crystal Rapids in 1983, and perhaps as at House Rock Rapids at low discharges, a rather large hydraulic jump approximately normal to the flow direction accomplishes much of the matching to tailwater conditions. The data on House Rock Rapids (Figures 10d and 11) suggest that the jet that emerges below the constriction is approximately critical,  $Fr \sim 1$ .

Channel expansions below a rapid are typically very sudden, and the flow streamlines generally do not follow the channel boundary curvatures. There is thus a separation surface between the "jet" that emerges from the constricted part of a rapid and recirculating flow in an eddy (a schematic illustration of the jet structure is shown in Figure 21). The relations between the jet, eddy, and beaches are documented by Schmidt and Graf (GCES, 1987). The separation surfaces between the flow and the eddies act as solid boundaries which can further constrict the emerging jet, in spite of the dramatic apparent enlargement of the channel. The strong "eddy fence" between the jet and the Slate Creek eddy at Crystal Rapids (Figure 22) may be an illustration of an instance where flow is reflected off of the boundary between a jet and an eddy; this eddy fence reached 3-4 m in height during the 92,000 cfs discharges.

The shape of the jet in the tailwater cannot be accurately predicted with available data, but laboratory data (Rouse, Bhoota, and Hsu, 1951) suggest that the jet will maintain constant diameter until it is several constriction diameters downstream (e.g., for a Froude number of 2, an ideal laboratory jet would maintain constant diameter for roughly 3 constriction diameters downstream). This is roughly the length of the region in which tailwaves are observed downstream of constrictions in rapids. In this region, the jet velocity appears to stay constant (Figures 10d, 12, and 13).

The length of the jet and its orientation change with discharge. This is shown dramatically at 24.5-Mile Rapids (Figure 23), as well as at Granite Rapids (Figures 2a and 2b).

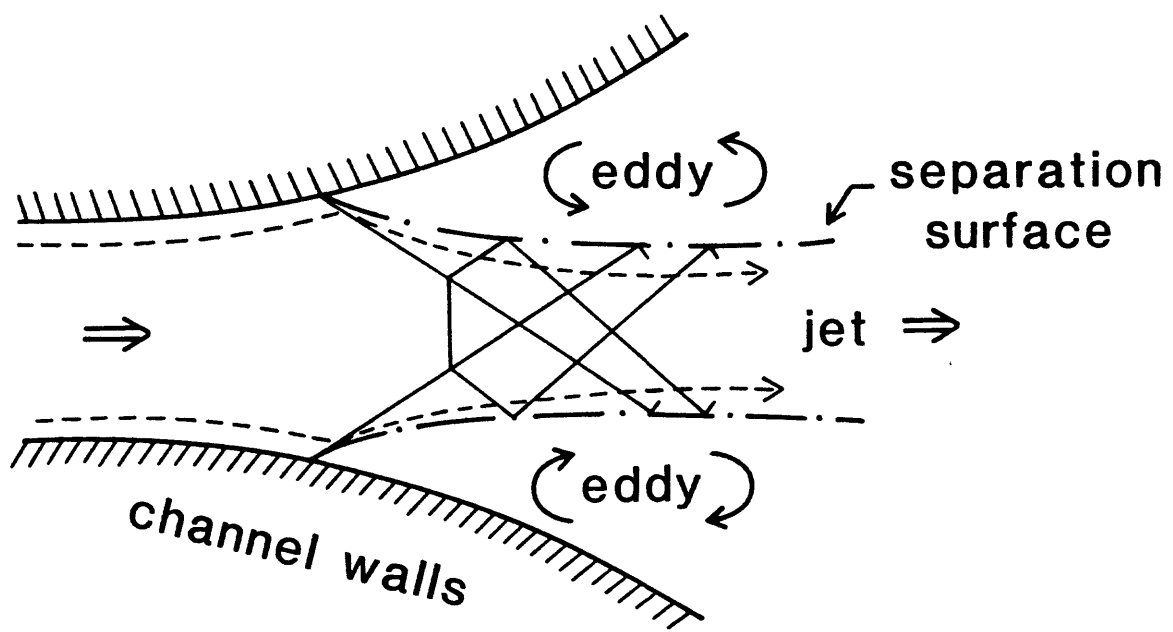
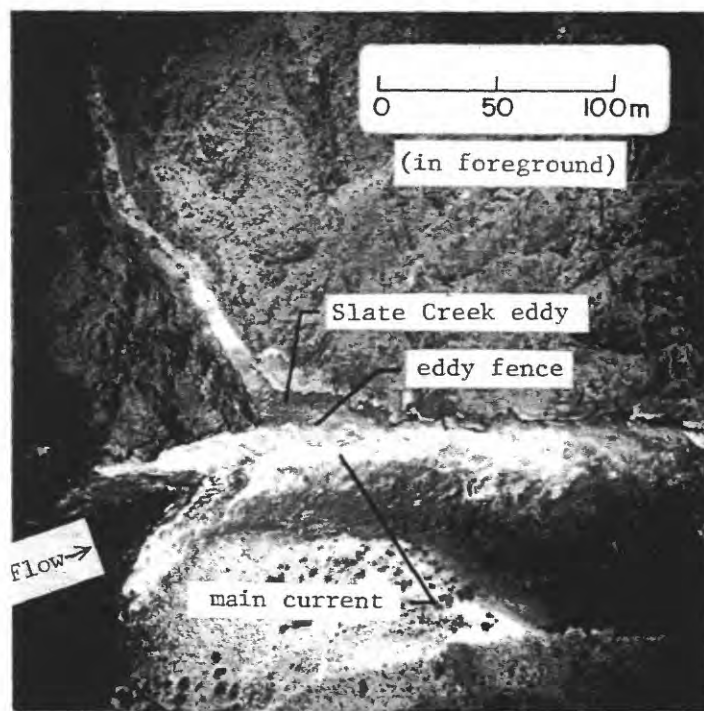


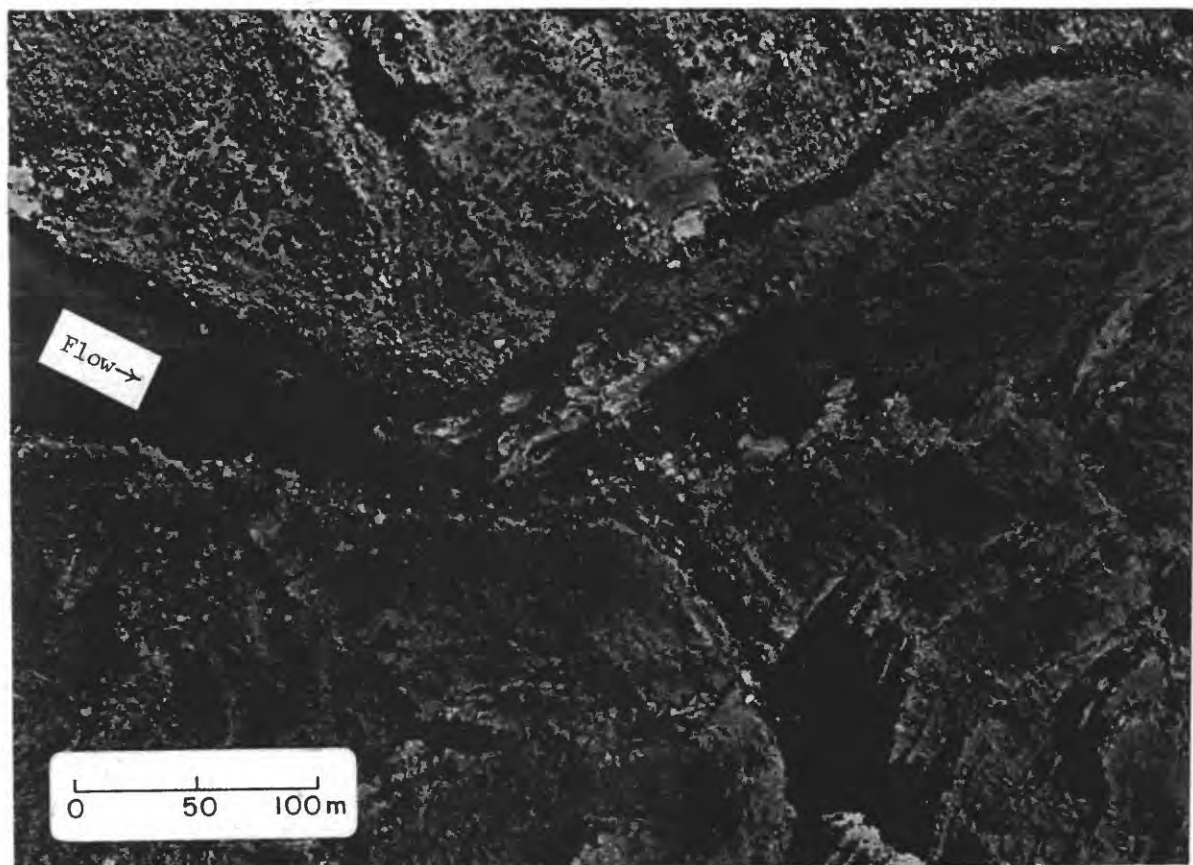
Figure 21. Illustration of the structure of a supercritical jet emerging from a constriction. From Chow (1959, p. 471; originally from Homma and Shima, 1952).

Although much of the energy that must be dissipated in the rapid (the excess backwater head, and the vertical elevation drop) is dissipated by the waves in the rapid and the bottom roughness of the channel, the fact that the flow still has a high velocity at the bottom of the rapid indicates that not all of the excess energy has been dissipated. Additional dissipation occurs through mixing between the relatively high-velocity water of the jet and the nearly stagnant water of the eddies that bound it in the tailwater. The motion of the jet induces circulation in the eddies, and the two flows (jet and eddy) mix in a mixing zone that expands around the separation line (Landau and Lifschitz, 1959, p. 131). For a very simplified geometry, the turbulent mixing zone looks as shown in Figure 24. The angles between the boundaries of the turbulent region,  $\alpha_1$  and  $\alpha_2$ , are different in the jet and in the eddy. These angles depend only on the geometry of the channel divergence--not on flow velocity--and must be measured experimentally. For expansion around a right angle corner, for example,  $\alpha_1=5^\circ$  and  $\alpha_2=10^\circ$  (Landau and Lifschitz, 1959, p. 132). The relative velocities of the jet and circulation flow (along A0 vs. B0 in Figure 24) also depend on geometry. For flow around a right angle the jet velocity is approximately 30 times the entrance velocity of the eddy flow. In the GCES studies, velocities in the jet are typically 4-5 m/s, and eddy circulation velocities are on the order of 0.5 to 1 m/s (Graf, unpublished data, 1986), suggesting that the complex geometry of the channel in the expansion is strongly influencing the velocity ratio between the main channel and the eddy.



**Figure 22.** Crystal Rapids at 30,000 cfs, showing the strong eddy fence that develops between the Slate Creek eddy and the main current (toward the top of the photograph). Note also gentler eddy downstream of the debris fan. Photograph by National Park Service, 1986.

23(a)



23(b)

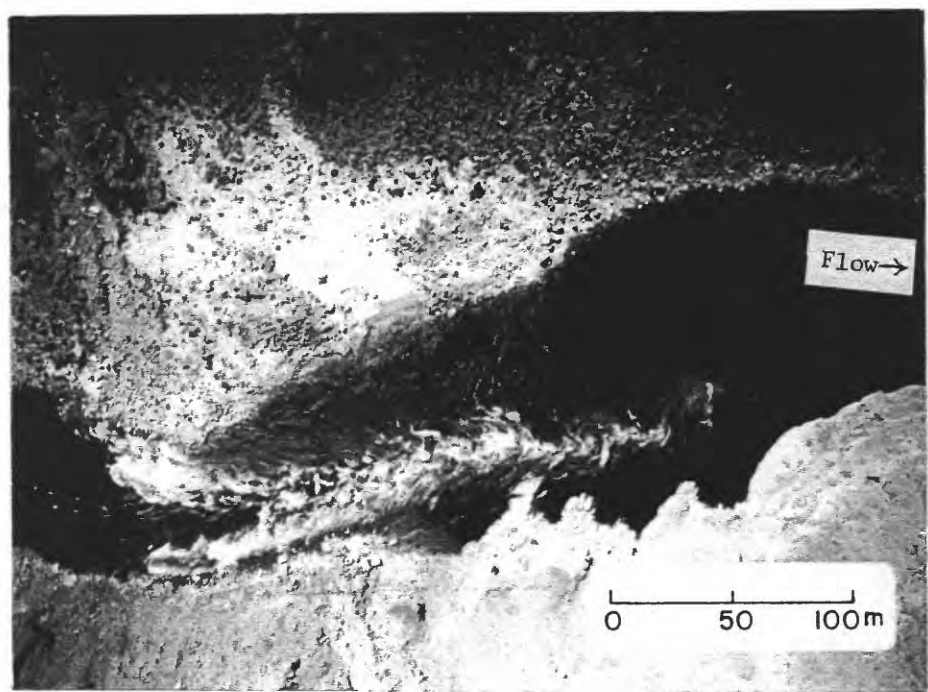


**Figure 23.** The tailwaves at 24.5-Mile Rapids at discharges of (a) 5,000 cfs, and (b) 30,000 cfs. Note the dramatic change in the orientation of the tail jet. Photograph (a) by U.S. Bureau of Reclamation, 1984; (b) by National Park Service, 1986.

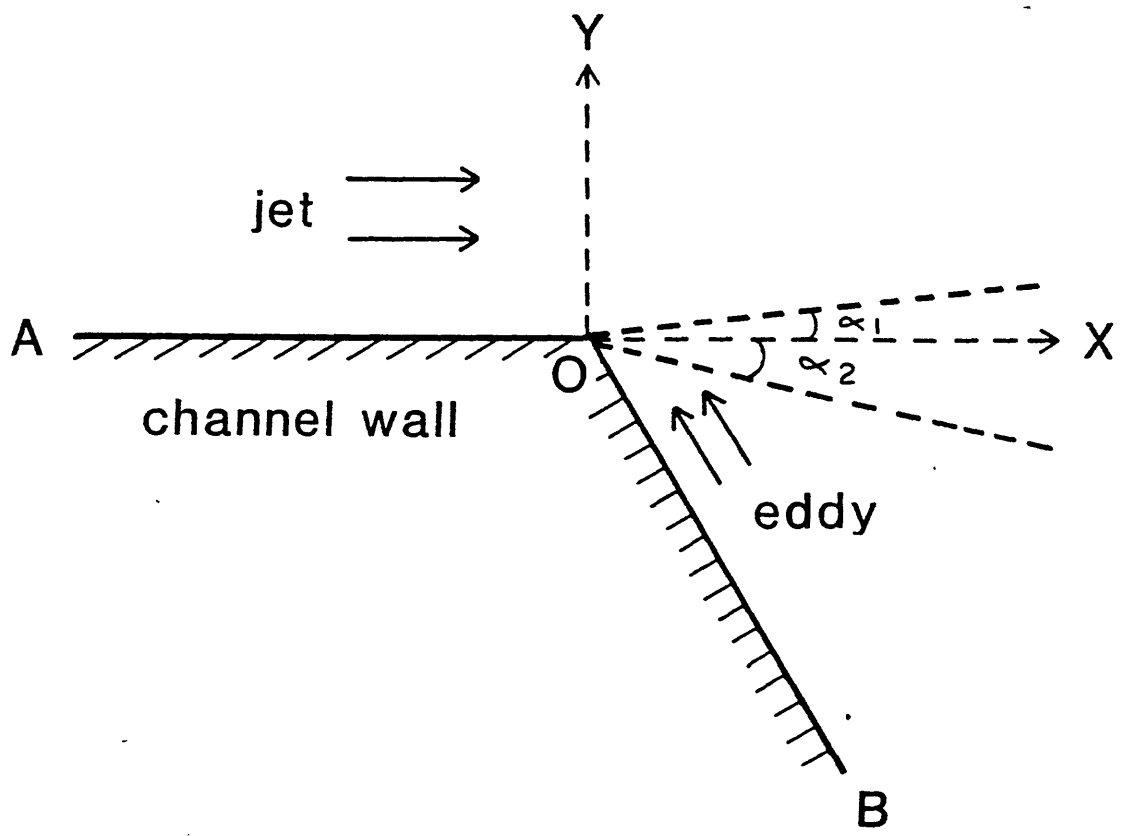


**Figure 24.** Mixing of jet and eddy water along the separation zone between these two regions. From Landau and Lifschitz, 1959, p. 131.

## 10. The Minor Effects—River Curvature

River curvature affects supercritical flow in much the same way that contraction and expansion of the channel affect the flow: it induces standing cross-wave patterns. Additionally, the curvature induces superelevation of the flow on the outside of the bend. An excellent discussion of these effects can be found in Chow (1959, p. 448).

The curvature influences measured velocities at House Rock Rapids. In the fastest part of the rapid, the flow velocities are systematically highest on the outside of the bend (Figure 10d).

The two walls of a curving channel do not act equally on all streamlines of the flow field. The outer wall turns in toward the flow, producing oblique hydraulic jumps (positive waves). The inner wall, turning away from the flow produces oblique expansion waves (which are not jumps, however). The disturbance lines thus produced by both walls reflect back and forth across the flow for a considerable distance downstream, causing a pattern of cross-waves (Figure 25). One of the most strongly curved rapids on the river is 209-Mile Rapids. The tongue of this rapid shows a unique set of cross-waves of several meters wavelength (Figure 26a). It is intriguing to speculate that these waves arise from the curvature of the river. The wavelength of cross-waves caused by curvature can be estimated to be  $\lambda=2w/\tan\beta$ , where  $w$  is the width of the channel at the constriction, and  $\beta$  is the wave angle related to Froude number defined above. Note that if the Froude number is near 1,  $\tan\beta$  varies dramatically (from  $\infty$  toward lower values) and there is therefore very large uncertainty in this calculation. Assuming that  $w=5$  m and that  $Fr=1.1$  (so that  $\tan\beta=2.2$ ), the wavelength for waves arising from river curvature is about 4.5 m (note that it is independent of the radius of curvature). The wave amplitude is given by  $a=u^2w/2r_cg$ , and does depend on river curvature,  $r_c$ . For a velocity of 3 m/s, and a radius of curvature of 25 m (estimated from Figure 26b), the peak amplitude of waves caused by river curvature is about 0.1 m (i.e., a few inches). The calculated and observe wavelengths and amplitudes agree within an order of magnitude and, while this is not a compelling argument for the interpretation of the cross-waves at 209-Mile Rapids as arising from river curvature, but suggests that the idea is plausible.

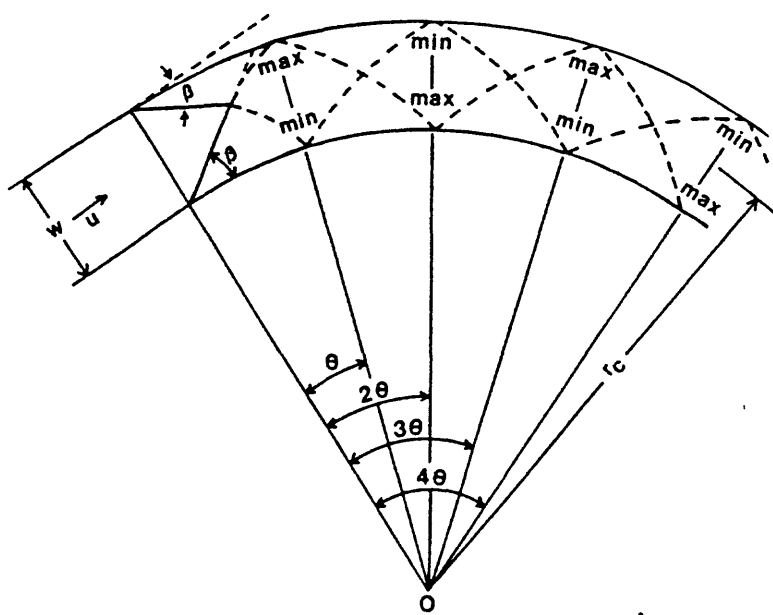
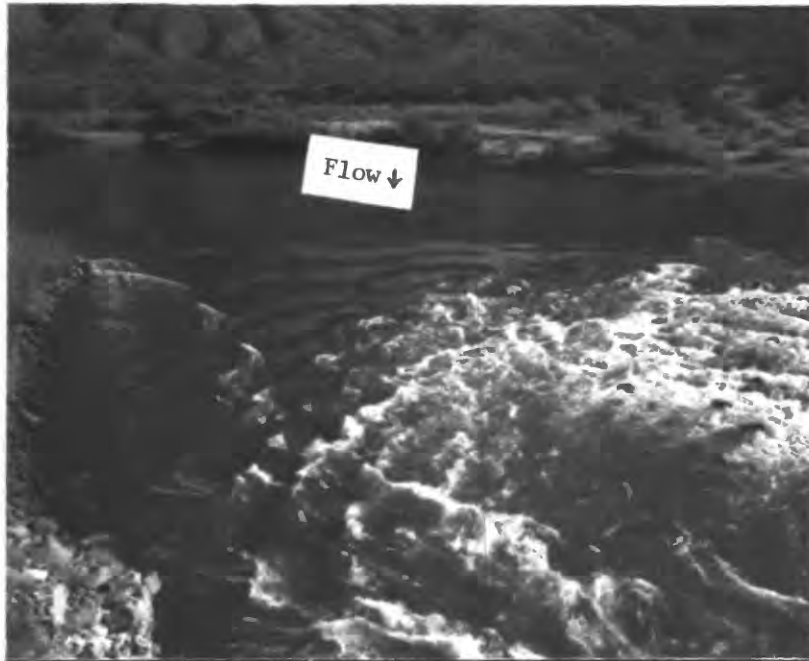


**Figure 25.** Cross-waves formed by curvature of a channel. From Chow (1959). The channel width is  $w$ ; the entering flow velocity is  $u$ . The wave angle is determined by the Froude number, as discussed in the text. The river curvature is approximated by a circular arc of radius,  $r_c$ . Cross-waves of maximum and minimum amplitude, max and min, occur as shown. See text for discussion and symbol notation.

26(a)



26(b)

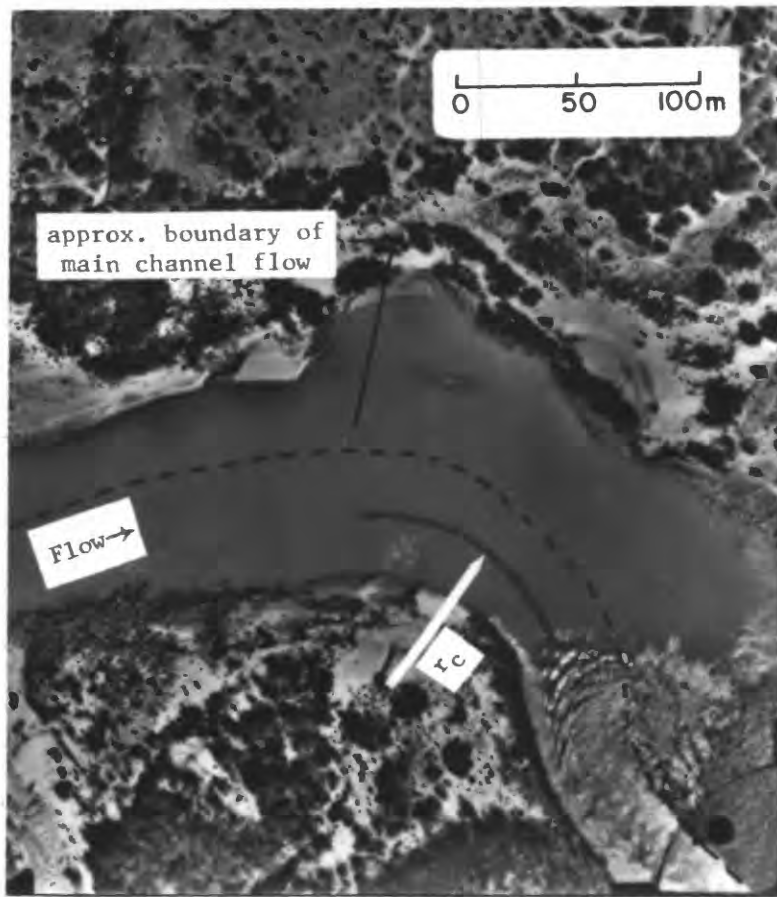


**Figure 26.** (a) Photograph of the tongue of 209-Mile Rapids, showing prominent cross-wave structure. The spacing of the cross waves is on the order of a few meters. This structure is not found on the tongues of other rapids, and may be a cross-wave structure due to the strong curvature of the river at 209-Mile Rapids. Photograph taken from shore by Jennifer Whipple. (b) Air photo showing the approximate boundary of deep flow that bends around the corner at 209-Mile Rapids. An estimated radius of curvature to the center of the curved flow (25 m) is indicated. The main channel flow in this region is about 5 m width. Photograph by U.S. Bureau of Reclamation, 1984 at discharge 5,000 cfs. The scale of the photograph is 1:3000.

## 11. Large Rocks in the Rapids

Most rapids have at least a few large boulders that present individual, sometimes formidable, obstacles. Some rapids are notoriously rocky at low discharges (Hance, Horn Creek, Deubendorff). The response of the river to an obstacle depends on whether the obstacle is in a subcritical flow region or a supercritical flow region (Figure 27).

If the flow is subcritical as it approaches the obstacle, and if it remains subcritical while flowing over the obstacle (that is, if the flow is deep), the upstream flow can adjust to the presence of the obstacle and diverge smoothly around it. The upstream flow "knows" of the presence of the obstacle because gravity waves driven by the water depth changes around the obstacle can propagate from the obstacle with a velocity  $(gD)^{1/2}$  that is greater than the flow velocity  $u$ . The size of the upstream region that is influenced can be many times the size of the perturbing obstacle. In principle, the flow would adjust smoothly to the presence of the obstacle everywhere; in practice, because of the viscosity of the water and the shear stresses that it can support, an eddy (a zone of recirculation) typically forms downstream of the obstacle (see Figures 6a and b). The "horseshoe vortices" that wrap around the obstacle usually cause both upstream and downstream scouring in an erodible channel. In extreme cases, the vortices form a cushion of water in front of the rock (e.g., at Lava, see the rock on the lower right side of the river illustrated in Figures 13a and b).

At a discharge that just submerges the obstacle, the water that flows over the top of it becomes supercritical because the upstream velocity is nearly maintained, but the water becomes shallow (Figure 27). The flow returns to subcritical conditions through a hydraulic jump, which is the wave associated with the rock. The height of the jump depends on the Froude number of the flow over the top of the rock. As discharge increases, the Froude number decreases because the depth of the water over the rock increases rapidly with discharge, whereas the velocity remains approximately constant or increases only slowly. At the discharge at which the Froude number returns to unity, flow over the rock returns to subcritical conditions, and the wave disappears ("washes out").

The behavior of waves around rocks embedded entirely in supercritical flow is more complex, because depth changes with discharge are less easily predicted. The most common occurrence of rocks in supercritical flow is near a shore where the flow maintains nearly the velocity of the main current, but becomes shallow. Many of the boulders show prominent V-shaped wakes typical of supercritical flow (see Figure 10a). When discharge increases to permit a stage sufficiently deep for subcritical flow, the wakes disappear.

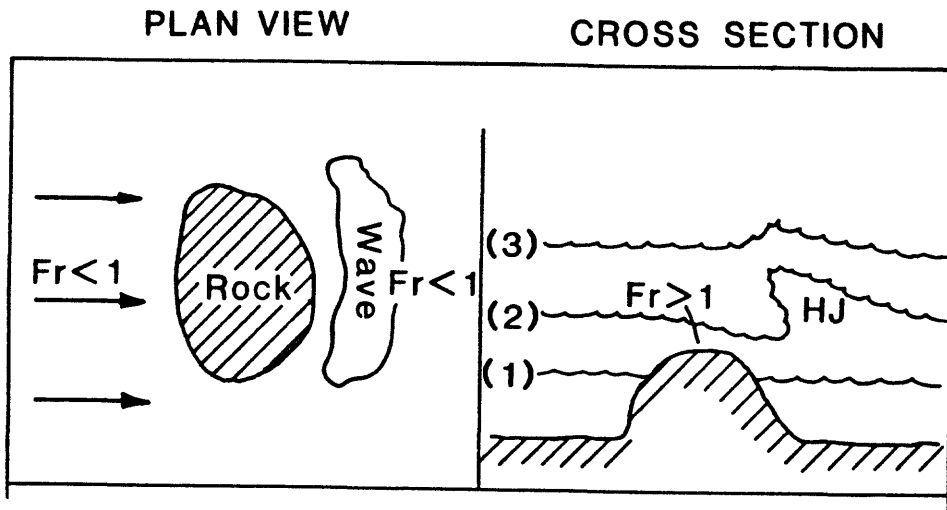


**Figure 27.** Schematic illustration of the response of a river to an obstacle on the bed when the flow changes from supercritical [(1) and (2)], to subcritical (3) as discharge increases. Fr refers to the Froude number; HJ indicates a hydraulic jump.

## 12. Movement of the boulders and contouring of the channel

The flow of water over a particulate surface can cause movement of particles by a variety of mechanisms: suspension and bed-load transport being the most commonly used terms (see Vanoni, 1975 for a comprehensive review of this subject). An excellent description of sediment transport through the Grand Canyon can be found in Howard and Dolan (1981).

The sedimentary material in the Colorado River bed consists of three major components: (1) alluvial fan deposits from tributaries (mud flows, debris flows, flood deposits) and talus/colluvium from steep canyon walls; (2) fine-grained sand and silt derived by reworking of the finer fraction of these deposits; and (3) cobble bars and rock gardens formed by the reworking of the coarser components of (1). The finer-grained material is mobile during even low stages of the river--for example, it moves during even the relatively small annual floods. Coarser debris may only move at rare peak floods. For example, the cobble bar at mile 209 was obviously emplaced at a discharge in excess of 100,000 cfs because it was not even submerged during the 1983 discharge of 92,000 cfs. Cobble bars are present in reaches where the width of the river is substantially greater than average because the flow loses its competence where the channel widens, e.g., they can be found downstream of the narrow section of a rapid where the river widens

and on the inside bends of broadly curving rapids. Some rocks and boulders may not be mobile at all, but may remain as a veneer of boulders on the bed at the debris fan (Howard and Dolan, 1981). Rocks between cobble size and the immobile size for a given location can be transported downstream short distances from the rapids in the expanding section, forming rock gardens.

This report focuses specifically on the relatively immobile boulders and rock gardens. No quantitative modelling has been done of the hydraulics of rapids in the Grand Canyon, except the work of Kieffer (1985) on Crystal Rapids. However, Graf (1979, 1980) analyzed the stability of boulders in the Green River and concluded that the largest boulders were stable and could not be moved during even the largest floods; by analogy, other authors have concluded that large boulders are also stable in the rapids in the Grand Canyon. The Colorado River in the Grand Canyon is capable of moving boulders comparable to those moved during the largest floods that are known from paleohydraulic reconstruction techniques (Baker, 1973; 1984).

Although there has been much documentation of the transportation of sediment past the gaging stations at Lee's Ferry and Grand Canyon (Bright Angel), as well as new measurements at the Little Colorado River, National Canyon, and Diamond Creek during the Glen Canyon Environmental Studies, little is known about the mobility of large particles in the vicinity of the rapids. The size and amount of material transported are positively related to water velocity, depth, and, therefore, discharge. The capability of the river to clear out debris fan material emplaced in the channel is therefore proportional to discharge and, within a rapid, to local variations in velocity and their changes as discharge changes.

One of the criteria available for the transport of large boulders is the Hjulstrom criterion, which relates water velocity to the size of the largest boulders that can be transported (Figure 28). Water-surface velocities of up to 7.5 m/s have been measured in this study, and velocities approaching 10 m/s are conceivable in rapids (Kieffer, 1975) at high discharges. From the Hjulstrom criterion shown in Figure 28, it can be seen that a velocity of 6 m/s would be capable of eroding a 0.5 m boulder (the upper curve) and could transport material out to 1-2 m diameter (the lower curve); these values depend on how the Hjulstrom curves are extrapolated. From the same figure, it can be seen that the Colorado River in full flood with a velocity of 9 m/s [as measured at Crystal Rapids in 1983, (Kieffer, 1983)] is capable of moving boulders of several meters diameter (in those places within rapids where the highest velocities are obtained). Surface float velocities of the magnitudes measured may indicate average fluid velocities that are 10-25% greater, i.e., 6-8 m/s at 5,000 cfs discharge. Referring to the Hjulstrom diagram, we can then conclude that the main channel of the river where these velocities are obtained is efficiently cleared of material up to about 1-2 m in size at discharges even at the lower end of the range of the Glen Canyon Dam generators (order of 10,000 cfs). Field studies, such as those that produced the lower zone of transport criteria in Figure 28, suggest that particle motion in natural rivers may begin at appreciably lower velocities.

A second criterion for boulder transport is the concept of unit stream power, originally introduced by Bagnold (1966) and recently applied to paleohydrogeologic problems by O'Conner et al (1986). The unit stream power is the stream power (rate of energy expenditure) per unit area,  $\omega$ . It was originally defined by Bagnold (1966) as

$$\omega = \gamma Q S_f / w = \tau u$$

where  $\gamma$  is the specific weight of the fluid,  $Q$  is the discharge (that component carried in the main channel),  $S_f$  is the friction slope,  $\tau$  is the total channel shear,  $w$  is channel width, and  $u$  is the mean channel velocity. A more convenient form of this equation is (O'Conner et al., 1986):

$$\omega = \gamma n^2 u^3 / R^{1/3}$$

where  $n$  is the Manning coefficient of roughness and  $R$  is the hydraulic radius of the channel (taken to be the main channel flow area divided by the immobile surface bounding it; the boundary between main channel flow is taken to be frictionless).  $\gamma$  is assumed to be  $9800 \text{ N/m}^3$  (clear water).

For example, at House Rock Rapids at 5,000 cfs discharge with an average velocity of  $6.5 \text{ m/s}$  and a depth ( $\sim$ hydraulic radius) of  $1 \text{ m}$  in the narrowest part of the rapid, the unit stream power is  $3300 \text{ N/m/s}$ . Available relations between unit stream power and sediment-transport relationships (from Williams, 1983; summarized in O'Conner et al., 1986, Figure 9) suggest that a river with this unit stream power could transport boulders up to approximately  $2 \text{ m}$  diameter. This conclusion is in good agreement with the inferences from the extrapolated Hjulstrom diagram.

Evidence that the Colorado has transported boulders of this size is preserved in the size distribution of boulders remaining as lag on the debris fans where they have been covered by the river at different discharges (Figure 29; 12 parts shown in order of downstream occurrence of the rapids). These measurements show that most debris fans are depleted in boulders less than  $0.5-1 \text{ m}$  diameter even up to the elevation on the debris fans that correspond to the  $92,000 \text{ cfs}$  discharge<sup>10</sup>.

---

10 In contrast, many small cobbles and rocks are present above the  $92,000 \text{ cfs}$  shoreline in some places, particularly on talus slopes (e.g., on the right bank of Hermit Rapids). Since large, long-duration floods of more than  $200,000 \text{ cfs}$  and, plausibly, more than  $300,000 \text{ cfs}$ , have been recorded with some certainty, this observation suggests that the slopes in these regions are sufficiently mobile on a time scale of decades to replace the smaller particles by down-slope movement. At Hermit Rapids this observation is supported by a second observation. Driftwood can be found about  $2 \text{ m}$  higher than the driftwood deposited at the  $92,000 \text{ cfs}$  flow in 1983. This driftwood presumably was deposited during the 1957 flood of  $125,000 \text{ cfs}$ . It is, in most places, covered by talus that has migrated downslope since 1957.

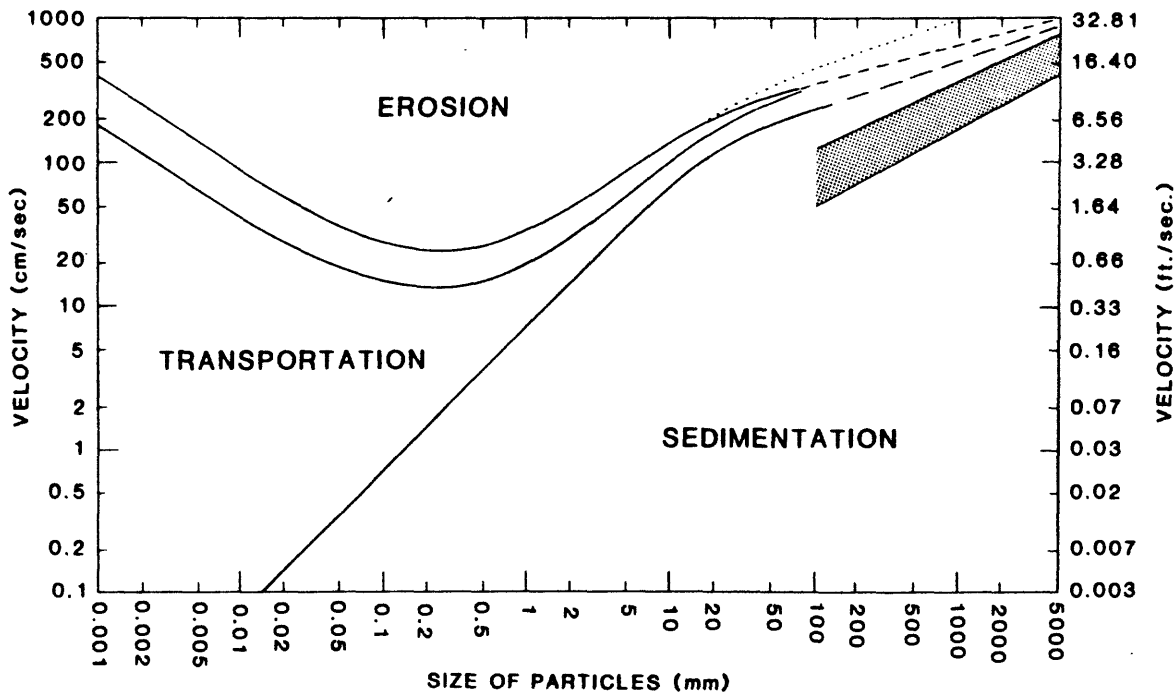
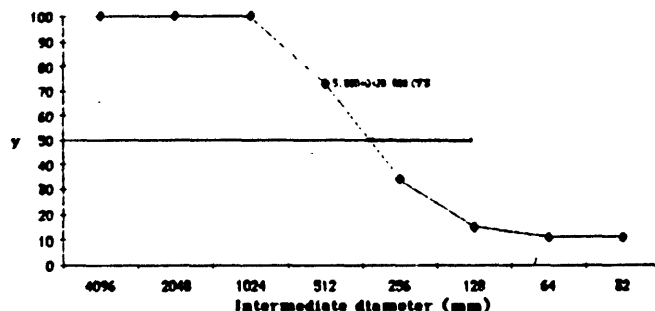


**Figure 28.** Summary of the relations between stream velocity and size of moveable boulders. The area on top represents the Hjulstrom criterion (Hjulstrom, 1935; as reported in Strand, 1986), extrapolated beyond particle diameters of 50 mm. The Hjulstrom criterion is for particles in a uniform bed. Bed roughness and particle shape appear to cause particles to move at lower velocities. The lower stipled area represents criteria developed by Helle (1969).

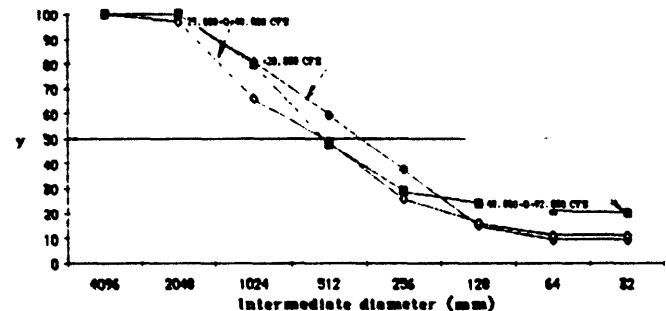
**Figure 29** (on next two pages). Size distribution of large particles measured at the places indicated at rapids. The twelve graphs are arranged in the order that the rapids occur along the river (see Figure 1). Elves Chasm, not on that map, occurs between Crystal Rapids and Deubendorff Rapids. The ordinate,  $y$ , is the per cent of particles smaller than the given (intermediate) diameter. The horizontal line in each part is to guide the reader's eye to the median diameter of the particles at the rapid.

**Figure 29, part 1 of 2.**  
(Figure caption is on previous page.)

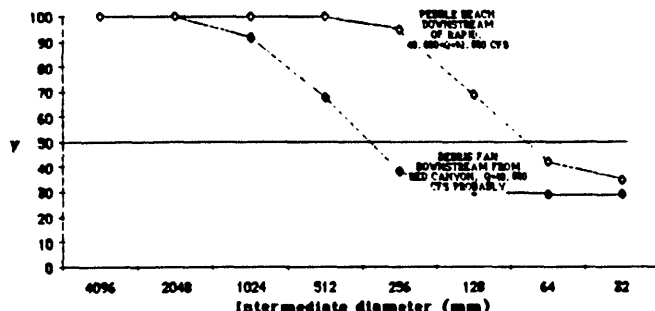
**(A) Boulder Size Distribution at House Rock Rapids**



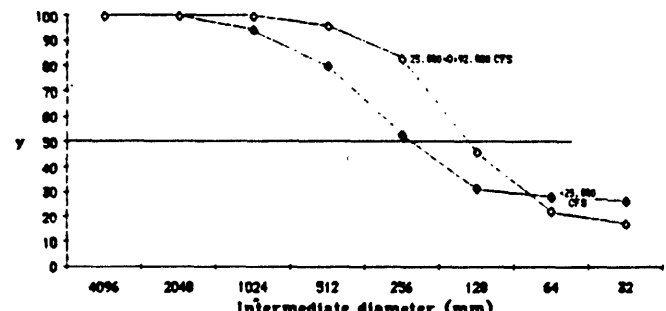
**(B) Boulder Size Distributions: 24.5-Mile Rapids**



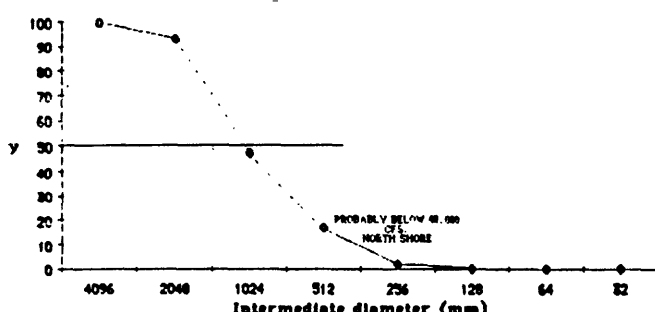
**(C) Boulder Size Distributions at Hance Rapids**



**(D) Boulder Size Distributions: Bright Angel Rapids**



**(E) Boulder Size Distribution at Horn Creek Rapids**



**(F) Boulder Size Distributions: Granite Rapids**

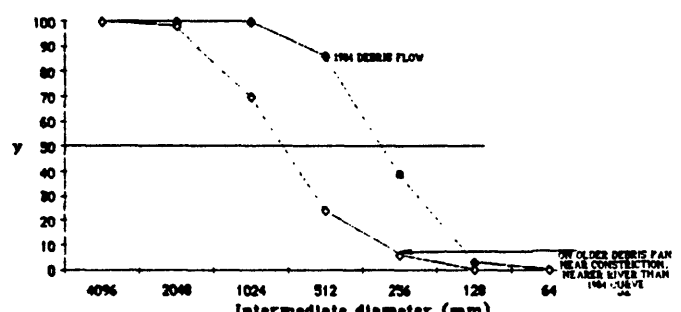
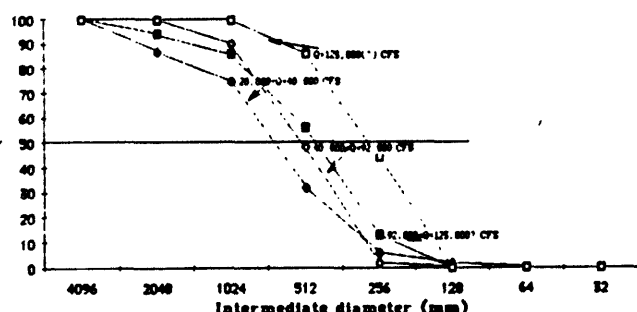


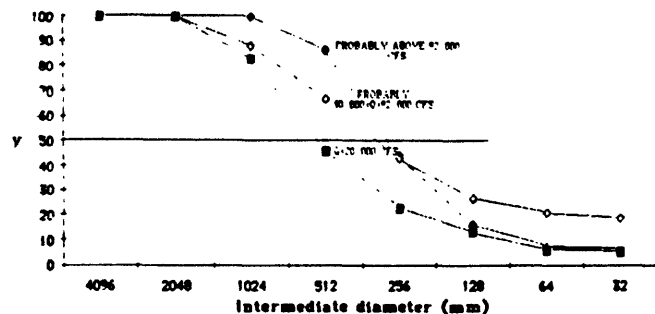
Figure 29, part 2 of 2.

(Figure caption precedes part 1 of this figure.)

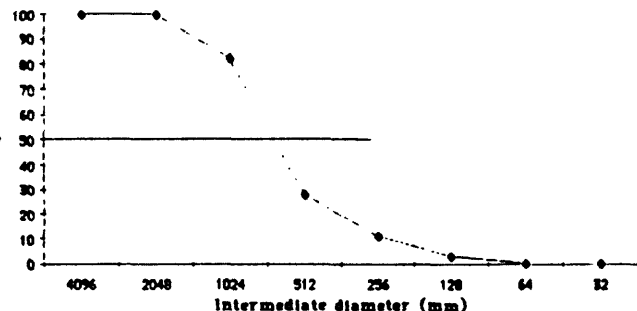
(G) Boulder Distributions: Hermit Rapids-North



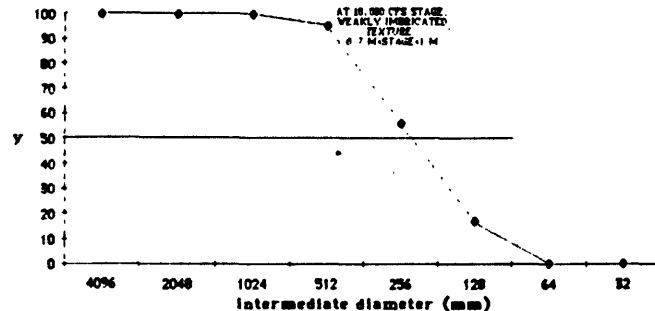
(H) Boulder Distributions: Hermit Rapids-South



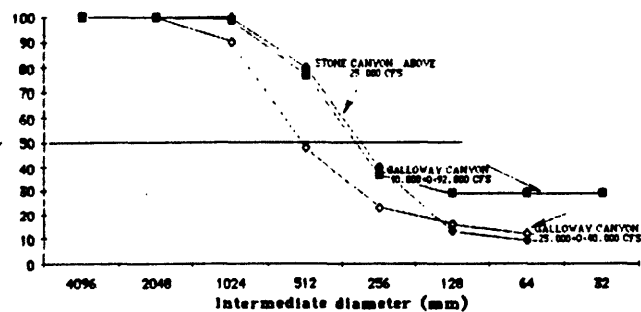
(I) Boulder Size Distribution at Crystal Rapids



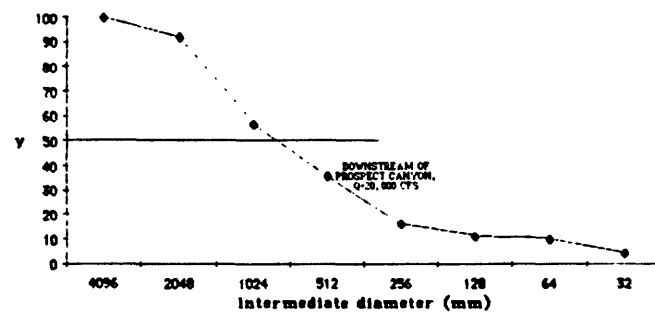
(J) Boulder Size Distribution at Elves Chasm



(K) Boulder Size Distributions: Deubendorff Rapids



(L) Boulder Distribution at Lava Falls Rapids



If a debris fan had a wide variety of particle sizes when it was emplaced (i.e., were unsorted), and if it were not graded in size laterally, then erosion of this fan by a large flood would be expected to remove larger particles low on the fan (where the flow is deepest and fastest), and to remove progressively smaller particles higher on the fan. The size distributions measured on the north and south banks of Hermit Rapids, at Bright Angel Rapids, and on the debris fan from Galloway Canyon at Deubendorff Rapids (refer to Figure 29 for data mentioned in this discussion) are consistent with such a simple emplacement and erosion model.

However, the boulder size distributions on the other debris fans are rarely as simple as this model suggests. The complexities appear because the initial particle size distributions are not known and the size distributions of the particles are not produced simply by erosion, but by a combination of erosion and replacement of material by deposition.

In the following discussion, the median size of material on a debris fan is used as a measure of the particle size. Each graph in Figure 29 has a horizontal line at the 50% level of size distribution to guide the reader's eye to the median size range.

The shortest, and therefore, in some ways, simplest histories exist in the new (1984) debris fans that can be found at Elves Chasm and at Granite Rapids. The data on the material at Elves Chasm were taken just above the stage level of 10,000 cfs discharge; it is known that when these data were taken no flood levels above 40,000 cfs had occurred. The boulders at Elves Chasm were emplaced while the Colorado was at about 40,000 cfs discharge. From the height of the erosion scarp carved into the debris above the place where the boulders were counted, it can be inferred that the water had been roughly 0.7-1 m deep. The size distribution in Figure 29 shows that the median size is 0.25 m. These boulders are weakly imbricated, indicating that they have been in a state of incipient motion. I believe that the size distribution can be interpreted as one in which there were originally more abundant small particles which have been removed by the discharges available. That is, a discharge of 40,000 cfs and a stage of roughly 1 m can move particles on the order of 0.25 m.

The same interpretation can be invoked to explain the boulder size distributions seen in the 1984 debris flow from Monument Creek into Granite Rapids. However, the interpretation is more complex there because examination of the debris flow upstream in Monument Creek shows that the debris was strongly sorted during travel toward the Colorado River. Field time did not permit us to obtain boulder sizes along different parts of the Monument Creek debris fan. However, the data obtained show that the debris of the underlying older debris flow, in which the median diameter is 1 m, is much coarser (a factor of 4) than the debris on the new flow (Figure 29). Even these coarsest boulders in the older debris flow are imbricated, suggesting that they have been at least incipiently mobile during the larger flood events. At 92,000 cfs, it can be estimated that water was approximately 5 m deep over these large imbricated boulders.

Outcrops of the 1966 debris flow at Crystal Rapids upstream in Crystal Creek show that it contained a wide variety of particle sizes when emplaced [(see also Webb (GCES, 1987)]. However, everywhere that the debris fan has been covered (up to 92,000 cfs in 1983) it is depleted in material less than 0.5 m diameter, and that the large particles remaining are imbricated. The flood history at Crystal Rapids is fairly well known (except for the initial ponding and breaching event when the debris fan was emplaced) and thus it can be stated that, unless the initial ponding and breaching event resulted in discharges temporarily greater than 92,000 cfs, discharges equal to or less than 92,000 cfs and water depths less than a few meters are responsible for the boulder size distribution observed.

At Horn Creek the median diameter is 1 m, and no particles were counted smaller than 0.128 m. At this rapids, there is apparently no supply of small pebbles and cobbles upstream, and the boulder distribution seen is interpreted here as a record of the erosive power of the river. Boulders less than 1 m in size apparently can be removed by large floods in Horn Creek Rapids.

A very similar size distribution is seen at Lava Falls Rapids, where the median diameter is 1 m. In contrast to the size distribution at Horn Creek Rapids, however, there is a spectrum of small particles at Lava, extending down below 0.032 m, the limit of sampling. Although we were not able to document the origin of the smaller particles in the limited field time available, I strongly suspect that the small particles were transported into the debris fan and trapped during waning floods. The data from House Rock Rapids can be interpreted similarly: the coarse particles are smaller than at Lava Falls (probably because of their sedimentary rather than igneous origin, and because the gradient of the Rider Canyon debris fan at House Rock Rapids is shallow), but material below 0.25-0.5 m has probably been removed by erosion, and replaced by a bed of cobbles and sand at the smaller sizes.

This is clearly illustrated at Hance Rapids: The debris fan from Red Canyon shows a large number of particles in the range between 0.1 and 2 m diameter, and only sand-sized material below 0.1 m. The sand has clearly been deposited by small floods of the Colorado River. In contrast, in the eddy below the rapids, the debris fan and larger rocks are completely mantled by the sand and pebble beach associated with the eddy. On this pebble beach, 50% of the particles are larger than 0.064 m. These pebbles are well rounded, imbricated, and clearly can be transported relatively easily downstream and through the eddy. The data from Bright Angel and 24.5-Mile Rapids appear to record a similar two-part process: erosion of fine material from the debris fans, and deposition of material of similar size back onto the fan. More work needs to be done in the field to document the origin of the smaller material on the individual fans.

The boulder size distribution story is perhaps most intriguing and informative at Hermit Rapids. On the south shore, the debris fan is coarsest near the river, where it has been subjected to the greatest depths. At depths submerged by a 20,000 cfs discharge the median

diameter is 1 m, and the smaller materials appear to have been reworked by floods. Higher on the debris fan, at levels submerged by flows greater than 40,000 cfs but lower than levels submerged by 92,000 cfs, the distribution is finer, with the median diameter being 0.25 m. At both levels, of pebbles and sand transported into the fan exist, as shown by the fine-grained material in these distributions.

In contrast, there are no fine particles (with less than 0.1 m diameter) on the north shore of Hermit Rapids. Here the slopes are mantled with actively creeping talus. High on the slopes the initial size distribution can be documented (in this one vicinity, debris from a flood with a stage approximately 1.7 m (5 ft) higher than the 1983 flood was found; this debris could be from the 1957 flood of 125,000 cfs, or from the 200,000 cfs flood about 60 years ago; I tentatively assign it as the 1957 flood event). The median size is 0.25 m. The cumulative flood events that have worked on this slope, including the large flood associated with the high stage found (125,000 cfs?) removed much of the material in the 0.25 m size range, leaving a residuum whose median size is 0.5 m high on the slopes and approaches 1 m on the lower slopes.

The hydraulic concepts outlined above, developed quantitatively for Crystal Rapids in Kieffer (1985), and supported by the field data reported here lead to the following model for the evolution of a fresh tributary debris fan with changing discharges of the Colorado River (summarized in Figure 30). The sequence shown in Figure 30 (a)-(f) represents but one cycle in recurring episodes in which debris fans are enlarged by floods in the tributaries and then modified by floods in the main channel. The beginning of the sequence is arbitrarily chosen as a time when the main channel is relatively unconstricted (Figure 30a). The river is suddenly disrupted and ponded by catastrophic debris-fan emplacement (Figure 30b), forming a "lake" behind the debris dam. The surface of the debris fan is shown as a "waterfall" in this model--to distinguish it from the rapid that evolves. As the ponded water overtops the debris dam, it erodes a channel, generally in the distal end of the debris fan (Figure 30c). This is the beginning of the evolution of the "rapid" from the "waterfall".

Unless the debris dam is massively breached by the first breakthrough of the ponded water, the constriction<sup>11</sup> of the main river is initially severe. Floods of differing sizes and frequency erode the channel to progressively greater widths, as shown in Figures 30c, 30d, and 30e. Small floods (Figure 30c) enlarge the channel somewhat, but constricted, supercritical flow is still present (e.g., the annual discharges from Glen Canyon Dam brought Crystal Rapids to the constriction of 0.25 between 1966 and 1983. Moderate floods (Figure 30d) enlarge the channel further and may widen the channel so that at lower discharges the flow is weakly supercritical or even subcritical (e.g., the 1983 high

---

<sup>11</sup> The word "constriction" is used specifically to indicate the ratio of the average channel width at the narrowest part of a rapid to the average unconstricted channel width upstream of the rapid.

discharges at Crystal widened the channel and weakened the waves characteristic of the 20,000 and 30,000 cfs discharges). At the same time that lateral widening is occurring, vertical scouring and headwall erosion of the channel are occurring (Figure 30f). Thus, the local gradient in the channel is changing, and new waves can arise as the channel geometry changes (e.g., the new, strong oblique waves on the tongue at Crystal can be attributed to concentration of the 2-3 m drop in bed elevation that had previously been distributed over much of the constriction into a small region at the head of the rapid by headward migration of the laterally widening channel, as in Figure 30f). The rare, large geologic floods which can no longer occur in the canyon carry this process further, possibly widening the channel sufficiently to allow subcritical flow at all discharges. This state has not been reached at Crystal Rapids.

### 13. Rapids and Rock Gardens

The supercritical flow in rapids produces high velocities capable of moving large boulders. As discussed in Kieffer (1985), and summarized in the diagrams of Figure 30, the boulders are transported hundreds of meters (up to about 1 km) downstream to form the "rock gardens" or cobble bars found below many rapids (see Figures 2a and 3). A rapid therefore evolves into two parts: the original debris deposit, and the rock garden (or cobble bar) below it, consisting of reworked debris. In early episodes of small floods, discharge through the constricted channel is strongly supercritical, and velocities are high enough in the constriction and in the supercritical flow zone, that large boulders can be moved by the river. They will be eroded from the constriction and the zone of supercritical flow, and deposited downstream in the region of slower subcritical flow. Thus, it is plausible to believe that rock gardens grow or are modified with the changing position of the supercritical flow and hydraulic jumps as discharge changes. The reports of changes in the configuration of the Crystal "rock garden" during the 1983 high discharges support this idea.

### 14. Summary: Processes and Their Relative Importance

The shape of the Colorado River channel in the vicinity of the debris fans depends on the relative frequencies of tributary and mainstem floods. Median, mean, and peak discharges through the Grand Canyon have been significantly altered by the construction and operation of Glen Canyon Dam (Dolan, Howard and Gallenson, 1974). Prior to dam closure, the median discharge was 8,200 cfs at Grand Canyon gaging station near Phantom Ranch). Between 1963 and 1974, the median was 12,800 cfs. The mean annual flood was 86,000 cfs, and the 10-year recurrence interval flood was 123,000 cfs. There tended to be two periods of high water each year--the largest during the spring melt (June) and the second--largest during the summer thunderstorms in July and August. The greatest floods known were about 300,000 cfs (Lee's Ferry, 1884) and 220,000 cfs in 1921. Floods exceeding 100,000 cfs occurred every few years in the early historic record. The last major floods prior to closure of the dam were 125,000 cfs in 1957 and 107,700 in 1958.

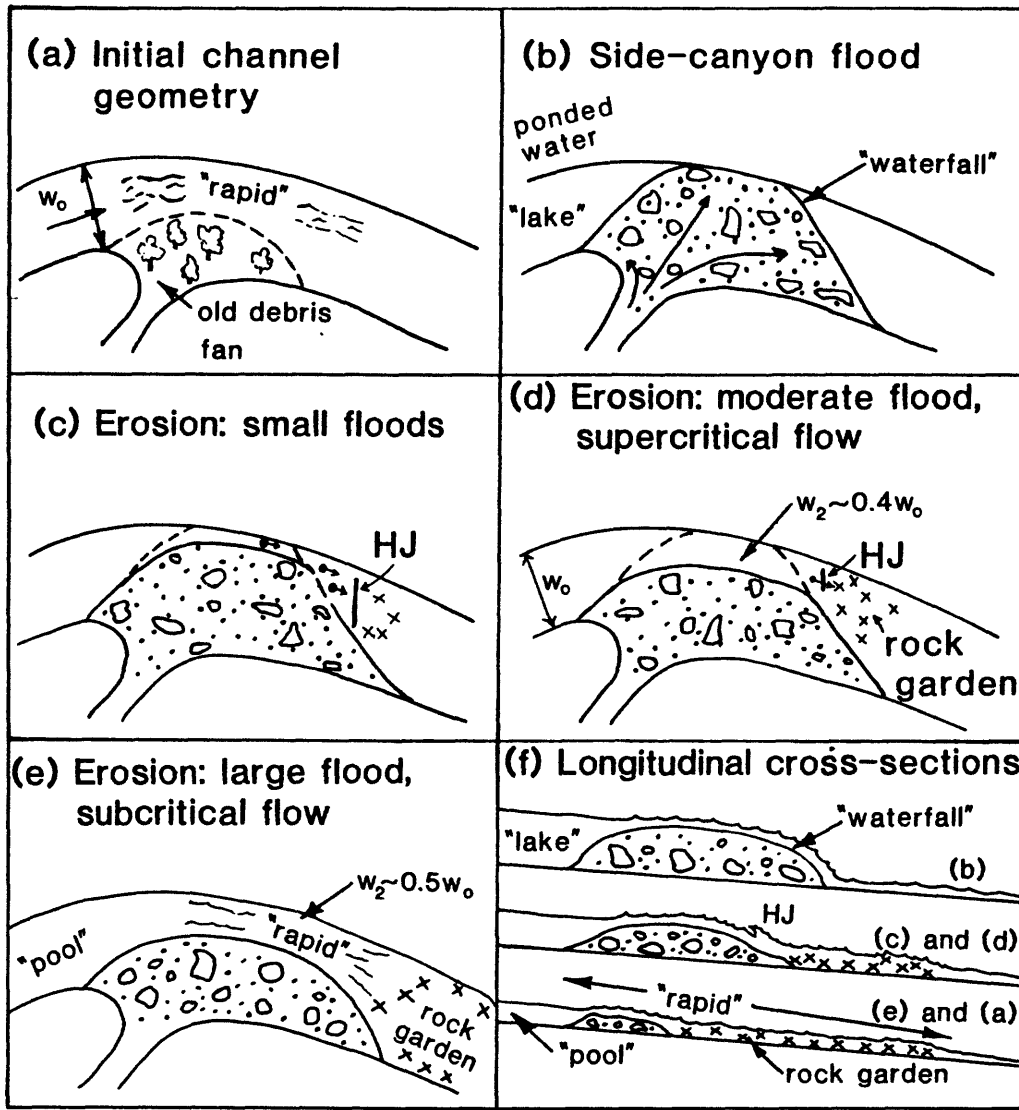


**Figure 30.** Schematic illustration of the emplacement and modification of debris fans, the formation and evolution of rapids, and the formation of rock gardens. See text for further explanation. (From Kieffer, 1985)

After dam closure, the mean annual "flood" was 28,000 cfs and the 10-year recurrence interval flood was 40,000 cfs. Maximum discharges through the power plants at the dam (about 30,000 cfs) are roughly the size of pre-dam summer floods caused by thunderstorm activity (Howard and Dolan, 1981). Only since 1983 have the peak discharges (up to 92,000 cfs) approached the pre-dam annual spring flood levels (80,000 to 125,000 cfs). It is therefore convenient to think of the dam discharges of three historical periods: (a) pre-dam; (b) prior to filling of Lake Powell to operational level (1962-1983); and (c) after filling of the Lake.

Howard and Dolan (1976) were able to compare pre-dam and post-dam air photos to conclude that in the first decade after dam closure, 27% of the tributary fans had built outward because of tributary flooding. Ten percent had built outward by more than 15 m. They concluded that "catastrophic narrowing and steepening of the rapids is very uncommon". However, in that time, and in the additional 12 years until 1986, severe changes (defined here to involve emplacement of boulders on the order of 1 m diameter) have occurred in enough of the tributary canyons to lead us to believe that on the time scale of decades major changes will occur in the rapids (e.g., at Bright Angel, Crystal, Granite, and 209-Mile, Elves Chasm; see Webb, GCES, 1987, for detailed discussion). The rapids will become steeper, rockier, and narrower, unless discharges adequate to remove the debris are permitted through the Canyon.

The data from Crystal Rapids in 1983 show that discharges of 92,000 cfs allowed part of the rapid to become cleared of boulders (the lower part in the constriction). However, the top part of the rapid (in the convergence) became steeper (Kieffer, 1985). It is not clear yet whether this is because the high discharge was not maintained for sufficient time for the debris to be carried away (to the rock garden), or if it is because 92,000 cfs is simply inadequate to clear the converging part of the rapid.

Field data suggest that natural floods larger than 92,000 cfs have contoured the river channel. Figure 31 shows a histogram of the constriction of the channel at more than 50 major old debris fans (age approximately  $10^3$ - $10^5$  years). At these debris fans the channel is typically 0.50 of the upstream width. In contrast, at Crystal Rapids during the years 1966 to 1983 when the discharge was held to less than 40,000 cfs, the constriction was about 0.25. The 1983 high water of 92,000 cfs enlarged the constriction to about 0.42. Extrapolation of the calculations for Crystal Rapids to higher discharges suggests that floods on the order of 400,000 cfs have contoured the channel of the Colorado River to its present shape at the older debris fans (Kieffer, 1985). Glen Canyon Dam discharges cannot reach this magnitude. Therefore, it is to be expected that the character of the rapids will change as tributaries flood if the discharges through Glen Canyon Dam do not exceed the power plant releases. The change will be toward more highly supercritical conditions as the constrictions become tighter both laterally and vertically.

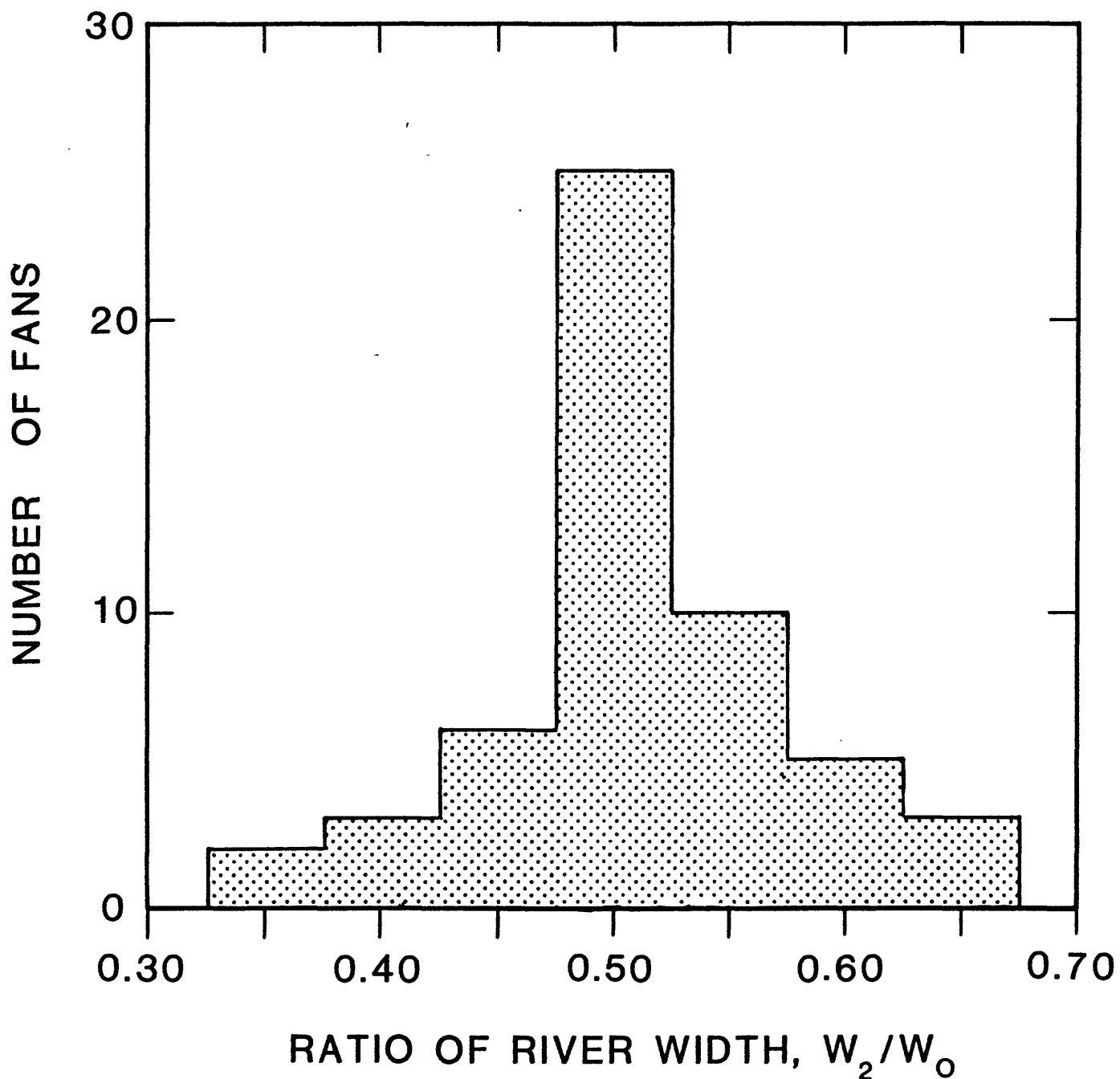


**Figure 31.** Histogram of constriction values of the Colorado River as it passes 59 of the largest debris fans in the 400-km stretch below Lee's Ferry (from Kleffer, 1985). These values are based on the widths of the surface water in the channel on 1973 air photos. The surface width of the water is not identical to average widths of an idealized channel. Thus, in this histogram, Crystal Rapids has a constriction of 0.33, whereas elimination of shallow channelized flow over the debris fan, and idealization of the channel to a rectangular cross-section, suggest that an average channel constriction is about 0.25 at Crystal. At the present time, a histogram based on actual channel constrictions cannot be made because of lack of detailed surveys of river bottom topography.

## V. OPERATING CRITERIA

Operation of Glen Canyon Dam should consider the effects of releases on the rapids in the following three ways:

1. Navigability of the rapids.
2. Safety of passengers in the rapids
3. Geologic evolution of the rapid-debris fan relations.

The proposed flow regime alternatives<sup>12</sup> include conditions which could affect navigability and safety. The larger boats cannot get through several of the rapids (Horn Creek, Hance) at discharges below about 5,000 cfs (exact determination of this discharge was not in the scope of this report, but could be determined from river-rafting companies). Therefore, the lowest discharges may have to be avoided because of this problem.

Passenger safety is determined largely by the strength of the waves. Further comments on this will be worked out with the NPS studies on boating safety. Safety conditions will depend on the hydraulic character of a rapid and on discharge. Consideration should also be given to the fact that the boatmen of many small boats (those which suffer the greatest accident rates) stop to scout the rapids. During fluctuating flows, discharges can change so rapidly that the hydraulic character of the rapids changes as people walk back to and board their boats. Thus, consideration should be given to the rate at which discharges fluctuate, as well as to the amplitude of the fluctuations.

Finally, it should be pointed out that peak discharges through Glen Canyon Dam can be sufficiently high to cause erosion of the Colorado River channel if it becomes constricted by fresh debris flows. Erosion began at Crystal Rapids at discharges on the order of 60,000 cfs (plus or minus about 10,000 cfs). Erosion could begin at greater or lesser discharges, depending on several factors: the early history of the debris fan (the days or weeks following its emplacement, the discharge at the time of emplacement; the particle sizes in the debris; the head of the river. Although the river channel has, in the past, been

---

<sup>12</sup> Briefly summarized the alternatives are: (1) Monthly base flow releases: relatively constant flows year round at about 10,000 cfs; (2) Maximized power plant releases: fluctuations varying with day, season, and month ranging from 1,000 to 31,500 cfs; (3) Maximized power plant releases with the range restricted between 8,000 and 25,000 cfs; (4) Base loaded power plant releases during the recreation season; maximized power releases for the rest of the year: 1-31,500 cfs except June, July, and August when flows would be held constant at 25,000 cfs; (5) Maximized fishery flows and altered power plant releases: discharges fluctuating between 1,000 and 31,500 cfs except during spawning, incubation, and initial growth periods for trout. These alternatives were formulated prior to recognition of the impact of the very high discharges between 1983 and 1986. Investigators have been asked to also consider the effect of these high discharges.

contoured by discharges of several hundred thousand cfs, the discharges possible from the dam can be a significant fraction of those peak floods (i.e., 10,000 cfs is about 10% of the natural annual peak flood, a few percent of the likely maximum natural flood; 92,000 cfs is about 20-25% of the estimated maximum natural flood) and can, therefore, produce a substantial fraction of the natural erosive capability.<sup>13</sup> Therefore, if there are fresh debris flows that constrict the channel, due consideration should be given to the effects of changing discharges on the hydraulics of the rapids in these regions. For boating safety, careful consideration should be given to the consequences of any "substantial" change of discharge at a rapid that has been newly modified by a major tributary debris flow (the meaning of "substantial" in cfs will depend on the particular circumstances at the rapid and cannot be specified a priori).

## VI. CONCLUSIONS

The work reported here is based on only two river field trips during flows ranging between about 7,000 and 25,000 cfs, and on 6-months funded time for the Principal Investigator. There are a number of direct follow-on observations that could provide further substantiation of the conclusions presented here. These recommend future work is based on the need to make observations over a wider range of discharges than were obtained during the work (e.g., note the limited discharges over which velocity and stream-line measurements were made; they do not extend the full range of the operating scenarios):

- (1) Hydraulic maps will exist for the 10 rapids at 30,000 cfs, and for many of the rapids at 92,000 cfs, but no velocity information exist at these discharges. Therefore, if a period of about 3 weeks of 30,000 cfs discharge or greater occurs, an expedition to document streamlines and velocities and recreate all of the camera and documentation sites should be made.
- (2) If flows above 50,000-60,000 cfs occur, stereo air photos of the rapids of interest should be flown so that additional hydraulic map information could be compiled.
- (3) Any unusually high or low discharges should be documented at the rapids. Substantial inquiries by the author have revealed amazingly little photographic documentation of the hydraulic patterns during the 1983 flood.
- (4) Laboratory modelling of flow in rapid-eddy systems is needed to understand the lateral transport of fluid and sediment between the main channel and the channel banks.

---

<sup>13</sup> This will be especially true if peak discharges from the dam coincide with natural floods from the Little Colorado River.

(5) Theoretical hydraulic analyses should be performed for the channel shapes now documented on the maps.

(6) The type of documentation represented here should be provided at any rapids deemed to be at high-risk for tributary flash floods.

Literature Cited

Bagnold, R.A., 1966, An approach to the sediment transport problem from general physics: U.S. Geological Survey Prof. Paper 422-I, 37 pp.

Bagnold, R.A., 1980, An empirical relationship of bedload transport rates in flumes and natural rivers: Royal Soc. of London Channels, McGraw-Hill, 329 pp.

Baker, V.R., 1973, Paleohydrology and sedimentaology of Lake Missoula flooding in eastern Washington: Geol. Soc. America Spec. Paper 144, 69 p.

Baker, V.R., 1984, Flood sedimentation in bedrock fluvial systems, in Koster, E.H., and Steel, R.J. (Eds.), Sedimentology of Gravels and Conglomerates, Canadian Soc. Petroleum Geol., Memoir 10, pp. 87-98.

Bakhmeteff (Bakhmetev), B. A., 1932, Hydraulics of Open Channels, McGraw-Hill, 329 pp. Birdseye, C.H., 1923, Plan and profile of the Colorado River from Lees Ferry, Arizona to Black Canyon, Arizona - Nevada, U.S. Geological Survey topographic maps, 21 sheets, scale 1:31,680.

Chow, V.T., 1959, Open-channel Hydraulics: McGraw-Hill, New York, 680 pp.

Dolan, R., Howard, A., and Gallenson, A., 1974, Man's impact on the Colorado River in the Grand Canyon: American Scientist: v. 62, pp. 392-401.

Dolan, R., Howard, A., and Trimble, D., 1978, Structural control of the rapids and pools of the Colorado River in the Grand Canyon: Science, v. 202, pp. 629-631.

G.C.E.S., Glen Canyon Environmental Studies, reports submitted to the Bureau of Reclamation, for archiving in NTIS, 1987. Graf, W.L., 1979, Rapids in canyon rivers: Journal of Geology, v. 87, pp. 533-551.

Graf, W.L., 1979, Rapids in canyon rivers: Journal of Geology, v. 87, pp. 533-551.

Graf, W.L., 1980, The effect of dam closure on downstream rapids: Water Resources Research, v. 16, pp. 129-136.

Helley, E.J., 1969, Field measurement of the initiation of large bed particle motion in Blue Creek near Klamath, California, U.S. Geological Survey Prof. Paper 562-G, 19 pp.

Hjulstrom, F., 1935, Studies of the morphological activity of rivers as illustrated by the river Fyris: Univ. Upsala [Sweden] Geol. Inst. Bull., v. 25, pp. 221-527.

Homma, M. and Shima, S., 1952, On the flow in a gradually diverged open channel: Japan Science Review, v. 2, no. 3, pp. 253-260.

Howard, A., and Dolan, R., 1976, Changes in fluvial deposits of the Colorado River in the Grand Canyon caused by Glen Canyon dam: Proc. First Conference on Scientific Research in the National Parks, pp. 845-851, New Orleans, Nov. 9-12.

Howard, A., and Dolan, R., 1981, Geomorphology of the Colorado River in the Grand Canyon: Journal of Geology, v. 89 (3), 269-298.

Ippen, A.T., 1951, Mechanics of supercritical flow: Trans. ASCE, v. 116, 268-295.

Ippen, A.T., and Dawson, J. H., 1951, Design of channel contractions: Trans. ASCE, v. 116, 328-346.

Kieffer, S.W., 1985, The 1983 hydraulic jump in Crystal Rapid: implications for river-running and geomorphic evolution in the Grand Canyon: Jour. Geol., v. 93, pp. 385-406.

Landau, L.D., and E.M. Lifshitz, 1959, Fluid Mechanics: Pergamon Press, Oxford, 536 pp.

Leopold, L., 1969, The rapids and the pools - Grand Canyon: U.S. Geological Survey Professional Paper 669, pp. 131-145.

Lighthill, J., 1978, Waves in Fluids: Cambridge Univ. Press., London, 504 pp.

O'Conner, J.E., Webb, R.H., and Baker, V.R., 1986, Paleohydrology of pool-and-riffle pattern development: Boulder Creek, Utah: Geol. Soc. America Bull., 97, 410-420.

Oxford English Dictionary (Compact Edition), 1971, Oxford Univ. Press, New York.

Powell, J.W., 1875, Exploration of the Colorado River and its Canyons: Smithsonian Inst. Govt. Printing Off., 291 pp., reissued by Dover Publs., New York, 1961.

Rouse, H., Bhoota, B.V., and Hsu, E., 1951, Design of channel expansions, Trans. ASCE, v. 116, 347-363.

Schmidt, J.C., and Graf, J.B., 1987, Aggradation and degradation of alluvial-sand deposits, 1965 to 1986, Colorado River, Grand Canyon National Park, Arizona, GCES.

Stevens, L., 1983, The Colorado River in Grand Canyon: A Guide, second edition, Flagstaff, AZ, 107 pp.

Strand, R.I., 1986, Water related sediment problems: Water Systems Management Workshop-1986, Session 4-1, U.S. Bureau of Reclamation, Denver, Colorado, pp. 1-30.

Turner, R.M. and Karpiscak, M.M., 1980, Recent vegetation changes along the Colorado River between Glen Canyon Dam and Lake Mead, Arizona, U.S. Geological Survey Professional Paper 1132, 125 pages.

Vanoni, V.A., 1975, Sedimentation Engineering: ASCE Task Committee, New York, 687 pp., Webb, R.H., Pringle, P.T., and Rink, G.R., 1987, Debris flows from tributaries of the Colorado River in Grand Canyon National Park, Arizona, GCES.

Williams, G.P., 1983, Paleohydrological methods and some examples from Swedish fluvial environments, I - Cobble and boulder deposits: Geografiska Annaler, 65A (3-4), p. 227-243.

Appendix A:

THE 1983 HYDRAULIC JUMP IN CRYSTAL RAPID: IMPLICATIONS FOR  
RIVER-RUNNING AND GEOMORPHIC EVOLUTION IN  
THE GRAND CANYON

FROM

THE JOURNAL OF GEOLOGY

V. 93

PP. 385-406

1985

# THE JOURNAL OF GEOLOGY

*July 1985*

## THE 1983 HYDRAULIC JUMP IN CRYSTAL RAPID: IMPLICATIONS FOR RIVER-RUNNING AND GEOMORPHIC EVOLUTION IN THE GRAND CANYON<sup>1</sup>

SUSAN WERNER KIEFFER  
U.S. Geological Survey, Flagstaff, Arizona 86001

### ABSTRACT

For the last 1,000 to 10,000 years, dozens of large debris fans have severely constricted the path of the Colorado River in the Grand Canyon, Arizona. At most of these fans, the narrowest part of the channel eroded by the river is 0.5 of the upstream width. At Crystal Creek, a debris fan was emplaced in 1966, constricting the channel of the Colorado River to about 0.25 of its upstream width between 1967 and 1983, forming a major rapid. In this paper the hydraulics of Crystal Creek rapid are described, and an analysis is presented to support the hypothesis that the major wave in the rapid was a normal wave (one type of hydraulic jump). Hydraulic jumps rarely occur in natural river channels with erodible beds, but one was present at Crystal Rapid because of the unusually severe constriction of the Colorado River by the 1966 debris fan. Observations on the hydraulics of the river during this time (including mid-1983, when progressively higher discharges culminated in excess of 96,000 cubic feet per second) have demonstrated that the velocity of water going through the constriction and into the hydraulic jump was so great that there was erosion of the Crystal debris fan in the vicinity of the jump. Each new level of record high discharges caused the river to erode a channel of sufficient width to reduce flow velocities below a threshold value required for movement of the larger boulders of the debris fan, thus contouring the fan toward a configuration more in equilibrium with the high discharges. A quantitative model for river debris fan shapes is proposed and is used to estimate prehistoric flood levels from the observed constrictions: the 0.5 value of river constriction found at the more mature debris fans in the Grand Canyon suggests that peak flood discharges of approximately 400,000 cubic feet per second (11,320 m<sup>3</sup>/s) have occurred.

### INTRODUCTION

In the first 400 km of its course below Lee's Ferry, Utah, the Colorado River passes about 60 large debris fans formed by the flooding of its tributaries (location map in fig. 1). Such tributary floods are a major source of boulders in the river channel through the Grand Canyon. Although the major features of the flood-produced fans can be stable for more than 100 years (Leopold 1969; Dolan et al. 1978; Graf 1979, 1980; Howard and Dolan 1979, 1981), the river has eroded them, with remarkable uniformity, so that the

narrowest part of the channel as it passes through these debris fans is about 0.50 of the mean upstream width (fig. 2). This geometric relationship has not previously been noted or explained by theories of dynamics of rapids in canyon rivers, and observations on the fate of large boulders and the erosional modification of the large debris fans have been lacking because of the rarity of the modifying events (Shoemaker and Stevens 1969).

The 1966 mudflow down Crystal Creek was the most recent in the series of major tributary floods that have built debris fans into the Colorado River at Crystal Creek (Cooley et al. 1977), with the narrowed channel being thus called Crystal Rapid. Since about 1965, discharges into the Colorado River through the Grand Canyon (and hence through Crystal Rapid) have been controlled at less than 30,000 cfs by the U.S. Bureau of Reclamation

<sup>1</sup> Manuscript received August 1, 1984; revised January 29, 1985.

[JOURNAL OF GEOLOGY, 1985, vol. 93, p. 385-406]  
No copyright is claimed for this article.  
0022-1376/85/9304-001\$1.00

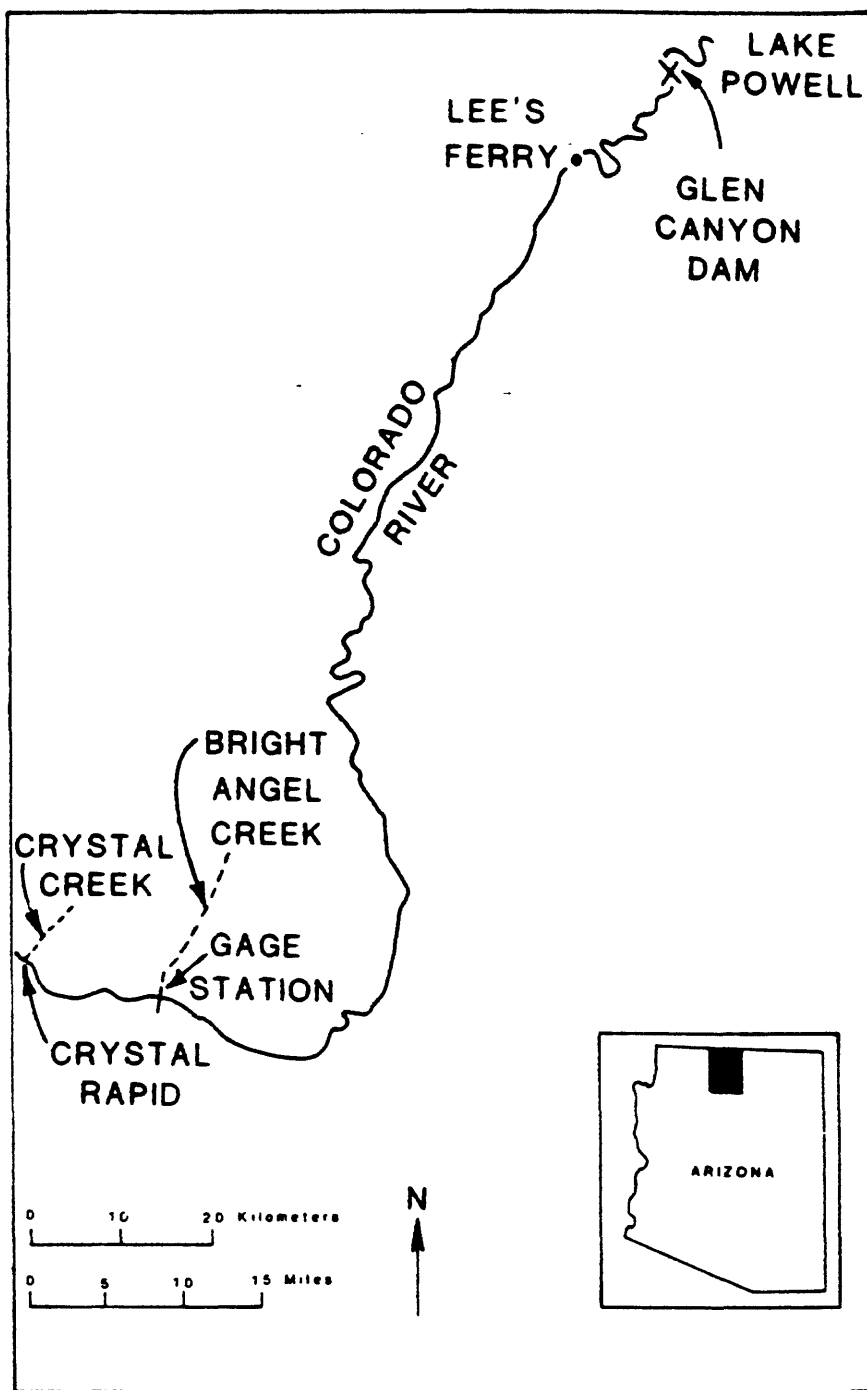


FIG. 1.—Location map of sites discussed in text.

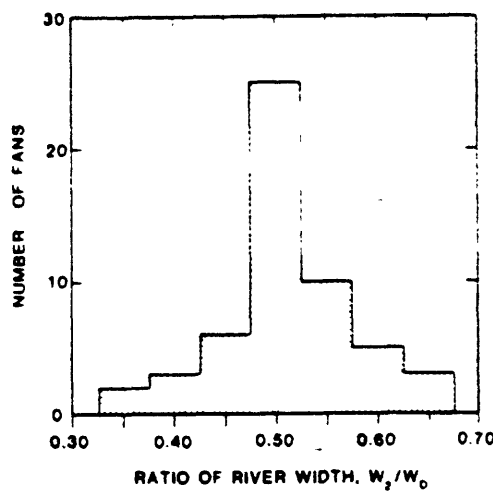


FIG. 2.—Histogram of constriction values of the Colorado River as it passes 59 of the largest debris fans in the 400-km stretch below Lee's Ferry. These values are based on the widths of the surface water in the channel on 1973 air photos (such as in fig. 4). As discussed in the text, the surface width of the water is not identical to the width of an idealized channel. Thus, in this histogram, Crystal Rapid has the value  $w_r/w_0 = 0.33$ , whereas elimination of shallow channelized flow over the debris fan and idealization of the channel to a rectangular cross-section suggests that an average channel constriction is about 0.25. At the present time, a histogram based on actual channel constrictions cannot be made because of lack of detailed surveys of river bottom topography.

normal levels of controlled discharges (Collins and Nash 1978). In 1983 Crystal Rapid became unusually hazardous, with one wave reaching trough-to-crest heights of more than 6 m as the discharge reached 50,000 to 70,000 cfs (fig. 3), drowning one rafter and seriously injuring dozens of others (Wolf 1983). Rare geologic events are only fortuitously documented, and they usually offer little opportunity for the rigorous observations required by the scientific method. The observations of the river-runners who navigated Crystal Rapids before and during this time have provided important and partially quantitative support for the hydraulic model presented in this paper.

*A Note on Units and Directions.*—The discharge of the Colorado River is accurately measured by the U.S. Geological Survey at the Bright Angel gage station, and the measurements are published in units of cubic feet per second (cfs). River-runners, who provided many eyewitness observations for this report, also estimate the discharges in cubic feet per second. Therefore, English units of discharge are used (10,000 cfs = 283 m<sup>3</sup>/s), but all other variables are given in metric units. In river navigation, "right" is the right side of the river when facing downstream—generally north in this case; left is generally south. "Above" means "upstream of," and "below" means "downstream of."

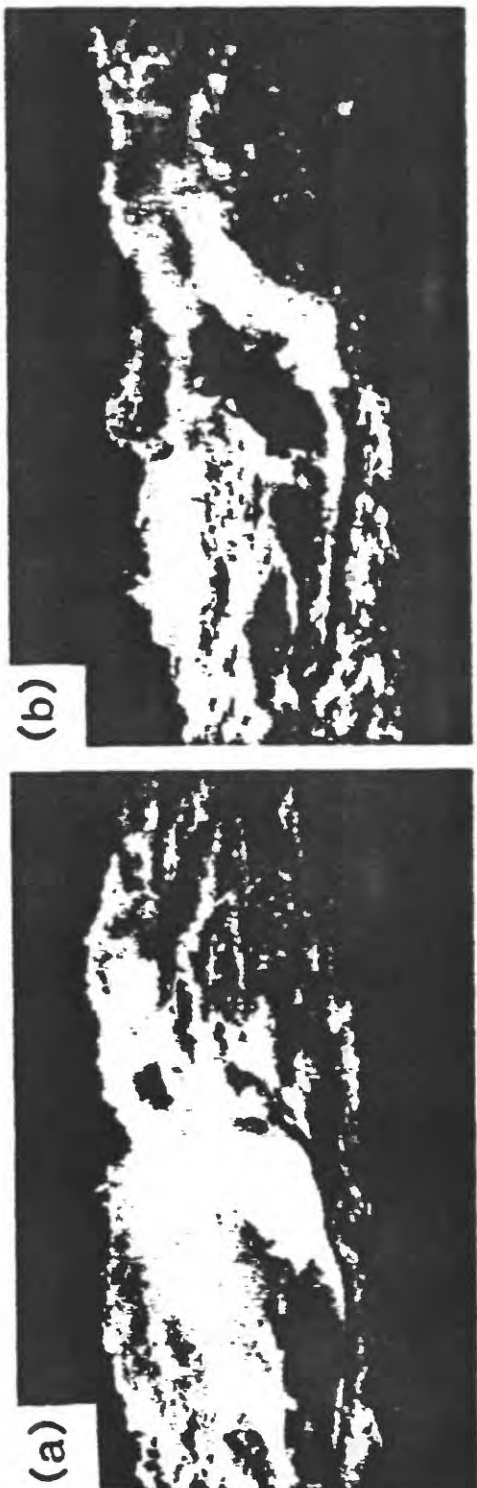
#### CHANNEL GEOMETRY AT CRYSTAL RAPID

*The Pre-1983 Channel.*—Since few survey data are available, the pre-1983 geometry of the Colorado River channel is unknown. The geometry has now changed substantially so this information is beyond recovery, except that which can be inferred from an interpretation of surface features present then.

When the discharge was 10,000 cfs, the surface width of the river narrowed from about 87 m upstream to about 35 m as the river passed around the debris fan (fig. 4). At all discharges, much of the surface width included shallow flow across the debris fan. Even at the peak discharge of 96,200 cfs the flow remained slow and shallow, as can be seen from the texture of the water surface in figure 5. However, the shallow water is not important in considering larger-scale features of the flow: field estimates of velocity, depth, and area of fan covered show that, at all discharges, less than 10% of the total flux is in-

to optimize water use for power generation at Glen Canyon Dam. Discharges typical of natural floods (e.g., as high as 300,000 cfs in 1884) had not flowed through Crystal Rapid before 1983 (U.S. Geological Survey, Water Resources Data for Arizona 1980). In June and July, 1983, however, record-high controlled discharges of up to 96,200 cfs were required to prevent Lake Powell from overtopping the Dam, causing rarely seen or documented geologic and hydraulic events and providing the opportunity to address the hydraulic relationship between the Colorado River and its debris fans.

In addition to their geomorphic significance, however, the hydraulic events during 1983 had a significant effect on commercial and private rafting in the Grand Canyon, where about 10,000 people each year navigate the 400-km stretch through the canyon. Boulders, waves, and eddies in Crystal Rapid have made raft navigation difficult even at



volved in the shallow flow. Most of the pre-1983 discharge was contained within a channel cut in the distal end of the debris fan on the south side of the river. This channel was substantially narrower in width than the surface extent of the water, even at the rate of only 10,000 cfs shown in figure 4.

Beyond the obvious bedrock boundaries, the path available for the river was narrowed by a rock ridge that extended from the south shore into the narrowest part of the channel (fig. 4). Water poured over the southern part of this ledge, creating the Crystal Rapid "Pour-Over." The projection of this ledge into the channel caused two eddies—one above the ledge in the mouth of Slate Creek, and one below. These eddies were present at all water levels, although their detailed configuration changed with discharge (figs. 4, 5, 6). The main part of the flow (see fig. 4a) was thus confined to a narrow, high-velocity channel between the eddies on the south and the debris fan on the north. Although the bottom profile was laterally irregular (see fig. 4c), in the following calculations it is assumed that this high-velocity channel was rectangular at all cross-sections and that it narrowed from an average width of 80 m upstream to 20 m at its narrowest point; the calculations can easily be done for a channel of arbitrary cross-section, but only the simplest assumption is justified by the scant data.

Little was known about the longitudinal slope of the main channel in 1983. The shoreline was measured to drop 2.5 m from Crystal Creek to a beach north of the main wave of interest (see figs. 4, 5, and 6), and the water surface was estimated to have dropped another 2.5-3 m through the Rock Garden. Fathometer data obtained before the 1966 mudflow (in 1965) suggest that the river bed dropped 7 m between the mouth of Crystal Creek and the bottom of the Rock Garden (Leopold 1984).

FIG. 3.—River raft (a) entering and (b) trapped in the large wave at Crystal Rapid on June 25, 1983 (photograph copyrighted by Richard Kocim; reprinted with permission). Pontoons on the raft are each 1 m in diameter; mid-section is about 3 m in diameter. More than 30 passengers are on board; one head is visible on lower left side of raft. From the scale of the raft, the trough-to-crest height of the wave can be estimated at more than 5-6 m.

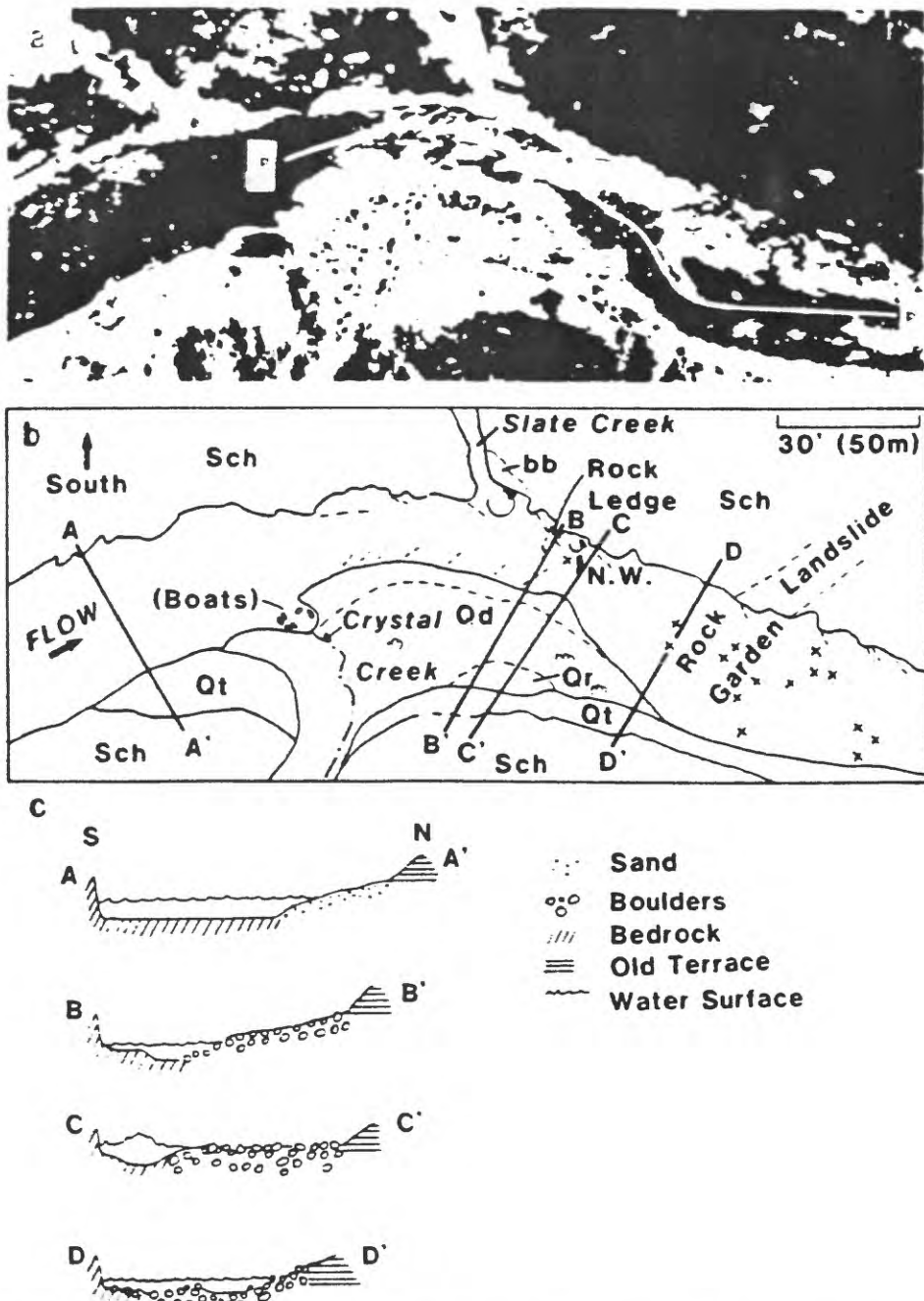


FIG. 4.—(a) Crystal Rapid on June 16, 1973 (U.S. Geological Survey Water Resources Division fair photo); discharge was about 10,000 cfs. (b) Key to features on (a). Other symbols are explained in figure 5. (c) Schematic cross-sections. Relative widths correct; vertical scale exaggerated. The river level at 30,000 cfs is shown by the limit of growth of tamarisk. Surface width of river upstream of rapid is about 87 m; surface width at narrowest point is about 29 m. Rise of debris fan from this river level to old alluvial terrace is about 5.5 m. Below the rapid, the river expands back toward more than 90-m width; the channel bottom is very irregular in this area and littered with boulders (the "Rock Garden"). Rocks in the Rock Garden are visible at 10,000 cfs, cause substantial waves at 30,000 cfs, and are submerged by 92,000 cfs (see fig. 5). Underwater extension of rock ledge is outlined, and assumed boundaries for deep channel are shown by light dashed line in (a). P-P' is the preferred navigation route. The normal wave of interest in this paper (indicated by N.W.) in (b) is not easily visible in (a). E-E' indicates the span of shore eroded by the 1983 high discharges; compare with figure 10.

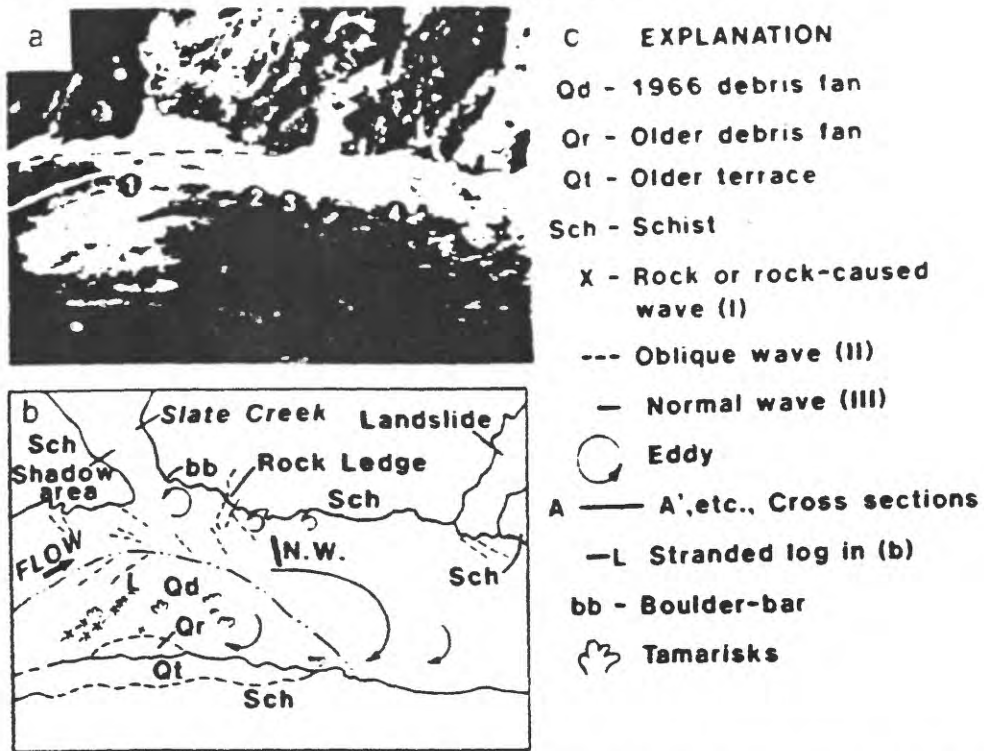


FIG. 5.—(a) Crystal Rapid at about 92,000 cfs on June 27, 1983. Scale is approximately the same as in figure 4(a) but altitude at which photo was taken and orientation differ slightly. (b) Key to features on (a). (c) Explanation of symbols. In (a) water lapping at the base of the alluvial terrace indicates a rise in level of about 5 m from the level shown in figure 4(a). Flow across upper half of debris fan is slow and channelized. Three types of waves discussed in the text are shown by different symbols: the wave that is the subject of this report is the normal wave (N.W.). Although this wave appears to be continuous with an oblique wave from the south shore, it was much larger than that oblique wave. The white line labeled with numbers refers to a path taken by kayaks, discussed in the text.

There is no evidence for sharp vertical drops (ledges) in the bed within this distance, except for the Pour-Over restricted to the south shore. A large rock set in the center of the main channel about 30 m below the Pour-Over, the avoidance of which (and of the hole and wave associated with it) was the primary goal of river-runners prior to 1983. The hole and wave were known as the "Crystal Hole." It was observed that this rock was just submerged at 6,000 cfs, from which its diameter can be estimated roughly at 2 ( $\pm 1$ ) m.

*The Post Mid-1983 Channel.*—After the high discharges of 1983, surface wave patterns were changed (fig. 6), indicating changes in the channel configuration. Most notable of these changes is the steepening of the rapid at its head; most of the drop through Crystal Rapid now occurs above Slate Creek.

After peaking at 96,200 cfs, the discharge did not drop below about 45,000 cfs for most of 1983. At this discharge a new, strong oblique wave appeared on the north side of the entrance to the rapid, opposite Slate Creek (fig. 6). It is, in late 1984, the largest wave in the rapid. At lower discharges this wave moves farther upstream and diminishes in size, but it is appreciable even at a discharge of only 6,000 cfs (these changes are addressed in the "Conclusions" section).

Although the depth of water in the channel at various discharges was not measured at Crystal Rapid itself, data are available from the U.S. Geological Survey's gaging station near Bright Angel Creek, 16 km upstream (table 1). Because of the similarity in channel size, gradient, and wallrock, similar conditions are assumed to have existed there and above Crystal Rapid. A loose constraint on

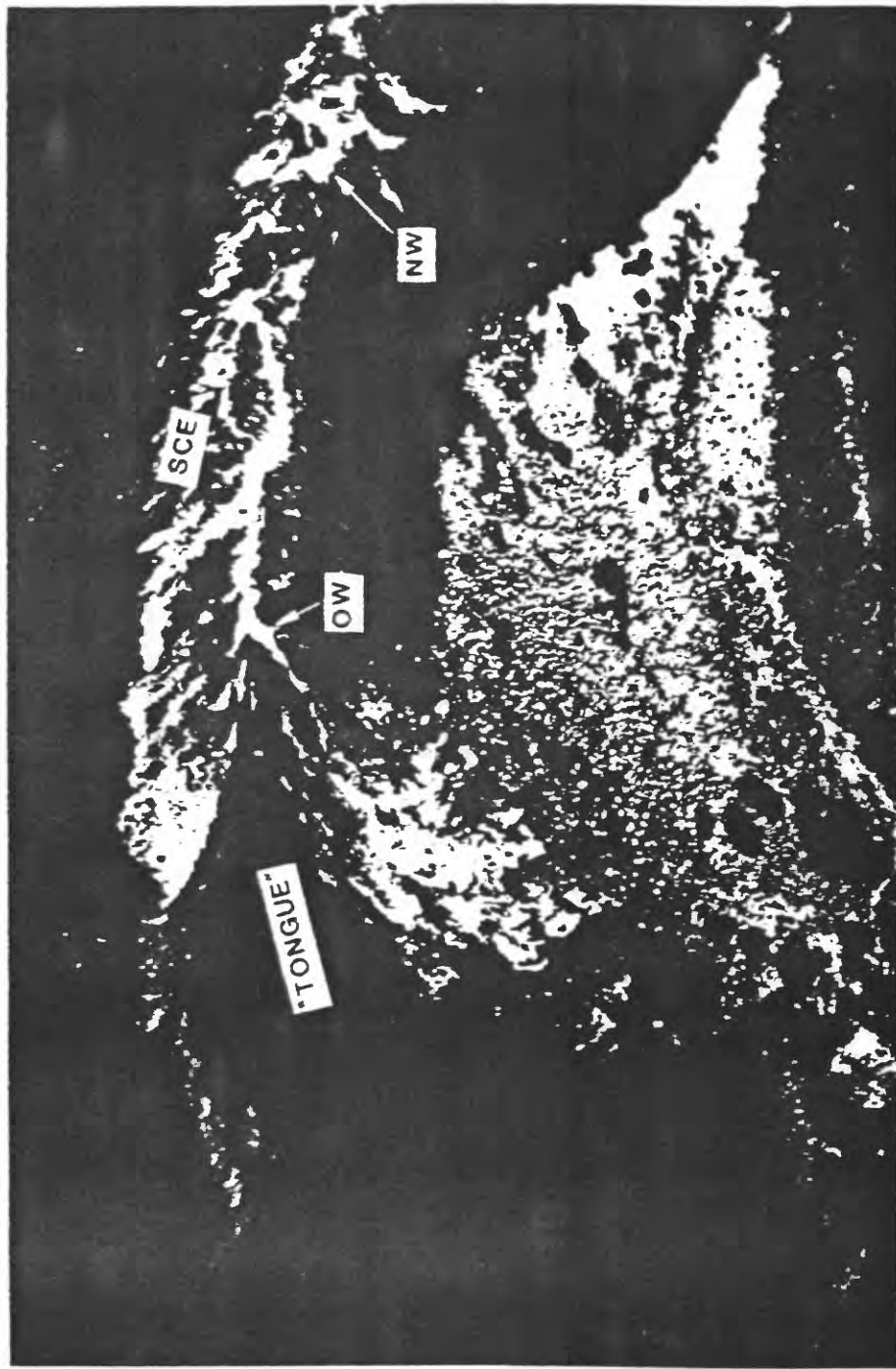


FIG. 6.—Air photo of the new configuration of Crystal Rapid at a discharge of about 45,000 cfs, taken on May 11, 1984. Photo courtesy of the National Park Service. NW indicates the normal wave discussed in this paper; its strength has diminished as a result of the high discharges of 1983. OW indicates the strong oblique wave that has become a major problem for navigation since the high discharges of 1983. SCE is centered on the large Slate Creek eddy

TABLE I  
DISCHARGE OF THE COLORADO RIVER AT BRIGHT ANGEL CREEK GAGING STATION

Date	A <sup>a</sup> (m <sup>2</sup> )	Q <sup>b</sup> (cfs, m <sup>3</sup> )	ū <sup>c</sup> (m/s)	D̄ <sup>d</sup> (m)	D <sub>g</sub> <sup>e</sup> (m)	D <sub>g</sub> <sup>f</sup> (m)	H <sup>g</sup> (m)
1982							
7-14	345.6	9060, 256	0.741	4.36	2.45	-1.91	4.20
7-21	472.0	20400, 577	1.23	5.96	3.91	-2.04	6.03
1983							
6-8	631.8	48700, 1378	2.18	7.97	5.92	-2.05	8.21
6-16	711.0	57600, 1630	2.29	8.97	6.52	-2.45	9.24
6-17	705.2	59700, 1690	2.40	8.90	6.41	-2.49	9.19
6-18	733.4	62300, 1763	2.41	9.25	6.37	-2.88	9.55
6-24	829.6	70000, 1981	2.39	10.47	6.72	-3.75	10.76
6-25	835.2	71500, 2023	2.42	10.54	6.69	-3.85	10.84
7-28 <sup>h</sup>	901.2	83000, 2349	2.69	11.37	7.50	-3.87	11.73

<sup>a</sup> The cross-sectional area, A, is measured by plumbing for depth D, at intervals across the width, w, of the river. Velocity, u<sub>0</sub>, is measured at each width-depth station.

<sup>b</sup> The discharge, Q, is calculated from individual w, D, and u<sub>0</sub> measurements.

<sup>c</sup> The mean velocity,  $\bar{u}$  =  $Q/A$ .

<sup>d</sup> The mean depth,  $\bar{D}$ , is taken as  $A/80$ , where 80 m is taken as the average width of a hypothetical rectangular channel.

<sup>e</sup> The gage height, D<sub>g</sub>, was provided by E. Buell, U.S. Geological Survey.

<sup>f</sup> The gage bottom, D<sub>g</sub><sup>f</sup>, is average gage bottom = D<sub>g</sub> - D.

<sup>g</sup> H is the specific head,  $H = \bar{D} - \bar{u}^2/2g$ .

<sup>h</sup> Peak discharge of 96,200 cfs occurred on 6-29-83 at 0400; at this time only stage was measured and discharge extrapolated from the measurements shown in this table (U.S. Geol. Survey Water Data Rept. AZ-R3 in press).

<sup>i</sup> For estimation of the specific head at high levels of discharge, the average depths ( $\bar{D}$ ), velocities ( $\bar{u}$ ), and specific heads ( $H$ ), given in table I were fit with simple power functions relating them to discharge. The measured average depths ( $\bar{D}$ ), velocities ( $\bar{u}$ ), and specific heads ( $H$ ) listed in table I were fit as follows:  $\bar{u} = (8.23 \times 10^{-3}) (Q)^{0.9}$ ,  $\bar{D} = (14.27 \times 10^{-3}) (Q)^{0.71}$ , and  $H = (4.88 \times 10^{-3}) (Q)^{0.66}$ , for Q in cfs.

the increase in water depth with discharge is also available from estimates of the elevation change of the water across the debris fan.

During the peak discharge of 96,200 cfs, for example, water covered the debris fan up to the base of an old alluvial terrace (fig. 5). Relative to the river level at 10,000 cfs, the following estimates are used: at 30,000 cfs, 1 m higher; at 50,000 cfs, 4 m; at 92,000 cfs, 5.5 m.

At Bright Angel, approximately 2.4 m of material was scoured from the main channel at discharges between 60,000 and 70,000 cfs, but further scouring did not occur at higher discharges. The changes in the bed observed since the high discharges suggests that erosion of a similar magnitude occurred in Crystal, and this assumption is used in the calculations presented below.

Water velocity varies through the length of Crystal Rapid, but the velocity in different regions has not been measured at most discharges because of the remoteness of the area and the difficulty of making systematic measurements in high velocity flows. On June 27, 1983, when the flow was at 92,000 cfs, the author obtained films of three kayaks going

through the rapid. For a kayak following approximately the route shown in figure 5b, the average velocities were as follows: immediately upstream of point 1, 8.5 m/s; point 1 to 2, 9.8 m/s; point 3 to 4, 8.7 m/s. The kayaks stalled to an average velocity of 3.3 m/s between the trough and crest of the wave before accelerating down the backside of the wave to a velocity of 8.5 m/s.

#### THE WAVES OF CRYSTAL RAPID

It is not commonly recognized that where a river passes across a debris fan waves can arise from different physical causes, and that for this reason, different waves can respond differently to changing discharges. At Crystal Rapid, there are three major causes of waves: (1) substantial obstacles in the bed, such as rocks (fig. 7a); (2) a converging or irregular shoreline, or a strong eddy that acts as an effective shoreline (fig. 7b); and (3) contraction and expansion of the flow as it goes through a channel of varying area (fig. 7c).

In all three instances, wave behavior depends on the Froude number of the flow:

$$Fr = u/(gD)^{1/2} \quad (1)$$

## HYDRAULIC JUMP AT CRYSTAL RAPID

393

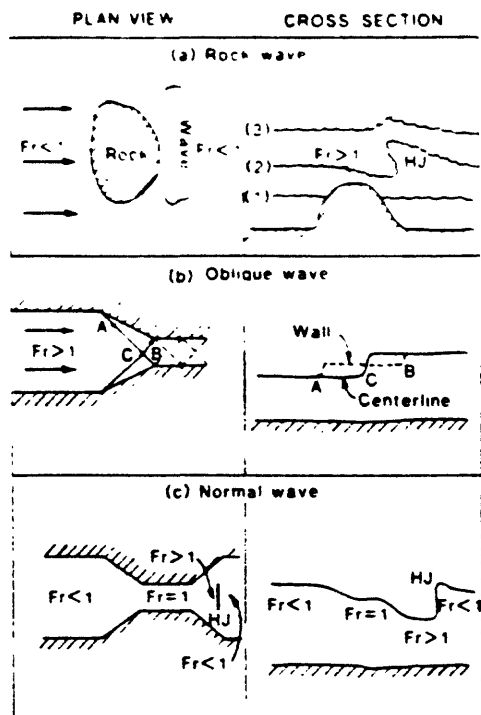


FIG. 7.—Schematic diagram of three types of waves found in river rapids. (left: plan view; right: cross-section) (a) Type 1 waves, caused by rocks. (b) Type 2 wave, caused by deflection of supercritical flow by convergence of a shoreline. These are oblique waves inclined downstream, commonly called "laterals" by river runners. (c) Type 3 wave, caused by severe convergence of the channel.

where  $u$  is mean flow velocity,  $g$  is the acceleration due to gravity, and  $D$  is mean depth of flow. The Froude number is the ratio of mean flow velocity to *critical velocity*, which, in turn, depends on water depth. Strikingly different wave phenomena occur in *subcritical* ( $Fr < 1$ ), *critical* ( $Fr = 1$ ), and *supercritical* flow ( $Fr > 1$ ) regimes.

At Crystal Rapid, waves of the first type (fig. 7c) arise from boulders and from projections of underwater extensions of ridges on the south shore (fig. 4). Along the north shore, even small (0.5-m-diameter) rocks created problems for rafts at low discharges, but the main obstacles were rocks 1 to 2 m in diameter. The infamous rock in the center of the constriction described above, and an equally infamous "orange rock" at the top of the Rock Garden (fig. 4) were the most prominent, but many others substantially complicated the flow.

Consider first a rock embedded in subcritical flow, which is the ambient condition of the flow in the Colorado River in the unobstructed channel. At a discharge that just submerges such a rock, the water that flows over the rock becomes supercritical because the upstream velocity is nearly maintained but the water becomes shallow (fig. 7a). The flow returns to subcritical conditions through a *hydraulic jump* (discussed in detail below), which is the wave associated with the rock. The height of the wave depends on the Froude number of the flow over the top of the rock. As discharge increases, the Froude number decreases because the depth of water over the rock increases rapidly with discharge, whereas the velocity remains approximately constant or increases only slowly. At the discharge at which the Froude number returns to unity, flow over the rock returns to subcritical conditions, and the wave disappears ("washes out"). Although it is difficult to quantify these ideas for a particular rapid without detailed measurements of water depth and flow velocity at specific rocks, it is useful to note that waves from boulders as high as 2 m in the "Rock Garden" below the constriction (see fig. 4) are strong at 10,000 cfs, moderate at 30,000 cfs, and are washed out at 92,000 cfs.

The behavior of waves around rocks embedded in supercritical flow is more complex because depth changes with discharge are less easily predicted. Flow can be supercritical near a shore where it maintains nearly the velocity of the main current but becomes shallow, e.g., along the north shore of the channel at Crystal. Many of the boulders in figure 4 show a prominent V-shaped wake typical of supercritical flow. (Note how their wakes resemble the waves emanating from an object in supersonic flow: there is a semi-quantitative comparison between supercritical and supersonic flow that the reader might find useful, e.g., Loh 1969). The problem of obstacles in supercritical flow will be dealt with below in "Application to the Hydraulics of Crystal Rapid."

Numerous oblique waves of the second type (fig. 7b) occur where the Crystal Creek debris fan deflects the flow southward and where the curving south shoreline deflects the flow northward (figs. 4-6). Several rock buttresses that extend into the water above

and below Slate Creek are the sources of oblique waves. The height of these waves increases with Froude number. The flow velocity decreases substantially across an oblique wave; therefore, moveable bed material transported into the wave at high velocity may be dropped downstream in the lower velocity region. Oblique waves thus can become stabilized by rocks and boulders, and a rather long oblique wave may consist of many smaller rock waves.

Another type of oblique wave is formed where fast-moving water in the main channel meets slow or stagnant water, such as where the main current collided with the Slate Creek eddy at high discharges (figs. 5 and 6). If the angle of intersection is small or if the velocity gradient across the boundary of the zones is small, the intersection of two different flows may be characterized only by a zone of shear without a prominent wave; such zones are known as "eddy fences" to river runners. If the angle of intersection is large or if the velocity gradient is large, a substantial wave may arise; waves of this type in the main channel surged as high as 3 m at 92,000 cfs (fig. 5).

Waves of the third type arise where flow is constricted by narrowing of the channel. If the constriction is severe, subcritical flow can accelerate to critical and then to supercritical conditions in passing through and out of the constriction. A strong wave will form downstream of the constriction; flow returns to subcritical condition as it passes through this wave. Such a wave stands approximately perpendicular to the flow direction and, because of this orientation, is called a "normal" wave. It is a hydraulic jump. The normal wave may not stand near any obvious source of perturbation of the flow (although it may be connected to weak lateral waves), and the height and position of the wave may change with discharge. This behavior was observed for the largest wave at Crystal Rapid during the high discharges of 1983, suggesting that it was a normal wave.

The size, location, and sound of this normal wave at Crystal Rapid changed with discharge. The trough-to-crest height was about 3 m at 20,000 cfs, and about 1 m higher at 30,000 cfs. At 50,000 to 60,000 cfs, boatmen and passengers reported that the wave surged

to a height between 5 and 9 m. It was verified photographically to about 5-6 m (fig. 3) and other photographs collected by the author. At 96,000 cfs, the wave surged between 3 and 4.5 m in height. At discharges over 50,000 cfs, the wave was located about 30 m downstream from its pre-1983 position at 20,000 cfs. Observers reported that at 50,000 to 60,000 cfs the wave emitted a low roar like a jet engine, but it did not generate the same loud roar at 96,000 cfs. However, loud, cannon-like booms that appeared to originate in the main channel occurred several times per minute. These sounds did not correlate with surges or declines in wave height and presumably originated from large boulders moving in the channel.

#### GENERAL ANALYSIS OF THE BEHAVIOR OF THE NORMAL WAVE

The behavior of the normal wave at Crystal Rapid can be analyzed by using the well-known equations of shallow-water flow (e.g., Rouse 1950; Brater and King 1976), although the channel geometry must be much simplified. The generalized geometry used is shown in figure 8a. Note the explicit assumption that there are no significant abrupt changes in bed elevation, i.e., that changes in water velocity are due to the overall slope of the bed and to width variations. In this analysis, the approximations of shallow-water theory are used: wavelengths of disturbances are assumed to be long and surface tension effects are assumed to be unimportant. The surface of the water is assumed to be at constant atmospheric pressure.

Quantitative analysis of the flow requires distinction of six different flow regimes, as shown in figure 8a: (0) an upstream state of unstricted uniform flow; (1) the convergent section of the channel upstream from the constriction; (2) the constriction [the ratio of width at a cross section taken through the constriction to upstream width in region 0 ( $w_2/w_0$ ) will be called the *constriction* of the river]; (3) the beginning of the divergence out of the constriction; (4) the end of the divergence; and (5) a downstream state of uniform flow not influenced by the constriction. Regimes (3) and (4) may be separated by a hydraulic jump, HJ.

At any cross section, the total energy of the

## HYDRAULIC JUMP AT CRYSTAL RAPID

395

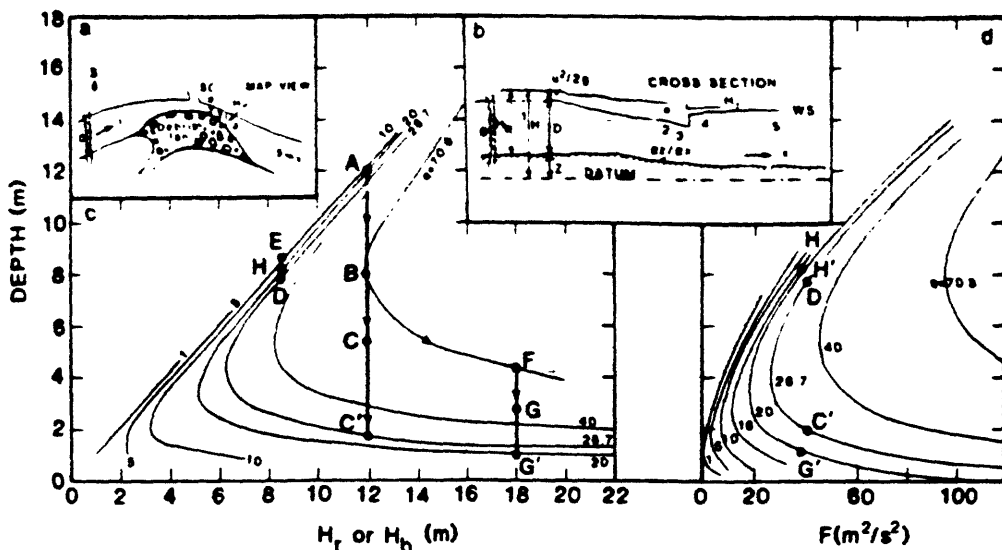


FIG. 8.—(a) Schematic map view of the river-debris-fan relations at Crystal Rapid. (b) Schematic cross-section. Regions 0,1,2,3,4,5 defined in text. HJ indicates a possible hydraulic jump; SC indicates position of Slate Creek. Water profile is for conditions of supercritical flow through the channel. (c) Depth-energy diagram. (d) Depth-force diagram. The curves are for different values of discharge per unit width,  $q$ . See text and appendix for discussion and explanation of symbols and paths shown.

flow,  $H$ , relative to an arbitrary datum is

$$H = H_r + z \quad (2)$$

where  $z$  is the elevation of the bed relative to the datum and  $H_r$  is the combined kinetic energy and potential energy of the water (relative to the bed), the *specific energy* (fig. 8b). Along the path of the river, the balance of energy is given by

$$\frac{dH}{dx} - \frac{dz}{dx} = \frac{dH_r}{dx} \quad (3)$$

where  $x$  is the distance downstream. The energy dissipation,  $dH/dx$ , in regions outside of flow discontinuities (discussed below) can be estimated from a Chezy, Manning, or Darcy-Weisbach equation if the flow is assumed to be gradually varied in these regions (e.g., see Brater and King 1976 or Richards 1983). Then,

$$\frac{dH}{dx} \sim \frac{u^2 n^2}{R^{4/3}} \quad (4)$$

where  $u$  is flow velocity,  $R$  is the hydraulic radius (approximately equal to depth), and  $n$  is the Manning coefficient. At high discharges

in the main channel of the Colorado the Manning coefficient averages 0.03. The bed of Crystal Rapid is much rougher than the main channel, and a value of  $n$  as high as 0.06 is plausible. In Crystal,  $u \sim 10$  m/s and  $R \sim 10$  m, so  $dH/dx \sim 0.017$ . This value is comparable to that of the slope ( $dz/dx$ ) in the upper part of the rapid (e.g., a drop of 2.5 m over the upper 150 m of the rapid), and the near equality of  $dH/dx$  and  $dz/dx$  suggests that the potential energy gain and energy dissipation approximately cancel. In this case

$$\frac{dH_r}{dx} \sim 0 \text{ i.e., } H_r \sim \text{constant} \quad (5)$$

This approximation greatly simplifies the analysis. Further examination of this assumption is given in the Appendix as an illustration of the use of figure 8c and 8d.

Values of specific head,  $H_r$ , are obtained from the Bright Angel measurements of flow depth (which give potential energy) and flow velocity (which give kinetic energy) (table 1). These measurements show that the ambient conditions of flow in regions 0 and 5 are subcritical at all discharges.

At a specific cross-section water depth and velocity are obtained from the equations of

mass continuity and energy conservation. Mass continuity for steady flow across two cross-sections of areas  $A_1$  and  $A_2$  requires that:

$$A_1 u_1 = A_2 u_2 = D_1 w_1 u_1 = D_2 w_2 u_2 \quad (6)$$

where  $w$  is the mean channel width and  $D$  is the mean water depth. The discharge is  $Q = A u$ . The specific energy of the flow,  $H_r$ , is then:

$$H_r = \frac{u^2}{2g} + D = \frac{q^2}{2gD^2} + D \quad (7)$$

where  $q = Q/w = Du$  is the volume flux per unit width, or *specific discharge*. For a given value of  $H_r$ , there are three roots  $D$  allowed by eq. (7); two are real and positive. These roots can be shown as a function of specific discharge on a depth-energy graph (fig. 8c).

For flow with constant specific head (that is, everywhere except across a hydraulic jump) the variation in depth is controlled solely by the specific discharge,  $q$ . For a given head,  $H_r$ , equations (6) and (7) show that the specific discharge,  $q$ , must be less than a limit,  $q_{max}$ , given by:

$$\left(\frac{q_{max}}{g}\right)^{1/3} = \frac{2}{3} H_r = D_c = \frac{u_c^2}{g} \quad (\text{for } H_r \text{ constant}) \quad (8)$$

A *critical depth*,  $D_c$ , and *critical velocity*,  $u_c$ , are implicitly defined in this equation. If  $Q/w_2$  is greater than  $q_{max}$ , the ambient river head,  $H_r$ , is not sufficient to allow all of the discharge through the constriction. Then  $H_r$  must be increased by the formation of a backwater to a new head (the *backwater head*,  $H_b$ ) in region 0 (illustrated in fig. 8b):

$$H_b = \frac{3}{2} \left[ \frac{(Q/w_2)^2}{g} \right]^{1/3} \quad (9)$$

Equation (8) then describes the flow with  $H_r$  replaced by  $H_b$ .

Flow with a given head can be in either of two regimes (called *conjugate states*) separated by the critical conditions at  $q_{max}$ : in one state (subcritical flow,  $Fr < 1$ ) the water is deeper than  $D_c$ ; in the other state (supercritical flow,  $Fr > 1$ ), it is shallower. In a channel

of the general shape of the Colorado River at Crystal Rapid, flow may be entirely subcritical, or entirely supercritical, or it may change from one state to the other. The specific discharge,  $q$ , will be greatest at the constriction, region 2. For a given specific head,  $H_r$ , if the total discharge,  $Q$ , divided by the constriction width,  $w_2$ , is less than  $q_{max}$  given by equation (8), and if the flow is subcritical in region 1, critical conditions will not occur in the constriction. The subcritical flow of region 1 accelerates to higher velocities and shallower depths through the constriction, and then decelerates back to greater depths in the diverging part of the channel.

On the other hand, if  $Q/w_2$  is greater than  $q_{max}$  allowed by  $H_r$ , water will pond behind the constriction until a backwater is formed that just allows  $Q/w_2$  to equal  $q_{max}$  for the backwater head,  $H_b$ . The backwater is essentially stagnant, and subcritical flow in regions 0 and 1 accelerates to critical conditions in region 2. The relative energies of the main channel flow upstream and downstream of the constriction determine whether the flow will return along a subcritical or supercritical path. In the case where a backwater has formed so that the energy of the river downstream,  $H_r$ , is less than the energy of the backwater,  $H_b$ , the flow will expand supercritically into the divergence. The return to ambient head is accomplished through a discontinuous transition—a *hydraulic jump*.

The depth change across the jump can be obtained from conservation of momentum. For any given discharge, there will always be two depths at which the forces at a given cross-section are the same (fig. 8d). The ratio of depth downstream of the jump ( $D_4$ ) to depth upstream of the jump ( $D_3$ ) is:

$$\frac{D_4}{D_3} = -\frac{1}{2} + \left( \frac{1}{4} + 2Fr^2 \right)^{1/2} \quad (10)$$

(In this context,  $Fr = Fr_3$ ; the position of the jump defines the boundary between the end of region 3 and the beginning of region 4.)

The velocities before and after the jump are simply related by the continuity equation (2). The new specific head in region 4,  $H'$ , is given by Bernoulli's equation applied to the flow after the jump:

$$u_4^2 = 2g (H' - D_4) \quad (11)$$

The location of the jump will be determined by the condition that  $H' = H_r$ . The equations were solved by computer, but an illustration of their solution by graphical techniques is shown in figures 8c and 8d and discussed in the Appendix as the justification for assuming constant specific energy in the analysis.

#### APPLICATION TO THE HYDRAULICS OF CRYSTAL RAPID

At a given discharge ( $Q$ ), the flow state is completely specified when the specific head ( $H_r$ ), the river width ( $w_0$ ), and the change in discharge through the constriction ( $q_0/q_2$ ) are given. The average river width used here for regions 0 and 5 is 80 m; the constriction of the river at the onset of the 1983 high discharges is assumed to have been 0.25. The specific energy of the flow is assumed to be given by the values at Bright Angel gage station, table 1. Calculated flow variables are shown as a function of discharge and ratio of specific discharges,  $q_0/q_2$  (fig. 9). As discussed above, it is assumed that all of the water goes through the constriction, so that  $q_0/q_2 = w_2/w_0$ . This assumption will be reexamined below, but, anticipating the validity of the assumption, the geometric term "constriction" will be used for this ratio.

The calculations indicate that at discharges of less than 12,000 cfs, flow through the assumed idealized channel should be subcritical if the constriction is 0.25. In detail, the potential energy gain arising from the drop in bed elevation at the top of the rapid is probably not compensated by the energy losses over this section, and the flow becomes weakly supercritical at the top of the rapid because of this energy gain (an illustration of this effect is discussed in the Appendix). Thus, in figure 4 (taken at 10,000 cfs), the "tongue" of smooth water extending into the rapid indicates supercritical flow. Over the course of the rapid, energy dissipation takes the flow back to subcritical conditions without need for a hydraulic jump at low discharge. The mid-channel rock caused a wave at the "Crystal Hole," of the type illustrated in figure 7a, but no obvious normal wave was present.

The calculations indicate that the available head,  $H_r$ , was not sufficient to allow the required flux through the constriction when discharges exceeded 12,000 cfs. A substantial

backwater (up to 5 m deep) was necessary (fig. 9a). Critical flow through the convergence, supercritical flow downstream of the convergence, and a normal wave to bring the supercritical flow back to subcritical downstream conditions resulted (fig. 9b-e). River runners experienced the backwater as the tranquil slow water above Crystal Rapid ("Lake Crystal") before the acceleration down the tongue of the rapid into the convergence. They experienced the normal wave, i.e., hydraulic jump, as the major obstacle in the rapid. The subcritical flow regime in the diverging section of the rapid below the hydraulic jump was either difficult to negotiate (at low to moderate discharges when the Rock Garden was exposed) or surprisingly simple and smooth (at high discharges when the Rock Garden was washed out).

As discharge increased from 12,000 to 50,000 cfs, the calculations indicate that the normal wave should have moved about 33 m downstream, which is in good agreement with observations.

The calculations suggest that the height of the jump would have increased continuously with increasing discharge if the channel geometry were constant at a constriction of 0.25 (the heavy line in fig. 9b). The observed wave heights were in good agreement with those calculated for a normal wave in a channel—until the discharge exceeded 60,000 cfs. At higher discharges the wave height was observed to decrease, rather than to increase toward the calculated value of 9 to 10 m. The observed decrease in wave height suggests that this quantity that I have been calling the "constriction," which is really the ratio of  $q_0/q_2$ , increased from 0.25 to about 0.40. If the effect of spillover of water across the debris fan was significant, the ratio of specific discharges  $q_0/q_2$  would not be equal to the geometric ratio,  $w_2/w_0$  because water that passed through region 0 would be detoured around region 2 and the ratio  $q_0/q_2$  could vary while  $w_2/w_0$  remained constant. For example, if the proportion of water bypassing region 2 increased with discharge,  $q_0/q_2$  would increase with discharge. Figure 9b shows that this would cause the wave height to decrease with increasing discharge. However, the estimated upper limit on spillover—about 10% of the total discharge—would correspond to an effective increase in the channel constric-

tion ratio of about  $10^7$  (e.g., from 0.25 to 0.275) and could not account for the substantial decrease in wave height observed.

It appears most plausible, therefore, that the path available for flow in the constriction widened, that is, that  $w_2/w_0$  actually changed. A change in  $w_2/w_0$  from 0.25 to 0.40 corresponds to about 12 m of widening. The widening could have occurred in two ways: (1) the size of the eddies constraining the flow along the south shore could have decreased with increasing discharge; or (2) erosion of the debris fan on the north shore could have occurred. Available photographs suggest that the eddy sizes remained relatively constant (perhaps because the eddy size is determined by the lateral dimension of the underwater protrusion of the rock ridge sketched in fig. 4a). Therefore, flow widening by eddy shrinkage is discounted.

Channel widening by erosion of the debris fan is the more likely process. Although data are sparse on conditions required for movement of large particles, velocities on the order of 9 m/s are required to move a 2-m diameter boulder, 11 m/s to move a 3-m boulder, and 13 m/s to move a 4-m boulder. These estimates are based on extrapolation of data from Schumm and Stevens (1973); Hjulstrom's criteria as extrapolated in Blatt et al. (1972); field observations on a natural stream by Helley (1969); and estimates of tractive force on large boulders. The calculations of conditions at Crystal Rapid during 1983 indicate velocities of exactly this range: at 50,000 cfs, with a constriction of 0.25, the velocity in the constriction ( $u_2$ ) is calculated to be 9 m/s and would increase to 14 m/s in region 3 ( $u_3$ ). Figures 9c and 9d. These numbers, and figures 9c and 9d, emphasize the important control that a constriction has on flow velocities and, by implication, on channel erosion.

If the channel contoured itself to keep  $u_2$  equal to the threshold velocity for transport of the major boulders, then by 60,000 cfs the channel would have enlarged to a constriction of about 0.30, a widening of 4 m; by 92,000 cfs, the constriction would have enlarged to 0.40, a widening of about 12 m. For contouring to reach these threshold values, erosion must occur rapidly compared to the duration of the high discharges. A rough calculation of erosion rate based on the number of rock impacts heard (about 1/minute; boul-

ders assumed to be 1 m diameter) suggests that 2200 m<sup>3</sup> could have been removed in 3 days. At this rate, the distal sector of a highly idealized fan, about 220 m<sup>2</sup> in area and 10 m in height, could have been eroded back the required 12 m during the few days that the maximum discharges were maintained.

On the basis of historical highest discharge and shoreline the documented post-1966 history of the Crystal debris fan can be divided into two parts: (1) pre-1983, when the maximum discharge had been at about 30,000 cfs and the highest shoreline had been at about the limit of salt cedar growth (fig. 4); and (2) post-1983, when the maximum discharge had been at 96,200 cfs and the highest shoreline had been at about the limit of currently preserved salt cedars (fig. 5). "Shoreline" as used here excludes slow channelized runoff and therefore does not correspond to river "stage." Evidence for the proposed channel erosion is preserved in the shorelines. Comparison of figs. 4 and 10 along the shore between E and E' and use of fig. 5 to demonstrate that this region was indeed between the constriction and hydraulic jump during the high discharges show that a substantial amount of material is missing. The shore prior to 1983 and the current shore here are much steeper than the general slope of the debris fan, and I interpret the steep banks to be channel walls carved during river erosion. Thus, the available evidence, though not conclusive or quantitative, supports the proposed idea that the channel was substantially widened by the 1983 discharges, and that in the past the channel has been subjected to erosion in the vicinity of the constriction.

High flow velocities cause channel widening, but channel widening in turn decreases flow velocities, as can be seen in figures 9c and 9d. Erosion should cease at a constriction when the constriction becomes sufficiently wide to pass the given discharge at a velocity equal to the threshold velocity for erosion. Erosion can continue, however, in region 3 of supercritical flow even after it ceases in region 2, because water accelerates from the constriction through the supercritical region (fig. 9c). As cited above, at 50,000 cfs, with the constriction still at 0.25, calculations indicate that the velocity  $u_3$  increases from 9 m/s at region 2 to 14 m/s just in front of the hydraulic jump. At 60,000 cfs, the con-

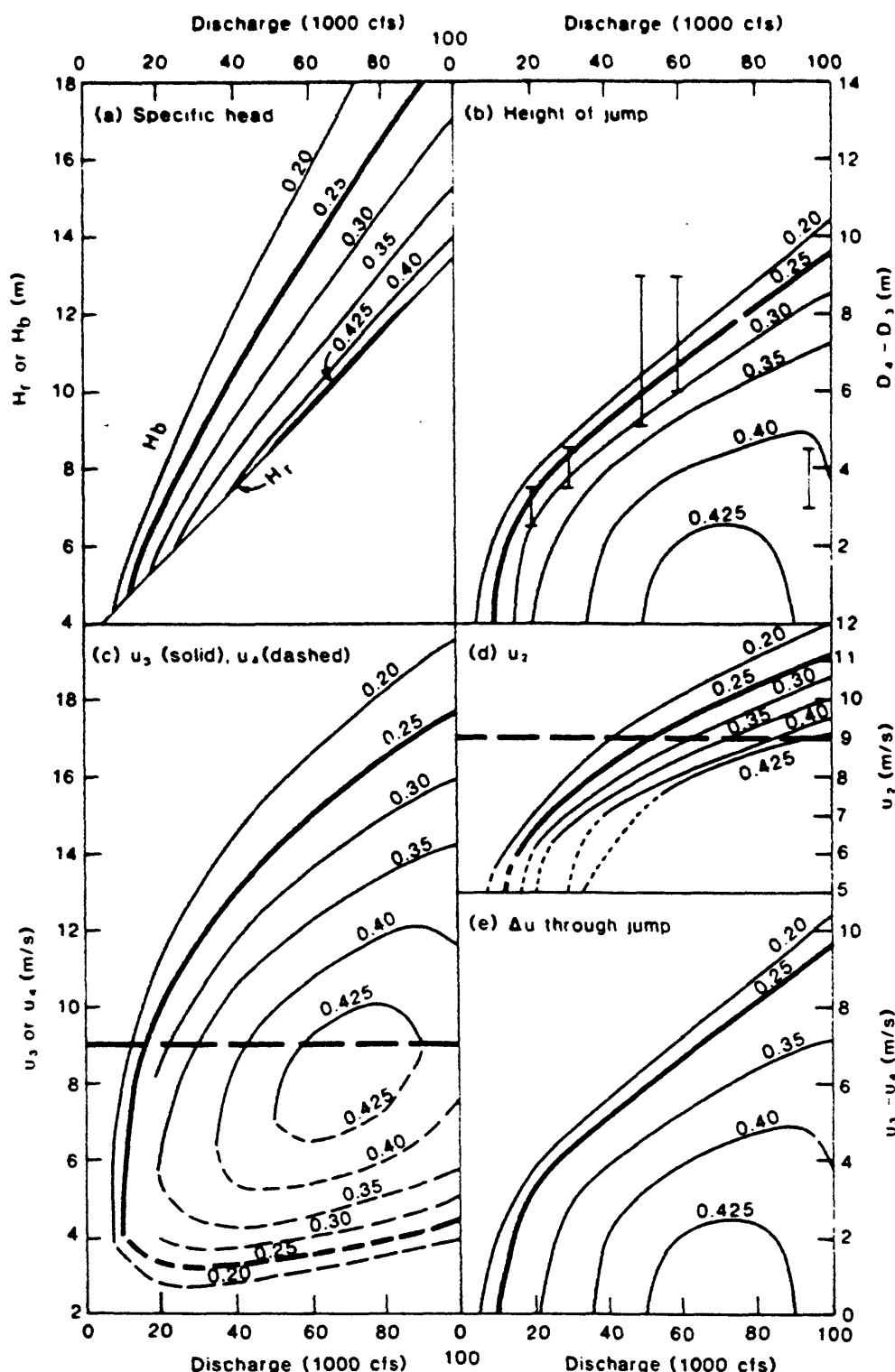


FIG. 9.—(a) Specific head ( $H_r$ ) measured at Bright Angel Creek vs. discharge, with backwater heads ( $H_b$ ) calculated for Crystal Rapid for the constrictions,  $w_2/w_0 = q_0/q_2$ , indicated. (b) Calculated height of the hydraulic jump for constrictions indicated. Bars denote observed values. (c) Calculated values of flow velocity in region 3 (top curves, solid lines) and region 4 (bottom curves, dashed lines) for constrictions indicated. Dashed line at 9 m/s indicates velocity at which larger boulders at Crystal Rapid can probably be moved by the current. (d) Calculated values of velocity in region 2 (the constriction) for constrictions indicated. Flow subcritical where dashed. (e) Velocity change through hydraulic jump that separates regions 3 and 4.

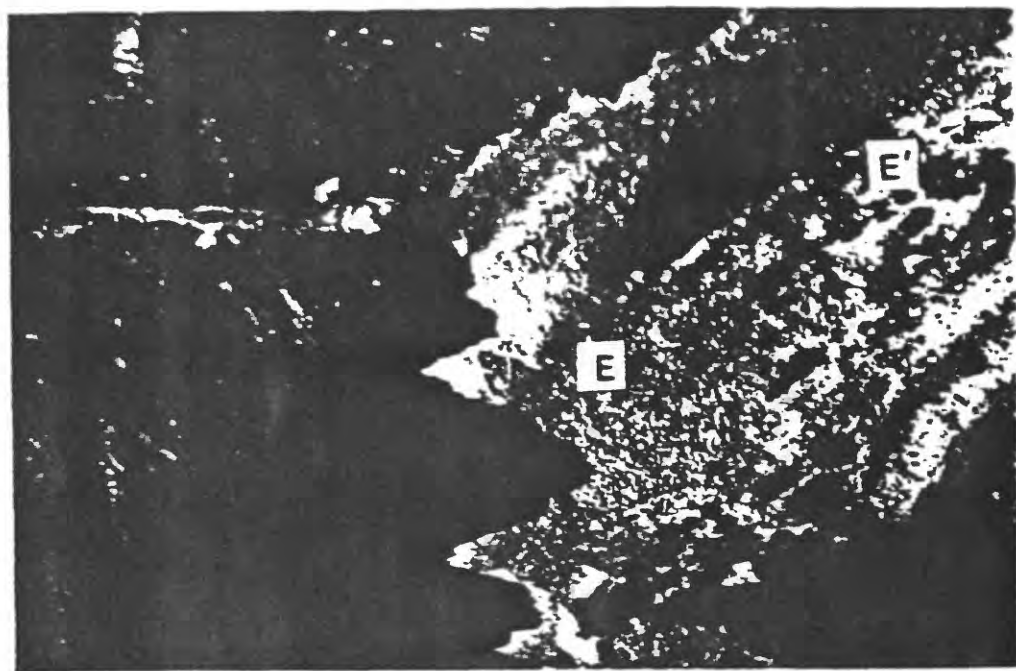


FIG. 10.—Photograph of part of Crystal Rapid obtained on Oct. 22, 1984 at a discharge of 6,000 cfs. Compare with figure 4a, taken in 1973 at 10,000 cfs. The equality of stage for the two different discharges suggests that either the bed in this photo is higher than in figure 4a, which could have resulted from post-flood sedimentation of fine material (e.g., as described by Howard and Dolan 1981, fig. 7), or that the depth-velocity relations within the rapid have substantially changed due to the change in channel shape. The author prefers the later explanation. Having noted the approximately equal stages in this figure and figure 4a, compare the span of shore between E and E' for evidence of erosion.

striction should enlarge to 0.3 to reduce  $u_2$  to 9 m/s, but  $u_3$  in front of the normal wave remains high at 13.6 m/s. At 90,000 cfs, a constriction of 0.40 will hold  $u_2$  to 9 m/s, but  $u_3$  is 11.6 m/s in front of the normal wave. Thus, under conditions of progressively higher discharge in the history the Crystal debris fan, the Colorado River should contour a nozzle of a shape appropriate to keep  $u_2$  equal to the threshold velocity for boulder transport and to keep region 3 of supercritical velocities as small as possible. It is therefore probably not a coincidence that at 92,000 cfs, the kayak velocities were 9.8 m/s from Slate Creek to the trough of the wave—a stretch that includes region 2 and the faster region 3. Given that the kayakers did not exactly follow flow streamlines and that they were paddling with great vigor when upright, this value of 9.8 m/s can be considered in reasonable agreement with the inferred threshold velocity of 9 m/s.

Water decelerates rapidly as it passes through the normal wave into region 4, and

the strong deceleration, as well as the great wave height, contributed to the rafting accidents at discharges of 50,000 to 60,000 cfs. The calculated velocity change through the wave was 10.7 m/s (35 feet/s or 24 miles per hour) at 50,000 cfs (fig. 9e). At 96,000 cfs with the constriction at 0.41, the calculated velocity change across the wave is 4.8 m/s. The kayaks were measured to decelerate from 9.8 to 3.3 m/s as they passed through the trough-crest region, in reasonable agreement with the calculated velocity change. Movies obtained by the author, as well as the sequence of photographs of which figure 3 is a part, show the large raft suddenly stopping as it hit the wave—a manifestation of the large velocity decrease across the hydraulic jump.

The large decelerations calculated for water when it passes through the normal wave from region 3 of supercritical flow into region 4 of subcritical flow suggest that this boundary will be a site of deposition of material scoured from regions 2 and 3. Experienced

## HYDRAULIC JUMP AT CRYSTAL RAPID

401

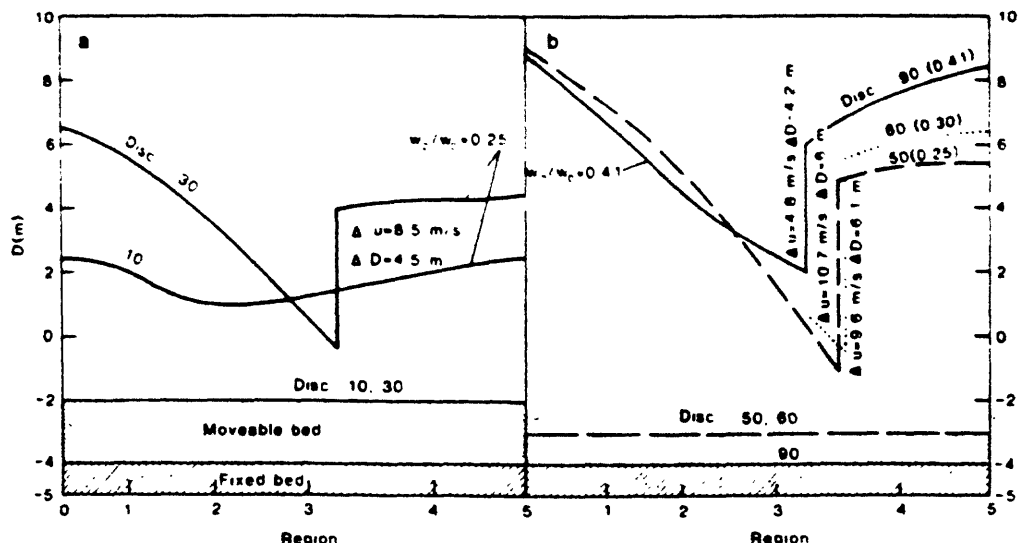


FIG. 11.—Schematic diagram of hydraulics at Crystal Rapid to discharges of 90,000 cfs. In each part, level of the water surface is obtained by taking the depth relative to a bottom whose behavior is that measured at Bright Angel Creek gaging station. Thus, erosion that occurred above 50,000 cfs is shown as a decrease in bottom level. (a) Subcritical flow at 10,000 cfs and supercritical flow at 30,000 cfs with a constriction of 0.25 in both cases. (b) Supercritical flow at 50,000, 60,000, and 90,000 cfs, with constriction widening as described in the text to maintain  $u_2$  at 9 m/s. For each supercritical-flow curve, height of hydraulic jump and velocity change across it are shown.

boatmen reported that the Rock Garden in the lower part of the rapid was substantially modified by the 1983 high discharges, and that it contains many new large boulders, some estimated to be greater than 2 m in diameter. These observations qualitatively support the erosion concepts developed above.

The major observation not explained by the calculations is the shape of the normal wave and the observed acceleration of the kayaks to 8.7 m/s downstream of it. The steepness of the wave on its back side cannot be accounted for by the two-dimensional theory used here. One possible cause of the interesting shape is stabilization by large boulders; however, observations of the river bed at 6,000 cfs by the author in October 1984 did not reveal any evidence of substantial material at this position in the bed. Descent of this steep backside by the kayaks undoubtedly contributed somewhat to their excess velocity beyond that predicted by the calculations. Part of the excess velocity may also have been obtained as the kayaks entered water that had high velocity but did not go through the wave.

The proposed hydraulic region in the various parts of Crystal Rapid is summarized in

figure 11. The calculated rise of the water surface across the debris fan with increasing discharge is about 6.5 m. A rise of about 5.5 m was observed. The agreement of the calculated and observed values must be considered good in view of the simplicity of the model, the uncertainty in extrapolating the bottom erosion from Bright Angel to Crystal, and the lack of observations and topographic control to estimate elevations of the flow at various discharges.

#### IMPLICATIONS FOR RIVER DEBRIS-FAN EVOLUTION

The dynamic interactions between the Colorado River and its tributaries have been described by Howard and Dolan (1979, 1981, esp. fig. 7), Dolan et al. (1978), and Graf (1979, 1980). The widely recognized pool-and-rapid sequence near tributary canyons (Leopold 1969; Dolan et al. 1978) arises from the rare emplacement of large debris fans at tributary mouths and their modification by large floods on the main river (see also Shoemaker and Stevens 1969), both events probably having time scales on the order of  $10^2$  to  $10^4$  years. A tributary flood raises the bed of the main river at the debris fan, dam-

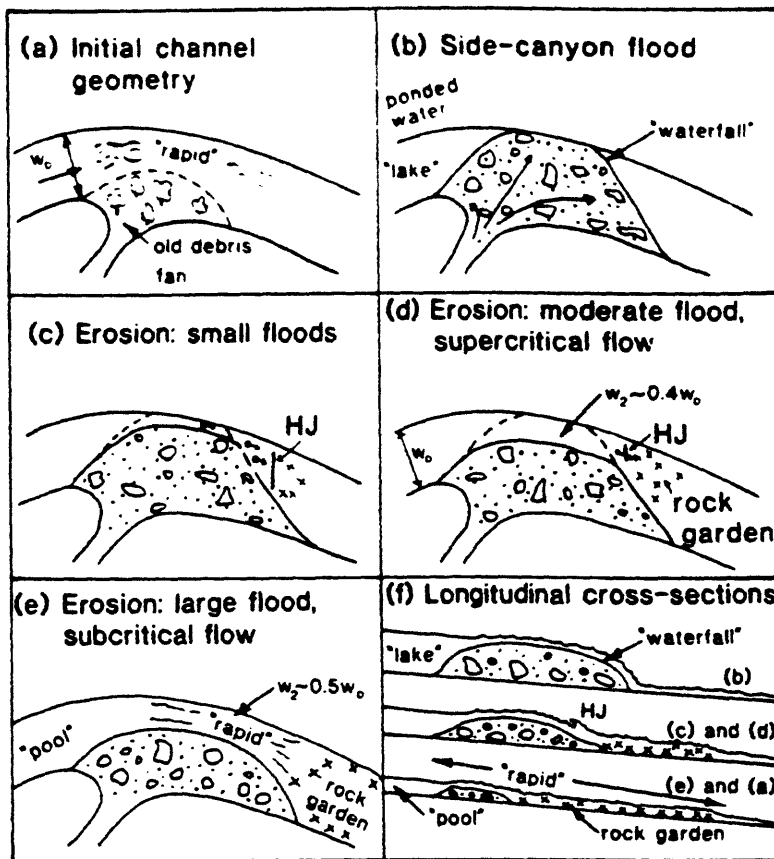


FIG. 12.—Emplacement and modification of the Crystal Creek debris fan.

ing the river; we might call this the "lake-and-waterfall" phase of "pool-and-rapid" evolution. Main-stream floods then remove the finer debris far from the fans and can shift some coarse debris downstream. Thus, the dam of tributary debris is lowered by erosion and the river bed below it raised by deposition. This general sequence of events has been confirmed by the events at Crystal between 1966 and 1984, and the analysis in this paper suggests a quantitative model for some intra-fan dynamics not previously recognized.

The proposed concept of river-debris-fan evolution in the Grand Canyon is summarized in the sequence shown in figure 12. This sequence represents but one cycle in recurring episodes in which debris fans are enlarged by floods in the tributaries and then modified by floods in the main channel. The beginning of the sequence is arbitrarily chosen as a time when the main channel is rela-

tively unconstricted (fig. 12a). The river is suddenly disrupted and ponded by catastrophic debris-fan emplacement (fig. 12b), forming a "lake" behind the debris dam. The surface of the debris fan is the "waterfall" in this model. As the ponded water overtops the debris dam, it erodes a channel, generally in the distal end of the debris fan (fig. 12c); this is the beginning of evolution of the "rapid" from the "waterfall."

Unless the debris dam is massively breached by the first breakthrough of the ponded water, the constriction of the main river is initially severe. Floods of differing sizes and frequency erode the channel to progressively greater widths, as shown in figures 12c, 12d, and 12e. Small floods (fig. 12c) enlarge the channel somewhat, but constricted, supercritical flow is still present (e.g., the annual discharges from Glen Canyon dam brought Crystal to the constriction of 0.25 between 1966 to 1983). Moderate floods (fig.

## HYDRAULIC JUMP AT CRYSTAL RAPID

403

12d) enlarge the channel further and may widen the channel so that at lower discharges the flow is weakly supercritical or even subcritical (e.g., the 1983 high discharges at Crystal widened the channel and weakened the waves characteristic of the 20,000 and 30,000 cfs discharges). At the same time that lateral widening is occurring, vertical scouring and headwall erosion of the channel are occurring (fig. 12f). Thus, the local gradient in the channel is changing, and new waves can arise as the channel geometry changes (e.g., the new, strong oblique waves at the tongue in Crystal can be attributed to concentration of the 2-3 m drop in bed elevation that had previously been distributed over much of the constriction into a small region at the head of the rapid by headward migration of the laterally widening channel, as in fig. 12f). Rare large floods (fig. 12e) carry this process further, possibly widening the channel sufficiently to allow subcritical flow at all discharges. This state has not been reached at Crystal.

A rapid like Crystal therefore evolves into two parts: the original debris deposit, and the rock garden below it consisting of reworked debris. In early episodes of small floods, flow through the constricted channel is strongly supercritical, and velocities are high enough in the constriction and in region 3 of supercritical flow so that large boulders can be moved by the river. They will be eroded from the constriction and region 3 and deposited downstream of the normal wave in region 4 of subcritical flow where flow velocities are smaller. Thus, it is plausible to believe that the rock garden grows or is modified with the changing position of the normal wave. The reports of changes in the configuration of the Crystal Rock Garden during the 1983 high discharges support this idea. Since the position of the hydraulic jump changes with discharge (which increases and decreases on many different time scales) and with channel constriction (which becomes less severe with time), changes in the rock garden can occur over a substantial distance in the rapid. At Crystal Rapid, the distance between the constriction and the furthest rocks in the Rock Garden is on the order of 1 km.

Depending on the relative upstream and downstream heads of the water and on the velocity required to move debris, two differ-

ent flow regimes and channel geometries could result from the highest discharges: (a) As widening occurs, flow velocities in the constriction could become lower than the threshold velocity for erosion, and erosion could cease while the channel geometry still required supercritical flow (as suggested in fig. 12d). (In this case, even though erosion no longer occurred in the constriction, modification of the debris fan could continue downstream of the constriction if velocities in the supercritical region 3 were sufficiently high for boulder transport.) (b) Alternatively, as widening occurs, velocities could remain sufficiently high for erosion to channel a width sufficient for subcritical flow (as suggested in fig. 12e). The choice of alternatives is determined by the relative upstream and downstream heads of the river at the rapid, and by the threshold erosion velocity. Calculations presented below suggest that alternative (b) is the general case for debris fan evolution on the Colorado River in the Grand Canyon—that is, that subcritical flow is obtained in the widening process. At some relatively arbitrary time in this sequence, the configuration of the river at the debris fan has evolved from lake-and-waterfall to pool-and-rapid, and, depending on the relative frequencies of the large floods on the main river and tributary, the sequence of fig. 12a-e is repeated.

The shape of the main stream at a debris fan at any instant of geologic time therefore reflects the contouring that occurred at the maximum discharge of the river since the last emplacement episode in the history of that debris fan, unless effects of sedimentation of the finer-grained, more transient material partially mask the larger scale erosion (e.g., Howard and Dolan 1981, fig. 7). The observation, summarized in figure 2, that the Colorado River is less constricted at most of the tributary debris fans than it is at Crystal Rapid suggests that these fans have seen higher discharges than Crystal, i.e., higher than 100,000 cfs. We know this to be true—a flood of 220,000 cfs occurred in 1921, and a flood estimated at 300,000 cfs occurred in 1884. It is reasonable to assume that even larger floods have occurred since the emplacement of many of these debris, a time that may exceed  $10^4$  years (Hereford 1983). (Note: the observations in fig. 2 and this dis-

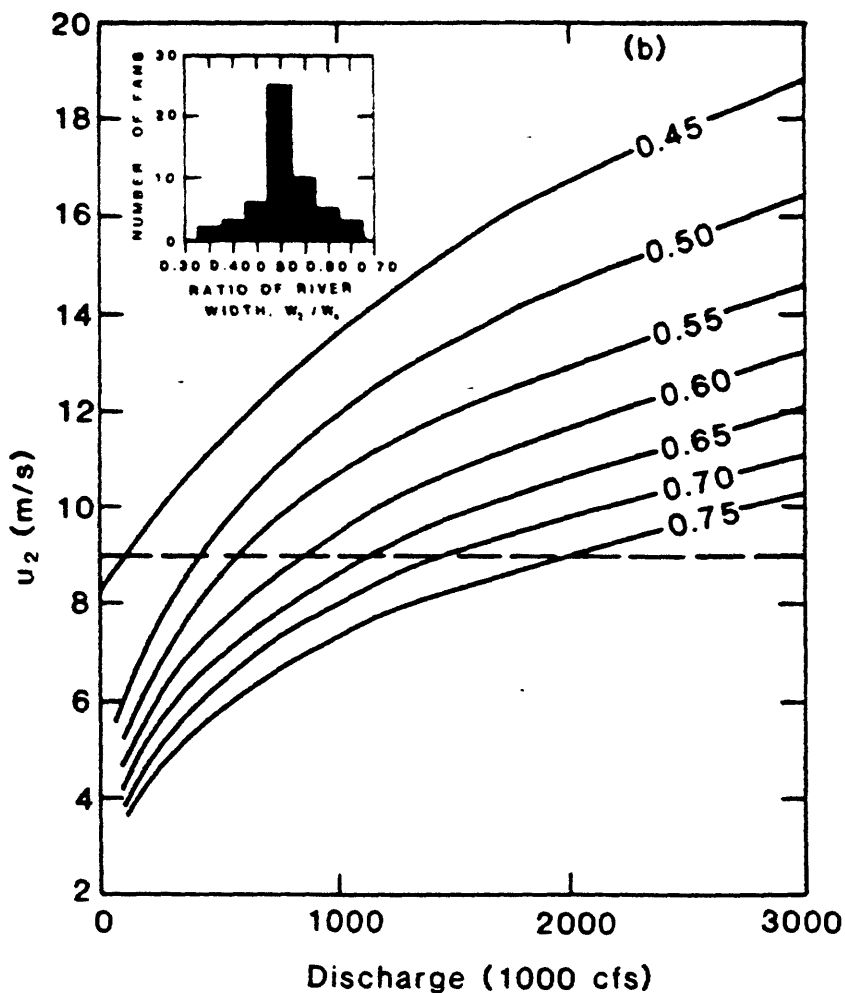


FIG. 13.—(a) Histogram of figure 2 reproduced. (b) Velocity in narrowest part of a constriction for flows extrapolated beyond 100,000 cfs. in comparison with threshold velocity (dashed line) assumed required for constriction erosion. Curves are labeled with values of constriction.

cussion apply only to those recent fans that emerge from tributaries and are currently active, not to some of the more ancient terraces along the Colorado that may have formed under substantially different climatic conditions.)

These observations suggest that the largest discharge in the life of these fans could be estimated from extrapolation of this analysis for Crystal discharges sufficiently high to obtain a constriction of 0.50 (fig. 13). In so doing, an assumption is made that channel erosion was sufficiently rapid to reduce the flow velocity to the threshold level at each flood. Extrapolation was done with the standard power functions relating depth, velocity, and head to specific discharge as described in

table 1, footnote i. In addition to the uncertainty introduced by these functions, there are uncertainties due to lack of knowledge of the vertical cutting of the bed at high discharges and to the role of overflow across the debris fan, which could become more significant at higher discharges.

The calculations show that if the discharges through Crystal Rapid were increased above 100,000 cfs., the present channel constriction of about 0.40 is too severe to prevent velocities in the constriction from rising above those required for erosion. For example, if the discharge rose to 300,000 cfs.,  $u_2$  would rise to 10.6 m/s in a channel with 0.41 constriction; therefore, the channel would widen. A widening to a constriction of 0.47

## HYDRAULIC JUMP AT CRYSTAL RAPID

405

would reduce the velocity back to 9 m/s. The hydraulic jump and supercritical flow regimes would disappear under these conditions. A constriction of 0.50 would be obtained at a discharge of slightly over 400,000 cfs (11,320 m<sup>3</sup>/s). Assuming that similar conditions hold at the other debris fans represented in the histogram of figure 2, this discharge represents an estimate for the largest flood in the Grand Canyon since these fans were formed.

As the channel widens, flow at low discharges becomes subcritical. Supercritical flow, even at the highest discharges, ceases when the constriction has reached 0.45. In the absence of supercritical flow, there is no normal wave. It is thus consistent with the calculations presented that there are few normal waves other than at Crystal Rapid on the Colorado River in the Grand Canyon—the river channel is sufficiently wide around the debris fans that supercritical flow does not occur (except the weakly supercritical conditions that arise when potential energy and dissipation are not exactly balanced in the upper reaches of rapids, as described in the text).

The constrictions of the Grand Canyon tributary debris fans are remarkably uniform at a value of  $w_2/w_0 = 0.5$  (fig. 2), especially when one considers variations in rapid size, fan size and composition, and vertical drop through the rapid. Variations in river constriction at different debris fans may indicate: (1) different erosional thresholds (e.g., due to different particle sizes or cementation of the fans); (2) different specific heads of the Colorado River along different reaches; (3) different flood histories of the Colorado in the vicinity of different debris fans (e.g., if the debris fans are of different ages or if temporary obstruction of parts of the Colorado River by debris or lava flows resulted in different flood levels along the Colorado); (4) different ages of the fans. For refinement of the estimate of peak discharge discussed above, these factors need to be examined at each fan of interest.

In conclusion, the ability of the Colorado River to contour its own channel probably accounts for the remarkable uniformity of constriction that the river exhibits as it passes around each of the major debris fans along its 400 km length in the Grand Canyon. During the high discharges of 1983, supercritical flow

of the Colorado River at the Crystal Creek debris fan brought the river and the debris fan substantially closer to a configuration characteristic of the one that would be obtained if natural flooding of the river still occurred.

**ACKNOWLEDGMENTS.**—I thank the U.S. Geological Survey staff in Flagstaff, Arizona, especially E. Buell, for kindly providing the Bright Angel gaging-station data and for helpful discussions on river hydrology. Numerous river runners provided descriptions of the flow at various stages; photographic documentation by Robert Melville was especially important. I also thank John Thomas of the U.S. National Park Service for arranging access to Crystal Rapid via helicopter on June 27, 1983, and Curt Sauer for arranging access on October 22–24, 1984, when the Bureau of Reclamation lowered the discharge to 6,000 cfs. The manuscript was greatly improved by the reviews by E. D. Andrews, E. Buell, P. Delaney, R. Hereford, H. Shaw, R. Shreve, B. Sturtevant, and by discussions with G. Billingsley. Director's Approval: July 19, 1984.

## APPENDIX

As an example of the use of the depth-energy and depth-force diagrams of figure 8c and 8d, consider the discharge of 50,000 cfs (1415 m<sup>3</sup>/s) flowing through a channel at Crystal assumed to narrow from 80 to 20 m. First consider the case of constant specific energy. The discharge per unit width in region 0 is 17.7 m<sup>2</sup>/s; in region 2 it is 70.6 m<sup>2</sup>/s. The ambient river head  $H_0$  is 8.4 m. This is insufficient to allow a flow of 70.6 m<sup>2</sup>/s through the constriction, so a backwater forms to increase the head to 12 m (point A). At this head the water flows through the constriction at a critical depth of 8.0 m, with a critical velocity of 8.8 m/s. Upon expansion into the divergence, the flow becomes supercritical as  $q$  increases (path B-C-C'). A hydraulic jump forms at the conditions C' where the dissipation across the jump returns the backwater head to the ambient downstream head of 8.4 m. The height of the jump formed for a given initial depth in front of the jump (e.g., C or C') can be found in part (d) of the figure. For example, at C', the depth in front of the jump  $D_1$  is 1.9 m at a discharge of  $q_1 = 26.7$  m<sup>2</sup>/s. The conjugate state on (b) is 7.9 m (point D), giving a jump height of 6 m. Referring back to part (c), point D plots at a new head of 8.4 m, as required to restore the flow to the ambient head. The flow then expands subcritically to the ambient downstream discharge, E.

The effect of increasing the specific head if the potential energy gain in the vertical drop through the rapid is not dissipated is shown by the alternate trajectory A-B-F, where B-F represents an extreme gain of 6 m head while the flow is in the constriction. A reasonable simplification of the geometry is that the steep downhill section is within the narrowest part of the channel (fig. 8b). The flow then becomes supercritical in the constriction, in this case at F, with  $Fr = 2.5$ . The depth is 4.3 m and velocity is 16.4 m/s. In the divergence the flow expands along path F-G-G' to a state where a hydraulic jump, if formed, would return the head from 18 m back to 8.4 m. By the same procedure as

before, point G' is plotted on (c) where the conjugate depth ( $H$ ) of 8.1 m is found. Expansion to state E (fig. 8c) in the divergence follows. Even for this case, in which the potential energy gain is about twice that plausible for Crystal, the calculated jump height (on c) is within 1 or 2 meters of that calculated without inclusion of the vertical drop of the bed and energy dissipation in the water. The height of the hydraulic jump is relatively insensitive to the potential energy gain. The few existing observations are insufficient to distinguish between the calculations with and without the potential energy gain. Therefore, the flow equations in the text are for the simplified case of  $H_r = \text{constant}$ .

#### REFERENCES CITED

BLATT, H.; MIDDLETON, G.; and MURRAY, R., 1972. Origin of Sedimentary Rocks. Englewood Cliffs, N.J.: Prentice Hall, 634 p.

BRATER, E. F., and KING, H. W., 1976. Handbook of Hydraulics. New York: McGraw-Hill, 14 Chapters.

COLLINS, R. O., and NASH, R., 1978. The Big Drops: Ten Legendary Rapids. San Francisco: Sierra Club Books, 215 p.

COOLEY, M. E.; ALDRIDGE, B. N.; and EULER, R. C., 1977. Effects of the catastrophic flood of December 1966, north rim area, eastern Grand Canyon, Arizona: U.S. Geol. Survey Prof. Paper 980, 43 p.

DOLAN, R.; HOWARD, A.; and GALENSON, A., 1974. Man's impact on the Colorado River in the Grand Canyon: Am. Scientist, v. 62, p. 392-401.

—; —; and TRIMBLE, D., 1978. Structural control of the rapids and pools of the Colorado River in the Grand Canyon: Science, v. 202, p. 629-631.

GRAF, W. L., 1979. Rapids in canyon rivers: Jour. Geology, v. 87, p. 533-551.

—, 1980. The effect of dam closure on downstream rapids: Water Resources Res., v. 16, p. 129-136.

HELLEY, E. J., 1969. Field measurement of the initiation of large bed particle motion in Blue Creek near Klamath, California: U.S. Geol. Survey Prof. Paper 562-G, 19 p.

HEREFORD, R., 1981. Driftwood in Stanton's Cave: a case for temporary damming of the Colorado River at Nankoweap Creek in Marble Canyon, in EULER, R. C., ed., The archaeology, geology, and paleobiology of Stanton's Cave: Grand Canyon Nat. Hist. Assoc. Mon. 6, p. 99-106.

HOWARD, A. D., and DOLAN, R., 1979. Changes in the fluvial deposits of the Colorado River in the Grand Canyon caused by Glenn Canyon dam, in LIN, R. M., ed., Proc. of the First Conf. Sci. Res. in the National Parks: Trans. Proc. U.S. National Park Service, New Orleans, no. 5, p. 845-851.

—, and —, 1981. Geomorphology of the Colorado River in the Grand Canyon. Jour. Geology, v. 89, p. 269-298.

LEOPOLD, L. B., 1969. The rapids and the pools-Grand Canyon: U.S. Geol. Survey Prof. Paper 669, p. 131-145.

LOH, W. H. T., 1969. Theory of the hydraulic analogy for steady and unsteady gas dynamics, in LOH, W. H. T., ed., Modern Developments in Gas Dynamics: New York: Plenum, pp. 1-61.

RICHARDS, K., 1983. Rivers: Form and Process in Alluvial Channels: London: Methuen, p. 58.

ROUSE, H., 1950. Engineering Hydraulics: New York: John Wiley, 1039 p.

—; BHOOJA, B. V.; and HSU, E., 1951. Design of channel expansions: Trans. Amer. Soc. Civil Eng., v. 116, p. 347-363.

SHOEMAKER, E. M., and STEVENS, H. G., 1969. The Green and Colorado River canyons observed from the footsteps of Beaman and Hillers 97 years after Powell: Geol. Soc. Amer. Abs., Rocky Mountain Sec., p. 73.

U.S. Geol. Survey, Water Resources Data, Arizona, 1980. (referenced as Water-Data Report AZ-(year)): U.S. Geol. Survey, Tucson, Az.

WOLF, T. J., Dec. 12, 1983. High Country News, v. 15, no. 22, p. 10-14.

## Appendix B: Summary of Project Objectives and Accomplishments

As stated in the text, the overall objective of work done under Interagency Acquisition No. 6-AA-40-04190 was documentation of the nature and shape of the channel of the Colorado River in the vicinity of the rapids and of the hydraulics of the rapids. The work was described under six objectives in the interagency agreement:

- (1) Classification of the origin of rapids in the Grand Canyon;
- (2) Selection of 12 rapids for intensive studies;
- (3) Development of hydraulic maps;
- (4) Collection of hydraulic data to calibrate calculations and hydraulic maps;
- (5) Analysis of the hydraulic and energy balances;
- (6) Integration of the measurements with the other sediment studies and recreation.

This work was funded for six months during FY-'86 and three months in FY-'87.

### Summary of achievement:

#### (1) Classification of the origin of the rapids of the Grand Canyon.

Nearly all rapids above boating difficulty level 4 were reconnoitered during the two river trips, and it was decided that a simple statement that the rapids arise from tributary debris flows, with reference to the detailed work of Howard and Dolan (1981) and Webb (GCES, 1987) was sufficient. Notebooks of "rapidforms" (a four-page form on which various geologic and hydraulic information about the rapids could be quickly noted as the boats floated through a rapid) were compiled, and the selection of twelve rapids for detailed study was based on the geologic observations of these rapids, and on consultation with the NPS, the BOR, and the USGS WRD. The rapids selected represent a range of interests from recreational use, to sediment-transport studies, to hydraulic studies.

(2) Selection of 12 rapids for intensive studies. The report describes the studies at 12 rapids (House Rock, 24.5-Mile, Hance, Cremation, Bright Angel, Horn Creek, Granite, Hermit, Crystal, Deubendorff, Lava Falls, 209-Mile), with additional data given for Elves Chasm. In the report, a generalized model for the structure of rapids and their evolution is developed, and each of the studied rapids is cited for specific phenomena. Description of the individual rapids in detail would require a very lengthy report; instead, the individual descriptions of rapids will appear as text on the final hydraulic maps.

(3) Development of hydraulic maps. Ten maps (one including two rapids) have been compiled and are in various stages of preparation for final publication for public purchase. The maps will be in the U.S.G.S. Miscellaneous Investigations Series, I-1897, parts A-J. Preliminary copies of all maps (except Bright Angel) were given to the NPS and BOR in July, 1986, in the form of data collection sheets for the NPS observers at rapids. Additionally, when requested, ozalid copies of base contour maps were provided to the BOR for the sediment modelling

effort. Samples of the maps are included as Figures 9-12 in this report. In consultation with Dave Wegner, BOR, it was decided in the spring of 1986 to illustrate the final maps with airbrush rendering of the hydraulic structures. This was approved by the BOR and USGS, and an extended contract agreement (for 3 months funding of the principal investigator plus map-making expenses) for FY-'87 was implemented. We expect the first of these maps to be available for public purchase in the fall of 1987, and most of them to be available by early 1988.

(4) Collection of hydraulic data to calibrate calculations and hydraulic maps. During the two river trips on which data were collected, five types of data were collected at each rapid: (1) photographic documentation of the river channel and hydraulics from camera sites that can be relocated; (2) time-lapse movie films of each rapid during fluctuating flows; (3) fathometer data in the channel above the rapid; (4) survey control data for the hydraulic maps; (5) movie footage of floats launched through the rapids. All movies have been copied by the BOR onto video for their use.

(5) Analysis of hydraulic and energy balances. Contour maps have been compiled for all of the rapids, using the control data obtained in the field. Airbrush maps have been completed for House Rock, Horn, Hance, Crystal, and Lava Falls, and will be finished for the remaining five rapids by summer 1987. Compilation of the hydraulic data from the movies onto the maps is only efficiently done after completion of the airbrush, since this provides the accurate hydraulic base. The five rapids completed to date are representative of the ten major rapids, and are the basis analysis of hydraulics and energy balances discussed in this report.

(6) Integration of the measurements with the other sediment studies and recreation. The preliminary hydraulic maps were put onto data sheets and a questionnaire was developed for the NPS observers to record hydraulic data on. In our amended FY-'87 contract, we are assuming the responsibility for duplicating these sheets, and providing an analysis of the data. We hope to do this in time for the data to be included in the recreation subteam report, but this is not required in the amendment. Hydraulic maps of the rapids were approximately doubled in length after discussions with Graf and Schmidt demonstrated that the increased information would help integrate the dynamics of the rapids with their work on eddies and beaches below the rapids. Bright Angel and Cremation Rapids were mapped specifically for their relation to the USGS WRD gage station studies. The study of boulder size distributions discussed in Section IV supplements studies of the finer-sized material done by other researchers, and also the study of Webb on the origin of this material in the tributary canyons. The products of this research are: (1) this report, a form of which will eventually be submitted to a published journal; (2) the hydraulic maps I-1897 A-J; (3) a 20-minute VHS video showing the major features of the 10 rapids (U.S.G.S. Open-File Report 86-503; and (4) miscellaneous interim products, such as copies of movie footage and preliminary hydraulic maps provided throughout the project to other investigators.

### Appendix C: Control for the Topographic Maps

Ten topographic maps (which will be published separately as U.S.G.S. Miscellaneous Investigation maps I-1897 A-J) have been prepared for this project in order to establish the geometry and roughness of the Colorado River channel. The compilation of the maps was done by Bonnie Redding of the Photogrammetry Section, Branch of Astrogeology, U.S.G.S., under the supervision of Sherman Wu. Scientifically accurate air brush illustrations were prepared to illustrate the hydraulic features by Patti H. Gray, of the Planetary Cartography Group, Branch of Astrogeology, U.S.G.S., Flagstaff, Arizona, under the supervision of Ray Batson.

Control for the maps was established by surveying approximately 10 points at each site with a Leitz Electronic Tachymeter. The control points were typically large boulders on the debris fans, or bedrock points that could be located in air photos. The 1984 low-discharge air photos of the Bureau of Reclamation were used as a base for the analytic photogrammetry. The maps typically cover the rapid and its shoreline from the upstream backwater to the downstream extent of the beach-eddy system below the rapid.

Elevation was documented from the river level to the old high-water vegetation line, that is, the channel is defined to discharges of about 125,000 cfs. The contour interval is 1 m, except on the flat parts of the debris fan where 0.5 m contours have been plotted. In most cases, absolute elevation could not be related to bench-marks (except at Bright Angel, Crystal, and Lava Rapids). The 15-minute quadrangle series, with 40-foot contour intervals, is not sufficiently accurate to allow specification of the elevation of the rapids. Therefore, in most cases, an elevation was assigned to the rapids based on the 1923 Birdseye profile of the river. The elevations used were not corrected for changing discharge during the Birdseye (1923) expedition, and therefore, the absolute elevations may be in error by a few meters. The errors in absolute elevation will not affect any hydraulic analyses.

The most serious error in the maps arises from the fact that ground control could not be established to all edges of the 1984 air photos--a requirement for establishing good relations between ground truth and internal photogrammetric coordinates. In an upriver-downriver direction the river frequently bends so that direct line-of-site surveying cannot be done, and limited time prevented establishing multiple hubs for the surveys. In a transverse direction, the photographs typically include the Tonto platform, and both time and line-of-sight conditions precluded surveying these distances. As a result, the gradient of the river has a larger uncertainty than would be desired for a map with 0.5 and 1-m contour intervals.

Comparison of the maps with the 1923 river profile and with surveying data obtained independently by Schmidt (GCES, 1987) suggests that the error in river slope is typically less than 1 m. Since most of these big rapids drop on the order of 5-8 m, the error in slope may be of the order of 15%. Errors in lateral dimensions on the map (e.g., distances to identifiable objects are estimated (from the averaging of the surveyed points to produce the maps) to be on the order of 2 m.

#### Appendix D: Measurement of Water Surface Velocities with "Yogis"

In order to measure water surface velocities, objects were floated through the rapids and their trajectories recorded on Super-8 movie film at 18 fps. The trajectories were then plotted on the hydraulic maps, using the air brush rendering of wave structures to locate the relative position of the floats in the river. Radii were drawn from the camera position to identifiable background features (typically to 10 or 12 features). The time at which the float crossed each radius was determined from the cumulative number of movie frames taken, using a Lafayette Analyzer movie projector. The path length between each radius was measured from the maps, and the velocity determined by dividing this distance by the time taken from one radius to the next. Each float was analyzed twice by two different people, and the average velocities were calculated.

In general, the floats were not launched at the same discharges that were used for creation of the hydraulic maps (5,000 and 30,000 cfs). On the preliminary maps in this report the measured velocities are shown. However, on the final maps of I-1897, a small correction will be attempted so that the velocity data correspond to the discharge portrayed on the hydraulic map. For example, at Lava Falls Rapids floats were launched at 7,000 and 10,000 cfs. This is not a wide enough range of discharge to permit conclusions to be drawn about the variation of velocity in a rapid with discharge, but the velocities in the backwater and convergent stretch of the river at Lava Falls were systematically 15% greater at 10,000 cfs than at 7,000 cfs, and the tailwave velocities were roughly 10% greater. No systematic difference was found in the velocities in the constricted, supercritical part of the flow (probably because the great turbulence gives such a wide spread of velocities that the average is unaffected by the small changes that may have occurred). In order to construct an internally consistent data set on the hydraulic maps, the trends suggested by available data such as these were used to extrapolate the measured velocities to the discharge shown on a hydraulic map on which the velocity is plotted. In the case of Lava Falls, the backwater and tailwater velocities measured at 7,000 cfs will be reduced by 10% to be plotted at 5,000 cfs on the hydraulic map.

Sophisticated floats were not warranted because of the high probability of loss of instruments. Large, bright-colored floats were needed because the camera had to be sited several hundred meters from the river in order to film the whole rapid and to have a large enough field of view that identifiable background features could be included (Figure D1 (a)). The floats used are shown in Figure D1 (a-d); they were nick-named "Yogis"<sup>1</sup>. They are 1 m high; 1/3 m diameter; and weigh 3 lbs. This weight is largely in sand stored in their bases. To aid in increasing their drag in the rapids, a garbage bag filled with water was tied to the Yogis. The Yogi's were typically oriented vertically (Figure D1(b))

---

<sup>1</sup> This reference is for purposes of identification only, and no endorsement of this product is intended by the U.S. Geological Survey.

or horizontally (Figure D1(c)) in the water, a combination that seemed to render an optimum blend of visibility and maximum water drag. The Yogi's were recovered at the bottom of the rapids by a kayaker and recycled (Figure D1(d)).

Unless weather conditions precluded extensive work, seven Yogi's were launched at each rapid: three in the hydraulic center; and one each at far right, mid-right, mid-left, and far left. In a few rapids, this sequence was done at "low water" (typically about 10,000 cfs) and "high water" (17,000 to 25,000 cfs). Even slight breezes affected the Yogi's in the backwaters, and in general, they were not launched when there was any wind.

The relation between water-surface velocities determined by the Yogi's, real water-surface velocities, and average water velocities is not known. Observations of a kayak in which the paddler was doing as little paddling as possible showed that the kayak went faster than the Yogis; it is known that a person in the water (with life-vest on, but feet into the water increasing drag) goes faster than a 16-foot boat. I therefore estimate that the Yogi velocities are on the order of 85% of an averaged river velocity for a given streamline. In this report, however, all quoted velocities are water surface velocities.

**Figure D1.** Plates showing the launching and recovery of floats at Granite Rapids. (a) A float is launched upstream of the rapid. Note the small size in comparison to the scale of the rapid. This is approximately the size that a float appears in the Super-8 movies of the experiment, because such movies had to be framed so that identifiable background and foreground features were included in the frame for location purposes. (b) and (c) Close-up views of the floats in the rapids, showing their most common orientations in the water. The floats had 3 lbs of sand in their bottoms, and were anchored with a rope tied to a garbage bag filled with water for additional drag in the water. (d) At the bottom of a rapid, a kayaker retrieves a float.

Figure D1 (Appendix D)

